Electronic Supplementary Material (ESI) for Chemical Communications.

Supporting Information

Concurrent Cu(II)-initiated Fenton-like Reaction and Glutathione Depletion to Escalate Chemodynamic Therapy

Ashwini Kumar[¥], Ayushi Chaudhary[¥], Bhumika Agrahari, Kajal Chaudhary, Pooran Kumar, Ritika Gautam Singh*

[1]Department of Chemistry, Indian Institute of Technology Kanpur, Kanpur 208016, Uttar Pradesh, India,
E-mail: rgautam@iitk.ac.in

*All correspondence should be addressed to rgautam@iitk.ac.in

Table of Content

EXPERIMENTAL SECTION

Physical methods and materials:

All the reagents and solvents were procured from commercial sources (such as TCI Chemicals, Alfa Aesar and Sigma-Aldrich) and used without purification unless otherwise mentioned. 3-Formyl-4-hydroxybenzoic acid, 5-Fluoro salicylaldehyde and 5-Nitro Salicylaldehyde were synthesized using reported literature.[1-3] Distillation setup was used for dry EtOH and toluene. $CDCl_3$ and DMSO-d_6 were used as solvents for ^1H and ^{13}C NMR measurements on JEOL 400 and 500 MHz spectrometers. The residual hydrogen signal of the deuterated solutions was used to reference the ^1H NMR chemical shifts. For ^1H and ^{13}C NMR spectroscopy, the chemical shift is reported as dimensionless values and is frequency referenced relative to TMS. Waters Micro mass Quattro Micro triple-quadruplet mass spectrometer was used to collect ESI-MS data. UV–visible spectra were obtained using a JASCO V–670 UV–Visible absorption spectrophotometer. FT-IR spectra were recorded on Perkin Elmer Spectrometer in the range of 400-4000 cm^{-1} using KBr pellets. Cyclic Voltammetry (CV) analysis was performed on CHI610E electrochemical analyser under oxygen-free conditions. The CV studies were performed on the $Cu(L2)_2$ complex (10^{-3} M) using 0.1 M [nBu$_4$N] [ClO_4] as a supporting electrolyte in DMF solvent at scan rate of 50 mV s^{-1}. The three-component electrode consisted of a glassy carbon working electrode, Ag/AgCl reference electrode, and Pt wire as the counter electrode.

All compounds reported in the article are >95% pure by reverse-phase high-performance liquid chromatography (HPLC) analysis. The compounds have also been characterized by other characterization techniques like ^1H and ^{13}C NMR, IR, EPR, and single crystal XRD.

Crystal Structure Determinations

Single-crystal X-ray data were collected on a Bruker SMART APEX CCD diffractometer using graphite-monochromated Mo Kα radiation (λ = 0.71069 Å) with the SMART suite of programs.[1] All data were processed and corrected for Lorentz and polarization effects with SAINT and for absorption effects with SADABS.2 Structural solution and refinement were carried out with the SHELXTL suite of

programs.[3] The structures were refined (weighted least squares refinement on F^2) to convergence. All the non-hydrogen atoms in all the compounds were refined anisotropically by full-matrix least-squares refinement. The lattice parameters and structural data are listed at the end of this Supporting Information. All the crystallographic data have been deposited in The Cambridge Crystallographic Data Centre; CCDC-**2252221** (**HL2**), **2251966** (**HL3**), **2251967 (HL5), 2251968 (HL4) , 2251965 (HL8) and 2251969 (Cu(L3)$_2$** contain the crystallographic data.

1. SMART version 5.628, Bruker AXS Inc., Madison, WI, USA, 2001.
2. G. M.Sheldrick, SADABS, University of Gottingen, Gottingen, Germany, 1996.
3. SHELXTL version 5.1, Bruker AXS Inc., Madison, WI, USA, 1997.

EXPERIMENTAL SECTION

Synthesis of 2-Amino-*N*-(1-phenylethyl) benzamide (1).

Isatoic anhydride (978.78 mg, 6 mmol) and (R)-1-Phenylethylamine (780 µL, 6 mmol) were dissolved in dry toluene (40 mL), in a clean and dry round bottom flask. The reaction mixture was stirred and refluxed at 100 °C for 6 h. Afterwards, the solvent was evaporated under low pressure using a rotary evaporator to obtain the desired white-brown product (Yield: 89 %). ^{1}H NMR (500 MHz, $CDCl_3$, δ ppm): 7.40 – 7.31 (m, 4H), 7.28 (ddd, *J* = 6.6, 3.9, 1.5 Hz, 1H), 7.25 – 7.15 (m, 2H), 6.69 – 6.61 (m, 2H), 6.28 (d, *J* = 6.4 Hz, 1H), 5.31 – 5.24 (m, 1H), 1.59 (d, *J* = 6.9 Hz, 3H). ^{13}C NMR (126 MHz, $CDCl_3$, δ ppm): 168.58 (s), 148.97 (s), 143.49 (s), 132.46 (s), 128.88 (2C), 127.36 (3C), 126.26 (2C), 117.46 (s), 116.67 (s), 49.03 (s), 22.11 (s).

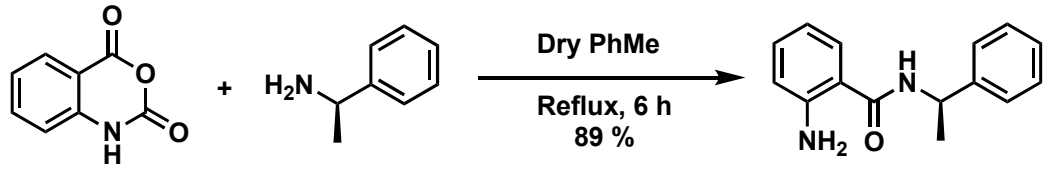

General Procedure A: Synthesis of HL1-HL8 ligands.

In an oven-dried Schlenk tube, 2-Amino-N-(1-phenylethyl) benzamide (**1**) and aldehyde (1:1 ratio) were taken and dissolved in ethanol. Acetic acid was added in catalytic amount (3-4 drops) and the reaction was refluxed for 4-6 h. After completion of the reaction, the reaction mixture was cooled to room temperature and solvent was removed in rotavapor. The crude solid product, then, washed with diethyl ether to obtain pure 'ONO' ligands.

(*R*,*E*)-2-((2-hydroxybenzylidene)amino)-*N*-(1-phenylethyl)benzamide (HL1).

Compound **HL1** has been synthesized by general procedure **A** using Salicylaldehyde (1 mmol, 104 µl, 122.12 mg) and **1** (1 mmol, 242.6 mg). Yield: 53%. ^{1}H NMR (500 MHz, $CDCl_3$, δ ppm): 8.53 (s, 1H), 7.94 (dd, *J* = 7.8, 1.4 Hz, 1H), 7.51 – 7.42 (m, 2H), 7.39 (dd, *J* = 7.7, 1.6 Hz, 1H), 7.34 (td, *J* = 7.6, 1.0 Hz, 1H), 7.29 (dd, *J* = 7.8, 1.4 Hz, 2H), 7.22 – 7.15 (m, 3H), 7.05 (d, *J* = 8.0 Hz, 2H), 6.98 (td, *J* = 7.6, 0.9 Hz, 1H), 6.81 (d, *J* = 6.7 Hz, 1H), 5.27 (p, *J* = 7.0 Hz, 1H), 1.54 (d, *J* = 6.9 Hz, 3H). ^{13}C NMR (125 MHz, $CDCl_3$, δ ppm): 165.67 (2C), 160.77, 147.42, 143.16, 134.20, 132.94, 131.93, 130.30, 128.68 (3C), 127.35, 126.88, 126.28 (2C), 120.11, 119.64, 119.03, 117.57, 49.99, 21.93. ESI-MS- (m/z): [M-H+]- calcd for [$C_{22}H_{19}N_2O_2$], 343.1447 found, 343.1446. FTIR (KBr), cm-1: 3309 *v* (-NH-)amide, 3065-2966 *v* (=CH)ar, 1640 *v* (-C=O-)amide, 1619 *v* (-C=N), 1529 *v* (C=C)ring, 758- 702 *v* (-CH).

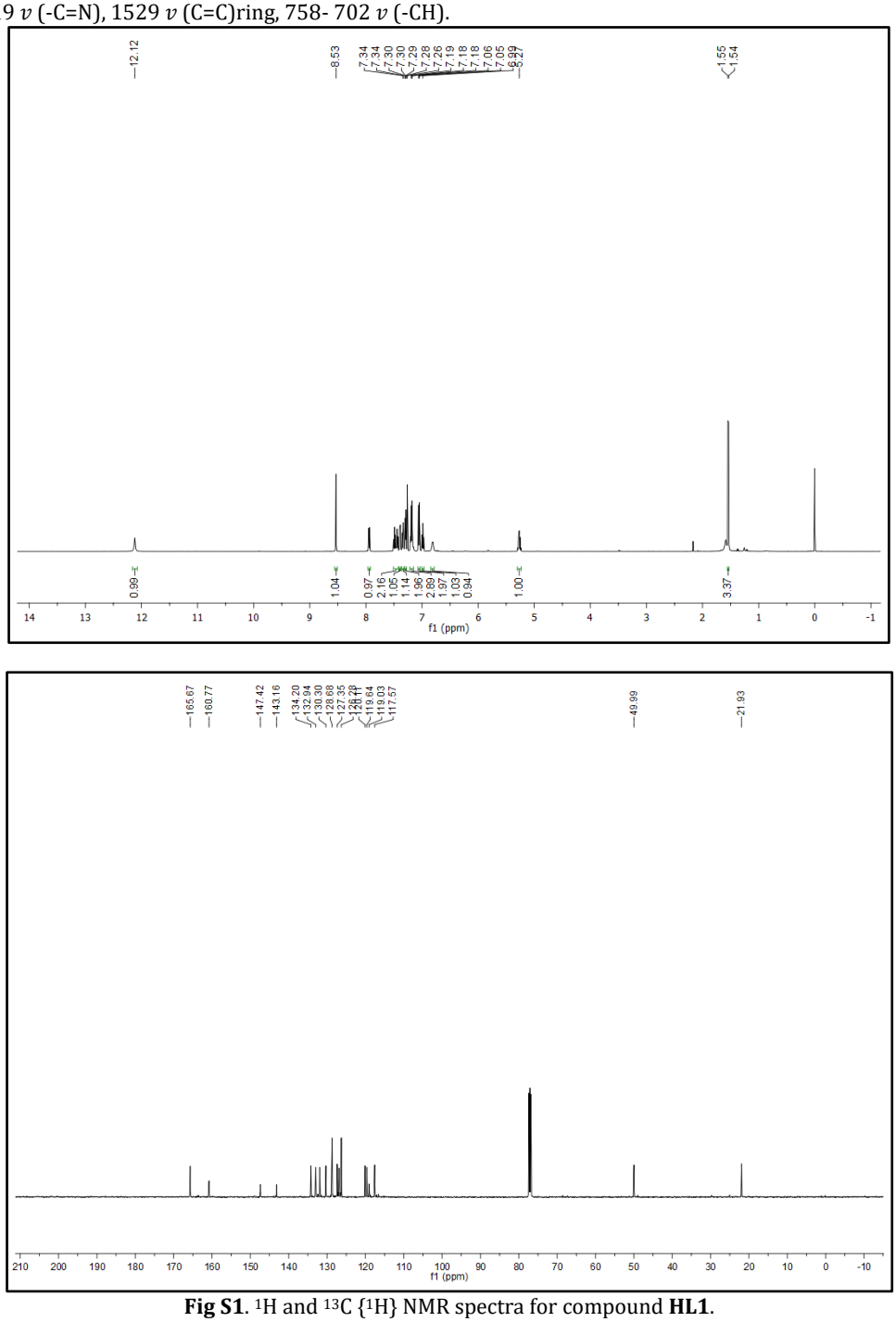

Fig S1. ^{1}H and ^{13}C {^{1}H} NMR spectra for compound **HL1**.

(*R*,*E*)-2-((3,5-di-*tert*-butyl-2-hydroxybenzylidene)amino)-*N*-(1-phenylethyl)benzamide (HL2).
Compound **HL2** has been synthesized by general procedure **A** using 3,5-di-*tert*-butyl-2-hydroxybenzaldehyde (1 mmol, 233.8 mg) and **1** (1 mmol, 240.3 mg). The compound was recrystallized in diethyl ether to get pure product. Yield: 47%. ^{1}H NMR (500 MHz, $CDCl_3$, δ ppm): 8.56 (d, *J* = 4.4 Hz, 1H), 8.02 (dd, *J* = 7.8, 1.3 Hz, 1H), 7.55 (d, *J* = 2.4 Hz, 1H), 7.49 (td, *J* = 7.7, 1.5 Hz, 1H), 7.40 – 7.29 (m, 4H), 7.24 (d, *J* = 2.4 Hz, 1H), 7.17 (tt, *J* = 4.3, 2.0 Hz, 3H), 7.11 (d, *J* = 7.3 Hz, 1H), 7.04 (dd, *J* = 7.9, 1.0 Hz, 1H), 5.28 (p, *J* = 7.0 Hz, 1H), 1.56 (d, *J* = 6.9 Hz, 3H), 1.49 (s, 9H), 1.36 (s, 9H). ^{13}C NMR (126 MHz, $CDCl_3$, δ ppm): 167.25, 165.66, 157.86, 147.71, 143.58, 141.54, 137.48, 132.11, 130.79, 129.41 (2C), 128.59, 127.69, 127.28, 126.78, 126.34 (2C), 120.36, 118.37, 50.10, 35.31, 34.41, 31.59 (3C), 29.61 (3C), 22.24. ESI-MS- (m/z): [M-H]- calcd for [$C_{30}H_{36}N_2O_2$], 455.2699 found, 455.2680. FTIR (KBr), cm-1: 3286 ν (-NH-)amide, 3063-2900 ν (=CH)ar 1627 ν (-C=O-)amide, 1588 ν (-C=N), 1434 ν(C=C)ring, 765- 702 ν (-CH).

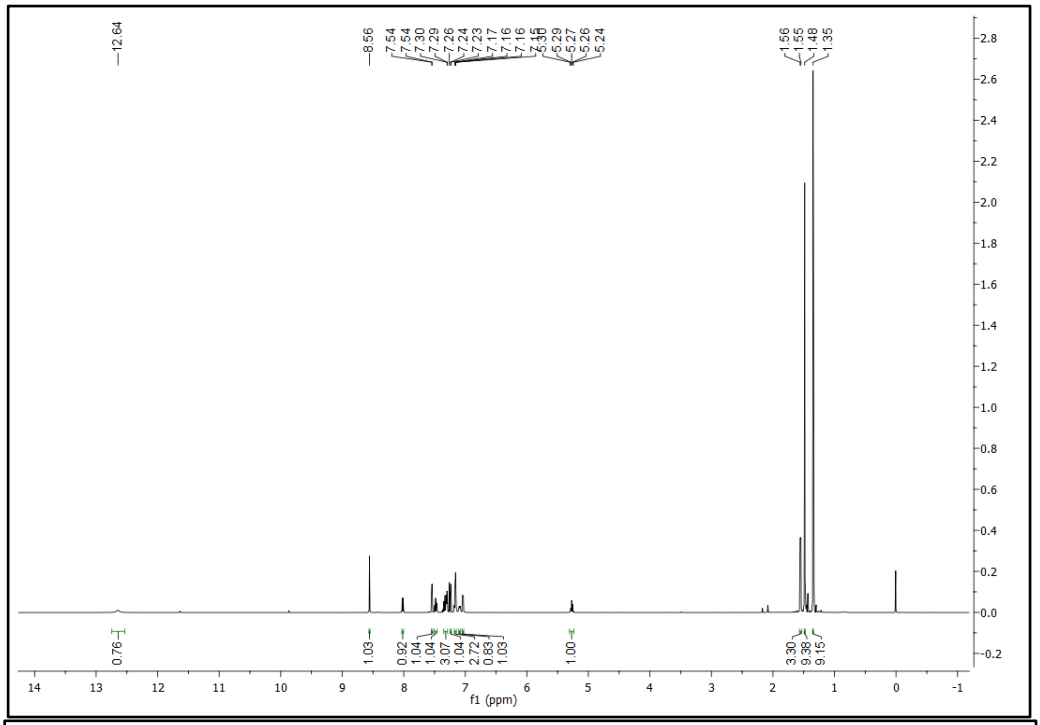

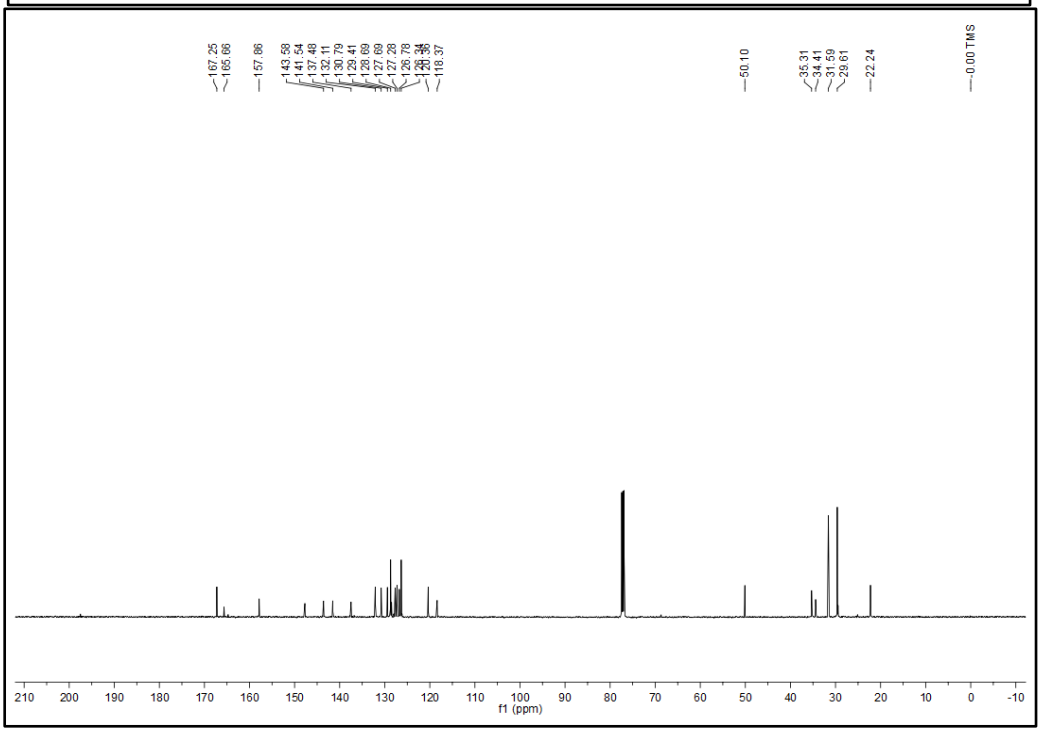

Fig S2. ^{1}H and ^{13}C $\{^{1}H\}$ NMR spectra for compound **HL2**.

(*R*,*E*)-2-((5-chloro-2-hydroxybenzylidene)amino)-*N*-(1-phenylethyl)benzamide (HL3).
Compound **HL3** has been synthesized by general procedure **A** using 5-chloro-2-hydroxybenzaldehyde (1 mmol, 156.7 mg) and **1** (1 mmol, 241.2 mg). Yield: 66%. ^{1}H NMR (500 MHz, $CDCl_3$, δ ppm): 8.45 (s), 7.83 (dd, *J* = 7.7, 1.4 Hz, 1H), 7.48 (td, *J* = 7.7, 1.5 Hz, 1H), 7.37 – 7.28 (m, 5H), 7.25 – 7.17 (m, 3H), 7.07 (dd, *J* = 7.9, 0.7 Hz, 1H), 6.98 (d, *J* = 8.8 Hz, 1H), 6.59 (d, *J* = 7.2 Hz, 1H), 5.27 (p, *J* = 7.0 Hz, 1H), 1.54 (d, *J* = 6.9 Hz, 3H). ^{13}C NMR (126 MHz, $CDCl_3$, δ ppm): 165.97, 163.97, 159.43, 146.72, 143.03, 133.85, 131.80 (2C), 129.95, 128.77 (2C), 127.40 (2C), 126.33 (2C), 124.19, 119.88, 119.20, 49.92, 21.83. ESI-MS^{+} (m/z): $[M-H]^{-}$ calcd for $[C_{22}H_{18}N_2O_2Cl]$, 377.1057; found, 377.1063. FTIR (KBr), cm-1: 3320 ν (-NH-)amide, 3056-2976 ν (=CH)ar, 1642 ν (-C=O-)amide, 1610 ν (-C=N), 1353 ν (C=C)ring, 704-703 ν (-CH).

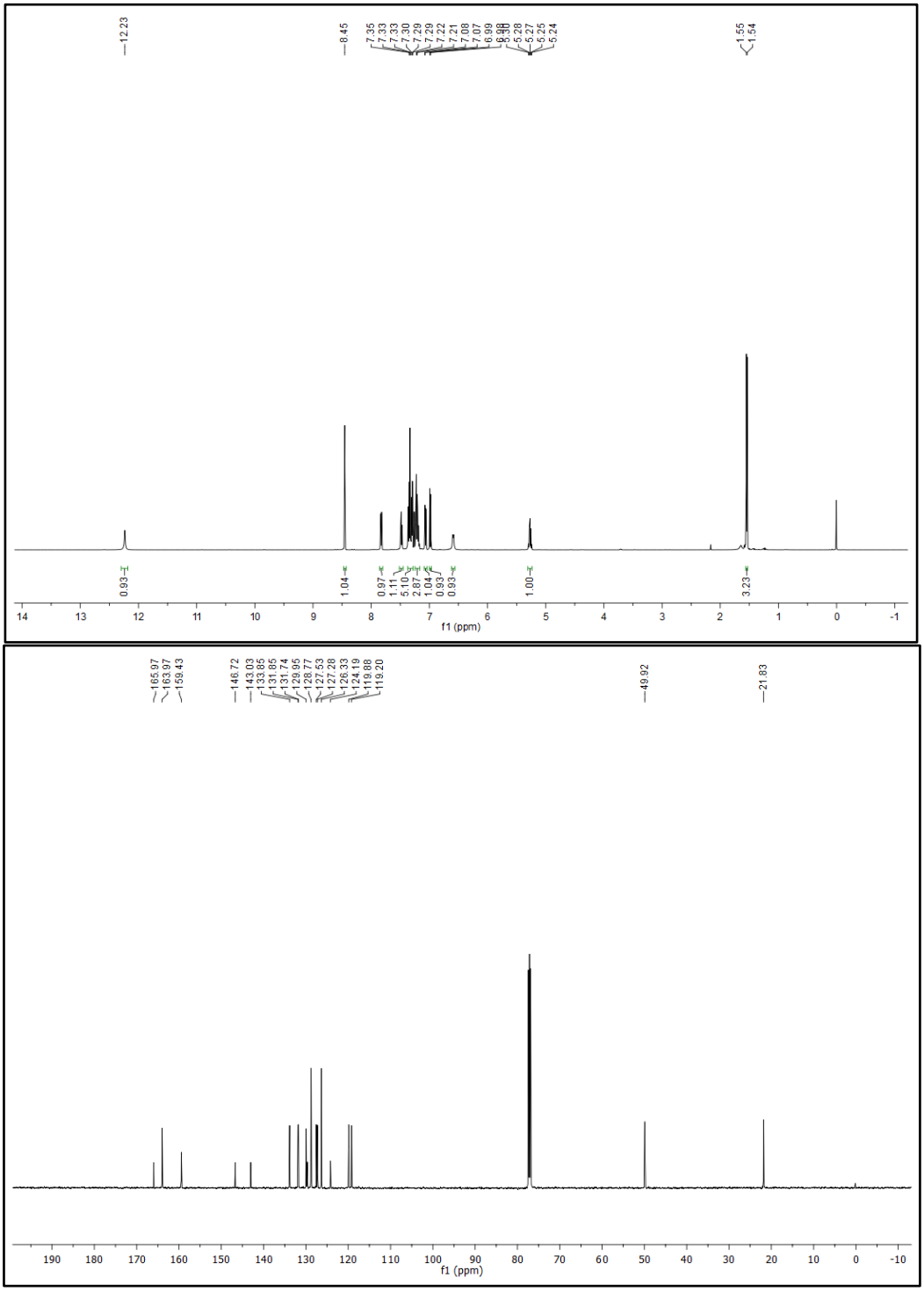

Fig S3. ^{1}H and ^{13}C {^{1}H} NMR spectra for compound **HL3**.

(*R*,*E*)-2-((5-bromo-2-hydroxybenzylidene)amino)-*N*-(1-phenylethyl)benzamide (HL4).
Compound **HL4** has been synthesized by general procedure **A** using 5-bromo-2-hydroxybenzaldehyde (1 mmol, 200.8 mg) and **1** (1 mmol, 240.3 mg). Yield: 58%. ^{1}H NMR (500 MHz, $CDCl_3$, δ ppm): 8.48 (s, 1H), 7.86 (dd, *J* = 7.7, 1.0 Hz, 1H), 7.56 – 7.49 (m, 3H), 7.40 – 7.30 (m, 3H), 7.30 – 7.21 (m, 3H), 7.10 (d, *J* = 7.8 Hz, 1H), 6.97 (d, *J* = 8.6 Hz, 1H), 6.59 (d, *J* = 6.9 Hz, 1H), 5.30 (p, *J* = 7.0 Hz, 1H), 1.58 (d, *J* = 6.9 Hz, 3H). ^{13}C NMR (126 MHz, $CDCl_3$, δ ppm): 166.08, 163.99, 160.02, 146.79, 143.14, 136.75, 134.89, 131.97, 129.93, 128.90, 127.54, 126.45, 120.58, 119.87, 111.14, 50.04, 21.95. ESI-MS^{+} (m/z): [M-H]$^{-}$ calcd for [$C_{22}H_{18}N_2O_2Br$], 421.0552; found, 421.0555. FTIR (KBr), cm-1: 3313 *v* (-NH-)amide, 3061-2976 *v* (=CH)ar, 1640 *v* (-C=O-)amide, 1524 *v* (-C=N), 1345 *v* (C=C)ring, 758- 702 *v* (-CH).

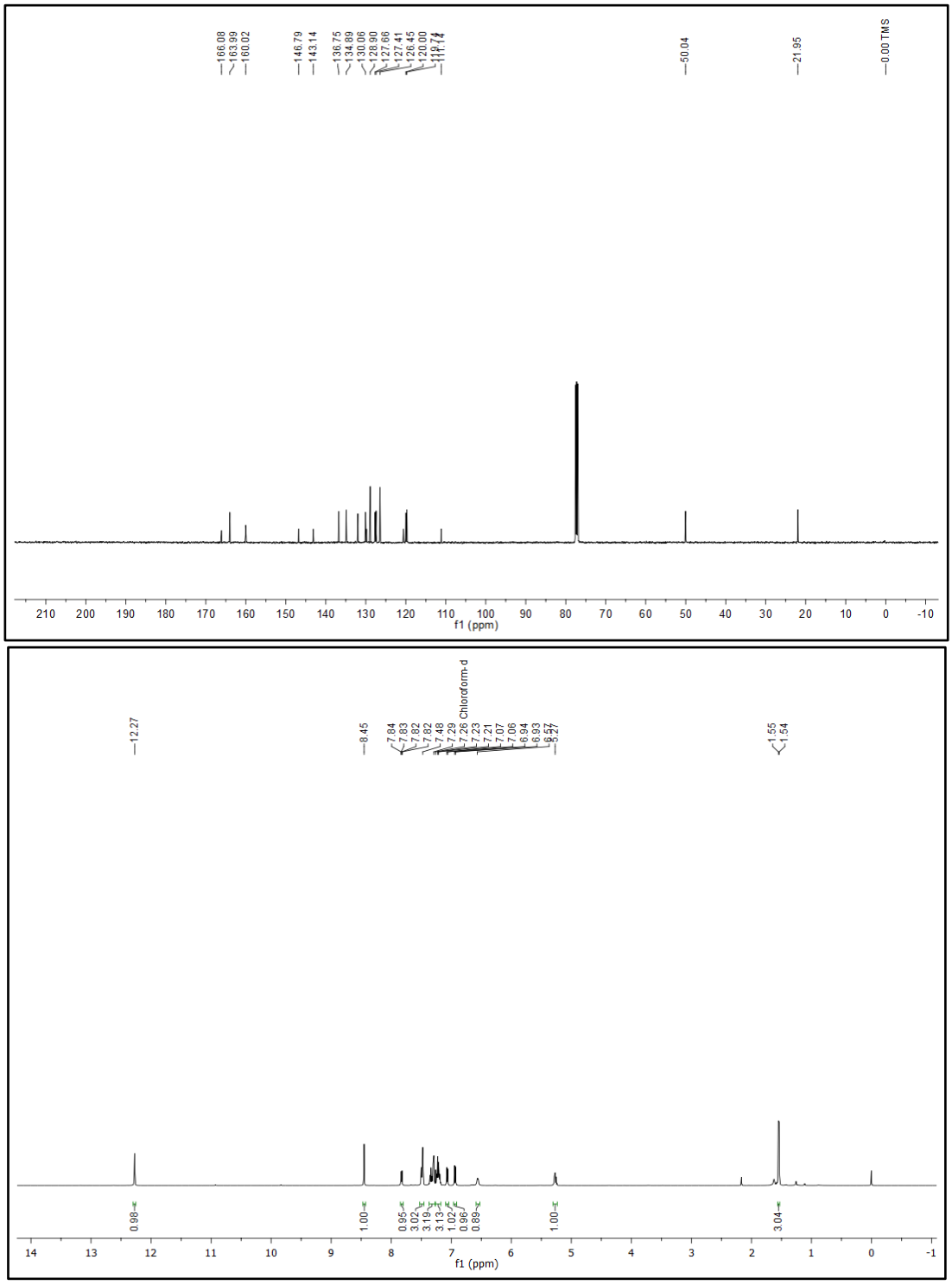

Fig S4. ^{1}H and ^{13}C {^{1}H} NMR spectra for compound **HL4**.

(*R*,*E*)-2-((5-fluoro-2-hydroxybenzylidene)amino)-*N*-(1-phenylethyl)benzamide (HL5).
Compound **HL5** has been synthesized by general procedure **A** using 5-fluoro-2-hydroxybenzaldehyde (1 mmol, 167.1 mg) and **1** (1.5 mmol, 356.3 mg). (Yield: 71%). ^{1}H NMR (500 MHz, DMSO-d_6, δ ppm): δ 11.99 (s, 1H), 8.46 (s, 1H), 7.86 (dd, *J* = 7.8, 1.4 Hz, 1H), 7.48 (td, *J* = 7.6, 1.4 Hz, 1H), 7.34 (dt, *J* = 8.1, 4.1 Hz, 1H), 7.29 (d, *J* = 6.7 Hz, 2H), 7.23 – 7.13 (m, 4H), 7.06 (dd, *J* = 8.2, 3.0 Hz, 2H), 6.99 (dd, *J* = 9.1, 4.4 Hz, 1H), 6.59 (d, *J* = 7.1 Hz, 1H), 5.26 (p, *J* = 6.9 Hz, 1H), 1.54 (d, *J* = 6.9 Hz, 3H). ^{13}C NMR (126 MHz, DMSO-d_6, δ ppm): δ 165.90, 164.12, 156.99, 156.69, 146.84, 143.04, 131.85, 130.00, 129.41, 128.72, 127.45, 127.18, 126.30, 121.35, 121.16, 119.87, 118.77, 117.54, 49.90, 21.83. ESI-MS^{+} (m/z): [M-H]$^{-}$ calcd for [$C_{22}H_{18}N_2O_2F$], 361.1352; found, 361.1381. FTIR (KBr), cm-1: 3290 ν (-NH-)amide, 3000-2900 ν (=CH)ar, 1636 ν (-C=O-)amide, 1617 ν (-C=N), 1472 ν (C=C)ring, 756- 699 ν (-CH).

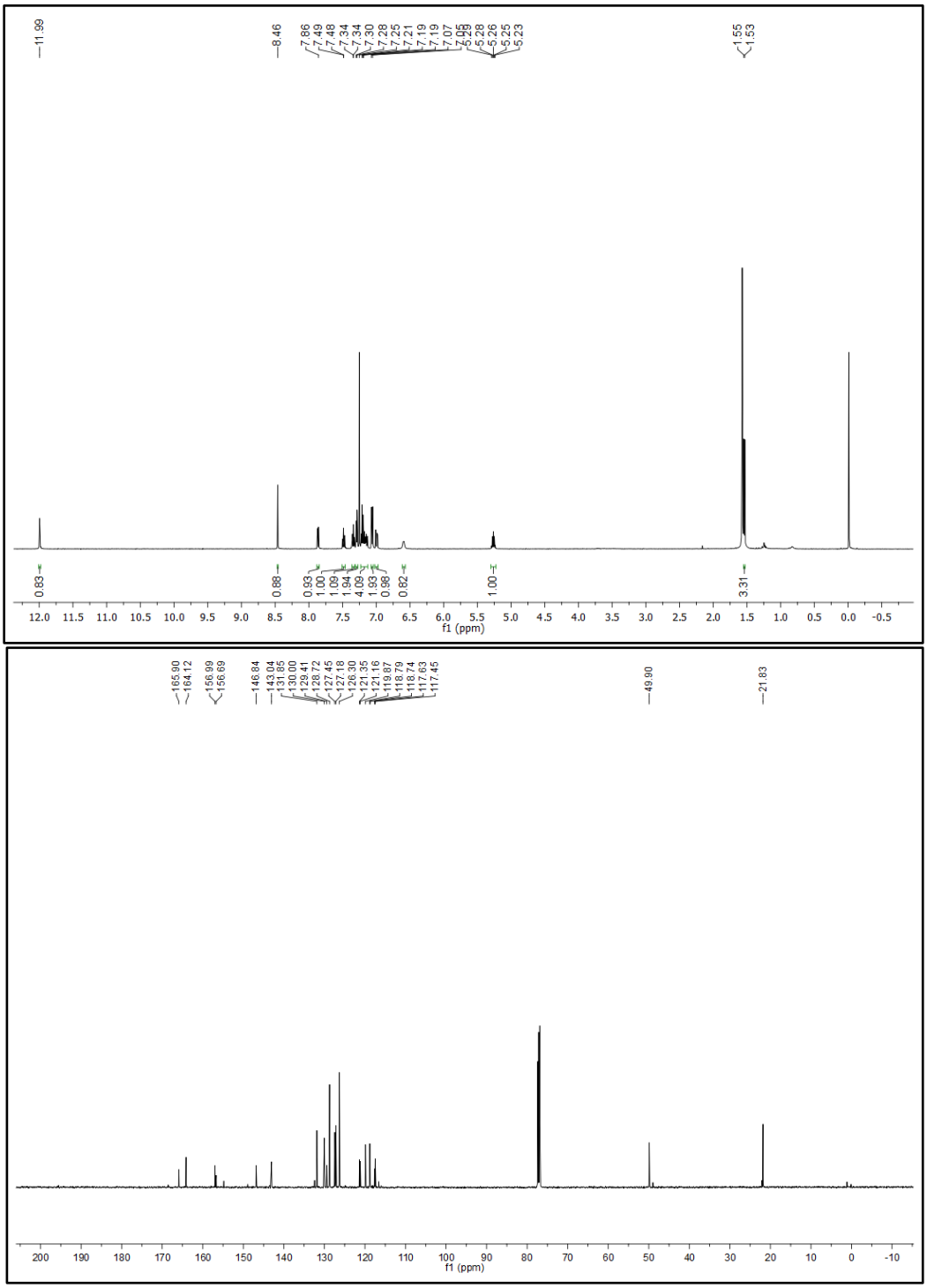

Fig S5. ^{1}H and ^{13}C {^{1}H} NMR spectra for compound **HL5**.

(*R*,*E*)-2-((2-hydroxy-5-nitrobenzylidene)amino)-*N*-(1-phenylethyl)benzamide (HL6).
Compound **HL6** has been synthesized by general procedure **A** using 5-nitro-2-hydroxybenzaldehyde (1 mmol, 167.1 mg) and **1** (1.5 mmol, 356.3 mg). Yield: 53%. ^{1}H NMR (500 MHz, DMSO-d_6, δ ppm): (s, 1H), 8.35 (d, J = 2.7 Hz, 1H), 8.29 (dd, J = 9.2, 2.7 Hz, 1H), 7.70 (dd, J = 7.7, 1.4 Hz, 1H), 7.55 – 7.51 (m, 1H), 7.39 (d, J = 7.7 Hz, 1H), 7.34 (s, 2H), 7.29 (s, 1H), 7.25 – 7.19 (m, 2H), 7.11 (d, J = 9.2 Hz, 1H), 6.22 (s, 1H), 5.35 – 5.28 (m, 1H), 1.11 (s, 3H). ^{13}C NMR (126 MHz, DMSO-d_6, δ ppm): 168.71, 167.73, 166.51, 165.50, 161.98, 145.98, 138.93, 132.27, 131.76, 129.40, 128.45, 127.29, 126.61, 120.01, 116.68, 115.11, 48.81, 46.86, 22.96. ESI-MS- (m/z): [M-H]- calcd for [$C_{22}H_{18}N_3O_4$], 388.1297; found, 388.1299. FTIR (KBr), cm-1: 3286 v (-NH-)amide, 3000-2900 v (=CH)ar, 1621 v (-C=O-)amide, 1532 v (-C=N), 1334 v (C=C)ring, 753- 698 v (-CH).

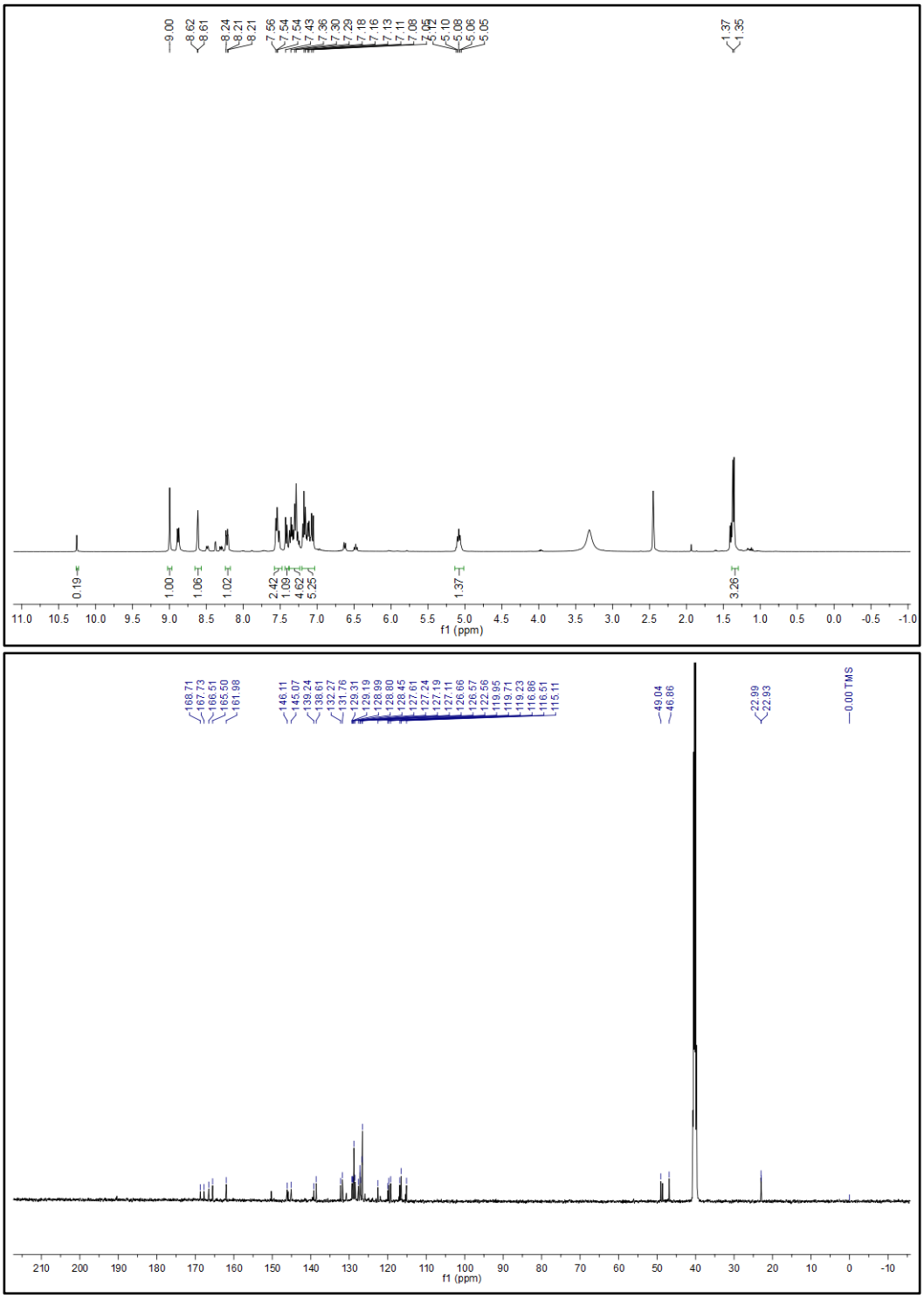

Fig S6. ^{1}H and ^{13}C {^{1}H} NMR spectra for compound **HL6**.

(*R*,*E*)-4-hydroxy-3-(((2-((1-phenylethyl)carbamoyl)phenyl)imino)methyl)benzoic acid (HL7).
Compound **HL7** has been synthesized by general procedure **A** using 3-formyl-4-hydroxybenzoic acid (2 mmol, 332.2 mg) and **1** (2 mmol, 481.9 mg). Yield: 60%. ^{1}H NMR (500 MHz, DMSO-d_6, δ ppm): 13.07 (s, 1H), 12.75 (s, 1H), 8.99 – 8.90 (m, 2H), 8.36 (d, J = 2.1 Hz, 1H), 7.98 (dd, J = 8.5, 2.1 Hz, 1H), 7.56 (t, J = 7.3 Hz, 2H), 7.44 (d, J = 7.9 Hz, 1H), 7.35 (dt, J = 20.5, 7.8 Hz, 3H), 7.20 (dt, J = 30.1, 7.2 Hz, 3H), 7.04 (d, J = 8.6 Hz, 1H), 5.11 (p, J = 7.0 Hz, 1H), 1.40 (d, J = 7.0 Hz, 3H).ESI-MS- (m/z): [M-H]- calcd for [$C_{23}H_{19}N_2O_4$], 387.1345; found, 387.1342. FTIR (KBr), cm-1: 3273 v (-NH-)amide, 3000-2900 v (=CH)ar, 1686 v (-C=O-)amide, 1611 v (-C=N), 1444 v (C=C)ring, 756- 695 v (-CH).

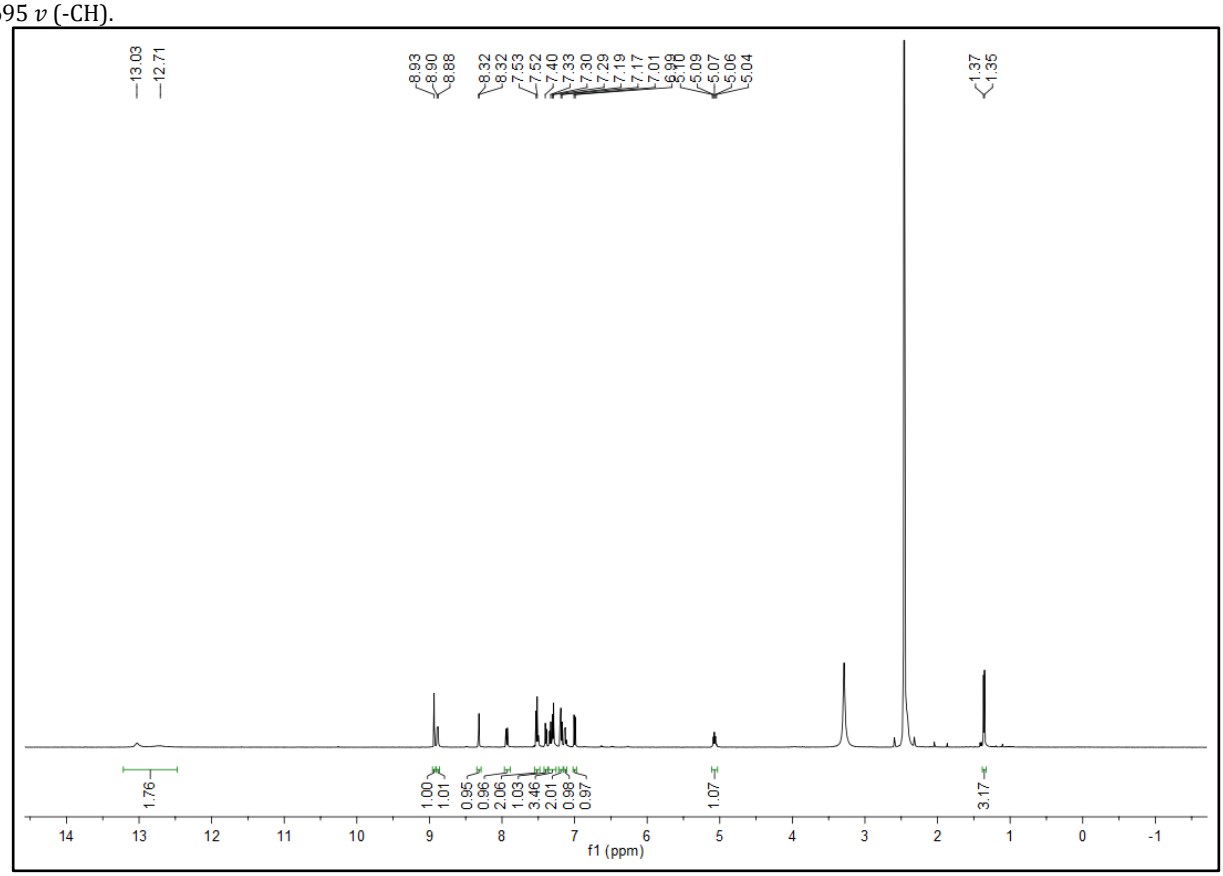

Fig S7. ^{1}H and ^{13}C {^{1}H} NMR spectra for compound **HL7**.

(*R*,*E*)-2-((4-(diethylamino)-2-hydroxybenzylidene)amino)-*N*-(1-phenylethyl)benzamide (HL8).
Compound **HL8** has been synthesized by general procedure **A** using 4-(diethylamino)-2-hydroxybenzaldehyde (1 mmol, 194.3 mg) and **1** (1 mmol, 240.3 mg). Yield: 53%. ^{1}H NMR (500 MHz, $CDCl_3$, δ ppm): 8.37 (s, 1H), 8.16 (dd, *J* = 7.8, 1.5 Hz, 1H), 7.67 (d, *J* = 7.3 Hz, 1H), 7.52 (td, *J* = 7.7, 1.6 Hz, 1H), 7.40 (dd, *J* = 5.3, 3.4 Hz, 2H), 7.34 (ddd, *J* = 9.2, 5.9, 1.1 Hz, 1H), 7.31 – 7.27 (m, 2H), 7.25 – 7.22 (m, 1H), 7.05 (dd, *J* = 7.9, 0.9 Hz, 1H), 6.37 (dt, *J* = 6.2, 3.1 Hz, 1H), 6.30 (d, *J* = 2.4 Hz, 1H), 5.35 (p, *J* = 7.0 Hz, 1H), 3.51 (p, *J* = 7.1 Hz, 4H), 1.63 (d, *J* = 6.9 Hz, 3H), 1.32 (t, *J* = 7.1 Hz, 6H). ^{13}C NMR (126 MHz, $CDCl_3$, δ ppm): 176.14, 163.44, 134.65, 131.43, 128.52, 127.12, 126.19, 125.56, 120.50, 104.35, 97.60, 49.99, 44.73, 22.29, 12.70. ESI-MS+ (m/z): [M+H]+ calcd for [$C_{26}H_{28}N_3O_2$], 416.2338; found, 416.2331. FTIR (KBr), cm-1: 3273 *v* (-NH-)amide, 2962 (=CH)ar, 1636 *v* (-C=O-)amide, 1571 *v* (-C=N), 1339 *v* (C=C)ring, 763- 699 *v* (-CH).

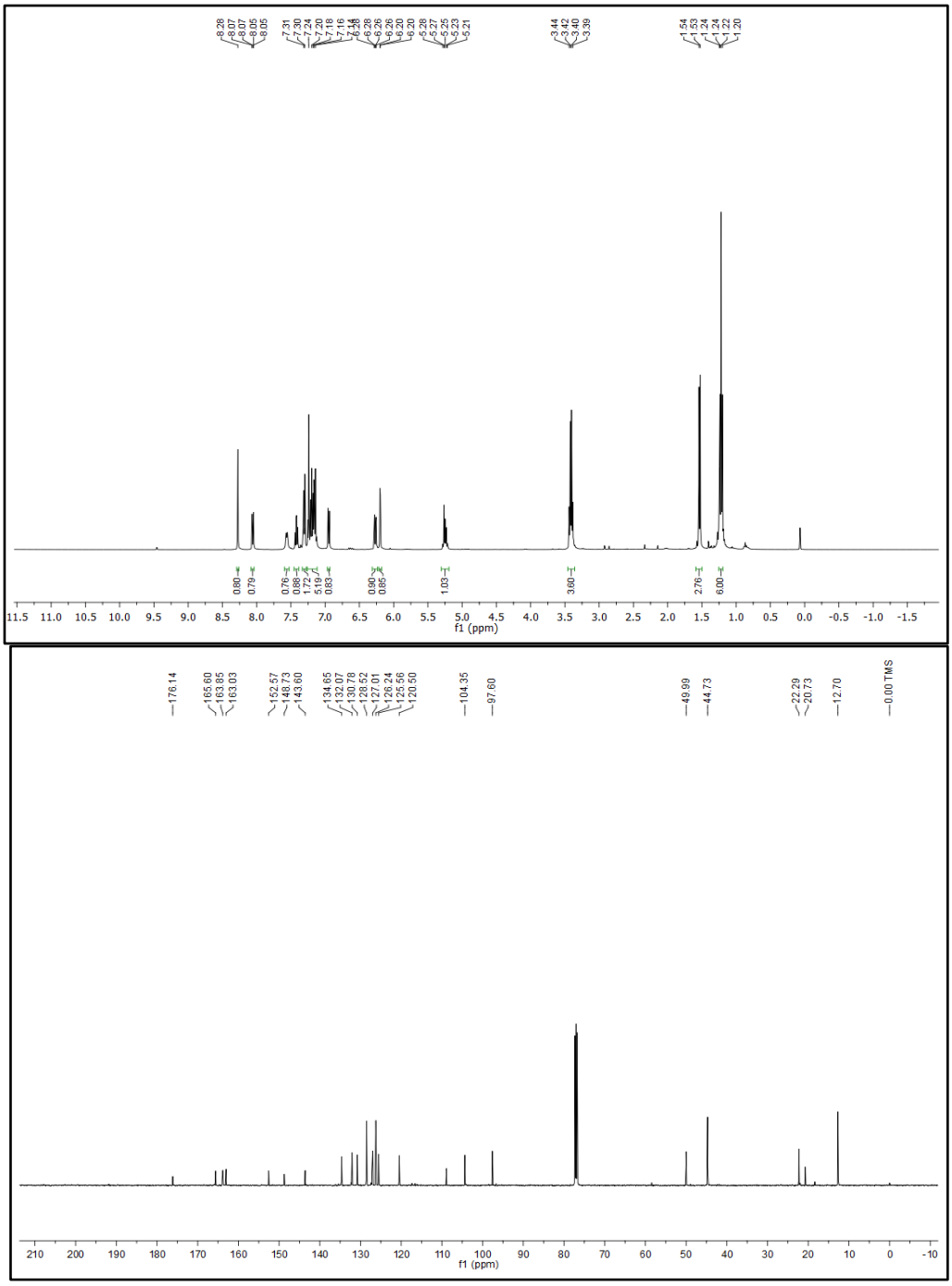

Fig S8. ^{1}H and ^{13}C $\{^{1}H\}$ NMR spectra for compound **HL8**.

Synthesis of copper complex. In a 25 ml round bottom flask, ligand HL1-HL8 (0.2 mmol) was dissolved in THF (10 ml). Afterwards, a solution of $Cu(OAc)_2 \bullet H_2O$ (0.12 mmol) in THF (5 ml) was added to the ligand solution in dropwise and stirred it for 1 h at room temperature. A sudden colour transition from orange to green/brown was observed. The progress of the reaction was monitored by UV-Visible absorption spectroscopy. The solvent was then removed through rotavapor, and the crude green/brown solid was then dissolved in DCM and filtered via celite plug. The compound then washed with diethyl ether to get the powdered green copper complex.

Cu(L1)$_2$. Followed same procedure as above with ligand **HL1** (0.2 mmol, 67.3 mg) and $Cu(OAc)_2.H_2O$ (0.12 mmol, 24.6 mg). (Yield: 76%) UV−Vis (Methanol) λ_{max} (ε), 283 nm (1247 mol^{-1} L cm^{-1}), 412 nm (5808 mol^{-1} L cm^{-1}),), 708 nm (208 mol^{-1} L cm^{-1}).ESI-MS^+ (m/z): $[M+H]^+$ calcd for $[C_{44}H_{39}CuN_4O_4]$, 750.2267; found, 750.2254. FTIR (KBr), cm^{-1}: 3227 ν (-NH-)$_{amide}$, 3058-2936 ν (=CH)$_{ar}$, 1611 ν (-C=O-)$_{amide}$, 1522 ν (-C=N), 1383 ν (C=C)$_{ring}$, 755- 697 ν (-CH).**Cu(L2)$_2$**. Followed same procedure as above with ligand **HL2** (0.2 mmol, 91.1 mg) and $Cu(OAc)_2.H_2O$ (0.12 mmol, 24.9 mg). (Yield: 67%) UV−Vis (Methanol) λ_{max} (ε), 302 nm (26450 mol^{-1} L cm^{-1}), 433 nm (10916 mol^{-1} L cm^{-1}), 705 nm (192 mol^{-1} L cm^{-1}).. ESI-MS^+ (m/z): $[M+H]^+$ calcd for $[C_{60}H_{71}CuN_4O_4]$, 974.4771; found, 974.4767. FTIR (KBr), cm^{-1}: 3065 ν (-NH-)$_{amide}$, 2964 ν (=CH)$_{ar}$, 1598 ν (-C=O-)$_{amide}$, 1533 ν (-C=N), 1306 ν (C=C)$_{ring}$, 748- 706 ν (-CH).

Cu(L3)$_2$. Followed same procedure as above with ligand **HL3** (0.2 mmol, 76.1 mg) and Cu(OAc)$_2$.H2O (0.12 mmol, 24.7 mg).. (Yield: 70%) UV−Vis (Methanol) λ_{max} (ε), 315 nm (7908 mol^{-1} L cm^{-1}), 424 nm (6216 mol^{-1} L cm^{-1}), 703 nm (132 mol^{-1} L cm^{-1}).. ESI-MS^+ (m/z): $[M+H]^+$ calcd for $[C_{44}H_{37}Cl_2CuN_4O_4]$, 818.1488; found, 818.1477. FTIR (KBr), cm^{-1}: 3313 ν (-NH-)$_{amide}$, 3061-2978 ν (=CH)$_{ar}$, 1608 ν (-C=O-)$_{amide}$, 1526 ν (-C=N), 1313 ν (C=C)$_{ring}$, 766- 705 ν (-CH).

Cu(L4)$_2$. Followed same procedure as above with ligand **HL4** (0.2 mmol, 84.7 mg) and Cu(OAc)2.H_2O (0.12 mmol, 25.5 mg). (Yield: 71%) UV−Vis (Methanol) λ_{max} (ε), 243 nm (43520 mol^{-1} L cm^{-1}), 423 nm (8481 mol^{-1} L cm^{-1}), 706 nm (276 mol^{-1} L cm^{-1}).. ESI-MS^+ (m/z): $[M+H]^+$ calcd for $[C_{44}H_{37}Br_2CuN_4O_4]$, 908.0457; found, 908.0424. FTIR (KBr), cm^{-1}: 3223 ν (-NH-)$_{amide}$, 2972-2915 ν (=CH)$_{ar}$, 1619 ν (-C=O-)$_{amide}$, 1510 ν (-C=N), 1376 ν (C=C)$_{ring}$, 754- 693 ν (-CH).

Cu(L5)$_2$. Followed same procedure as above with ligand **HL5** (0.2 mmol, 71.9 mg) and $Cu(OAc)_2.H_2O$ (0.12 mmol, 24.7 mg). (Yield: 78%) UV−Vis (Methanol) λ_{max} (ε), 282 nm (19063 mol^{-1} L cm^{-1}), 427 nm (8726 mol^{-1} L cm^{-1}), 703 nm (324 mol^{-1} L cm^{-1}). ESI-MS^+ (m/z): $[M+H]^+$ calcd for $[C_{44}H_{37}F_2CuN_4O_4]$, 786.2089; found, 786.2057. FTIR (KBr), cm^{-1}: 3231 ν (-NH-)$_{amide}$, 3000-2900 ν (=CH)$_{ar}$, 1609 ν (-C=O-)$_{amide}$, 1524 ν (-C=N), 1453 ν (C=C)$_{ring}$, 756- 699 ν (-CH).

Cu(L6)$_2$. Followed same procedure as above with ligand **HL6** (0.2 mmol, 80.6 mg) and $Cu(OAc)_2.H_2O$ (0.12 mmol, 24.3 mg). (Yield: 54%) UV−Vis (Methanol) λ_{max} (ε), 370 nm (19685 mol^{-1} L cm^{-1}), 706 nm (84 mol^{-1} L cm^{-1}). ESI-MS^+ (m/z): $[M+H]^+$ calcd for $[C_{44}H_{39}CuN_4O_4]$, 750.2267; found, 750.2254. FTIR (KBr), cm^{-1}: 3256 ν (-NH-)$_{amide}$, 2917-2841 ν (=CH)$_{ar}$, 1608 ν (-C=O-)$_{amide}$, 1538 ν (-C=N), 1467 ν (C=C)$_{ring}$, 766- 692 ν (-CH).

Cu(L7)$_2$. Followed same procedure as above with ligand **HL7** (0.2 mmol, 77.8 mg) and $Cu(OAc)_2.H_2O$ (0.12 mmol, 24 mg). . (Yield: 57%) UV−Vis (Methanol) λ_{max} (ε), 257 nm (27380 mol^{-1} L cm^{-1}), 402 nm (7395 mol^{-1} L cm^{-1}), 699 nm (96 mol^{-1} L cm^{-1}). ESI-MS^+ (m/z): $[M+H]^+$ calcd for $[C_{44}H_{39}CuN_4O_4]$,840.1969; found, 840.1972. FTIR (KBr), cm^{-1}: 3256 ν (-NH-)$_{amide}$, 2917-2841 ν (=CH)$_{ar}$, 1608 ν (-C=O-)$_{amide}$, 1538 ν (-C=N), 1467 ν (C=C)$_{ring}$, 766- 692 ν (-CH).

Cu(L8)$_2$. Followed same procedure as above with ligand **HL8** (0.2 mmol, 83.18 mg) and $Cu(OAc)_2.H_2O$ (0.12 mmol, 24.5 mg). (Yield: 69%) UV−Vis (Methanol) λ_{max} (ε), 235 nm (31913 mol^{-1} L cm^{-1}), 412 nm (40172 mol^{-1} L cm^{-1}), , 699 nm (276 mol^{-1} L cm^{-1}).. ESI-MS^+ (m/z): $[M+H]^+$ calcd for $[C_{52}H_{57}CuN_6O_4]$, 892.3737; found, 893.3722. FTIR (KBr), cm^{-1}: 3221 ν (-NH-)$_{amide}$, 2972 ν (=CH)$_{ar}$, 1566 ν (-C=O-)$_{amide}$, 1486 ν (-C=N), 1348 ν (C=C)$_{ring}$, 756- 702 ν (-CH).

Figure S9: Characterization ESI-MS and HPLC of $Cu(L1)_2$

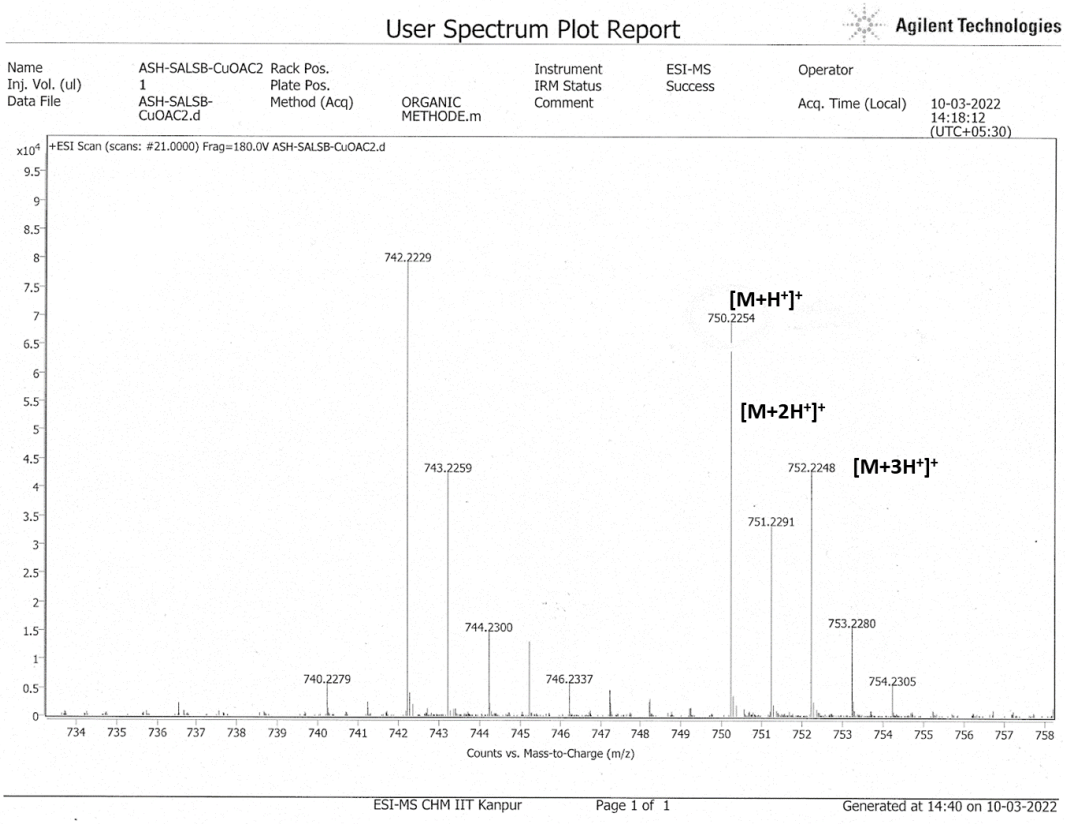

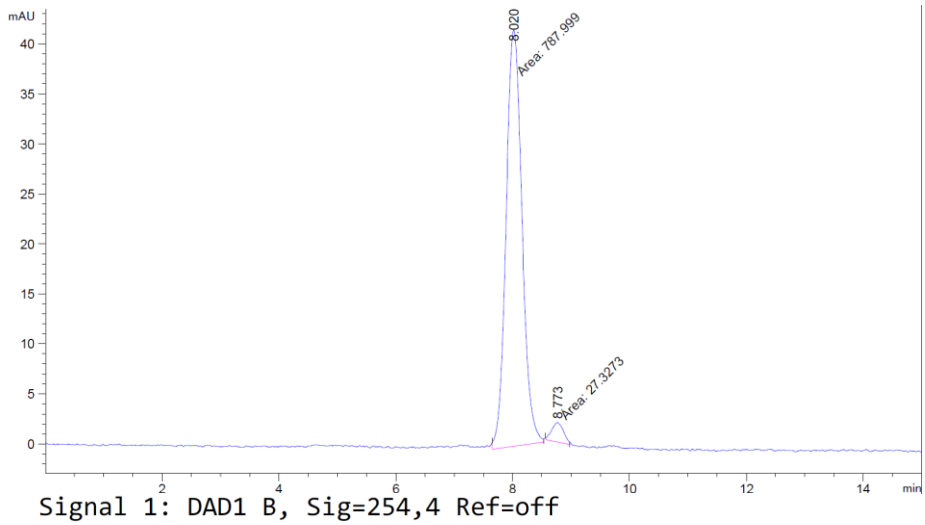

Signal 1: DAD1 B, Sig=254,4 Ref=off

Peak #	RetTime [min]	Type	Width [min]	Area [mAU*s]	Height [mAU]	Area %
1	8.020	MM	0.3154	787.99945	41.63994	96.6483
2	8.773	MM	0.2342	27.32733	1.94456	3.3517

Characterization ESI-MS and HPLC of HL1

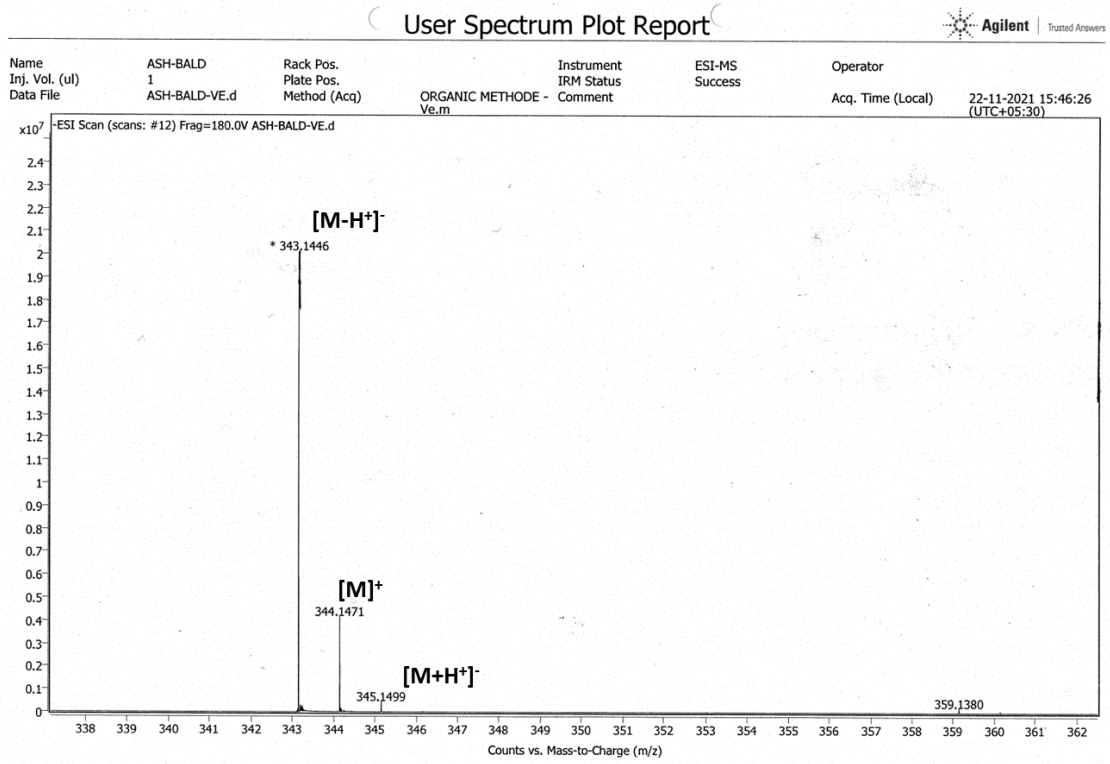

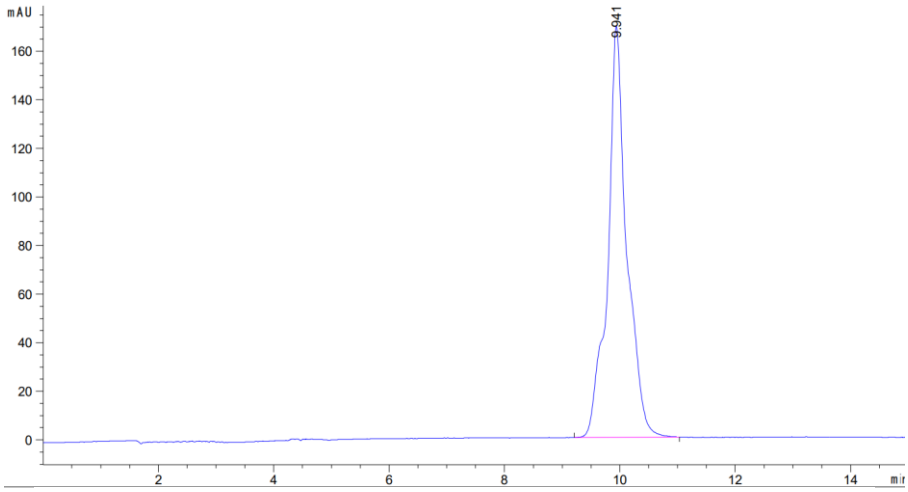

Signal 1: DAD1 B, Sig=254,4 Ref=off

Peak #	RetTime [min]	Type	Width [min]	Area [mAU*s]	Height [mAU]	Area %
1	9.941	BB	0.3202	3889.67334	169.18007	100.0000

Figure S10: Characterization ESI-MS and HPLC of $Cu(L2)_2$

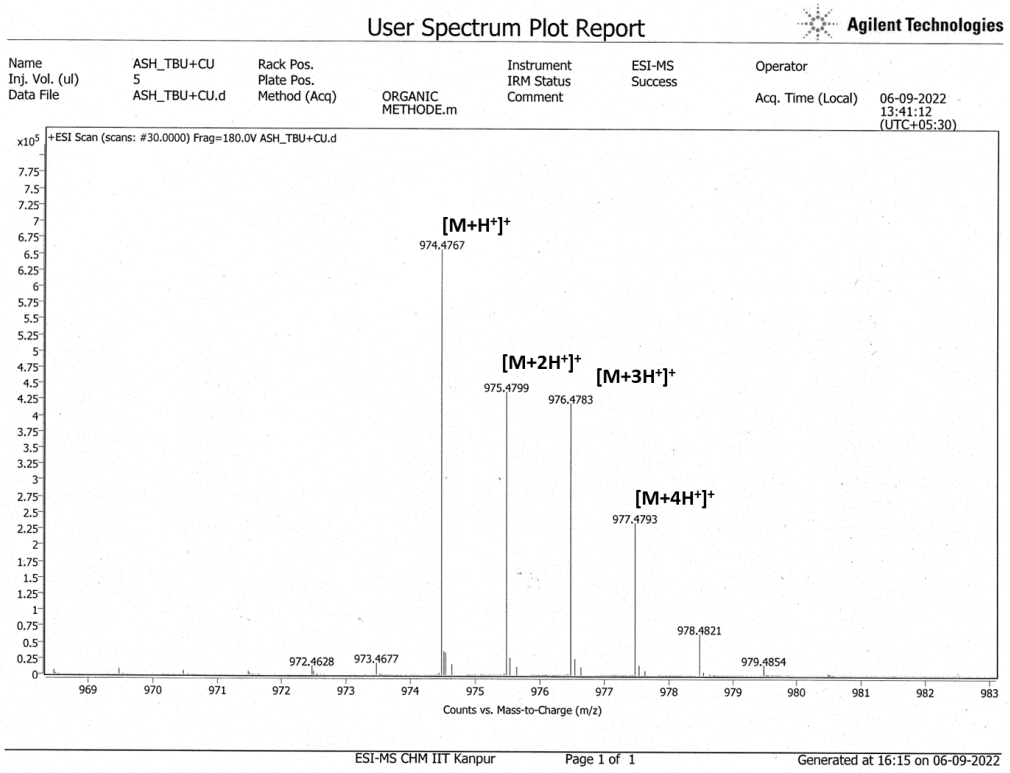

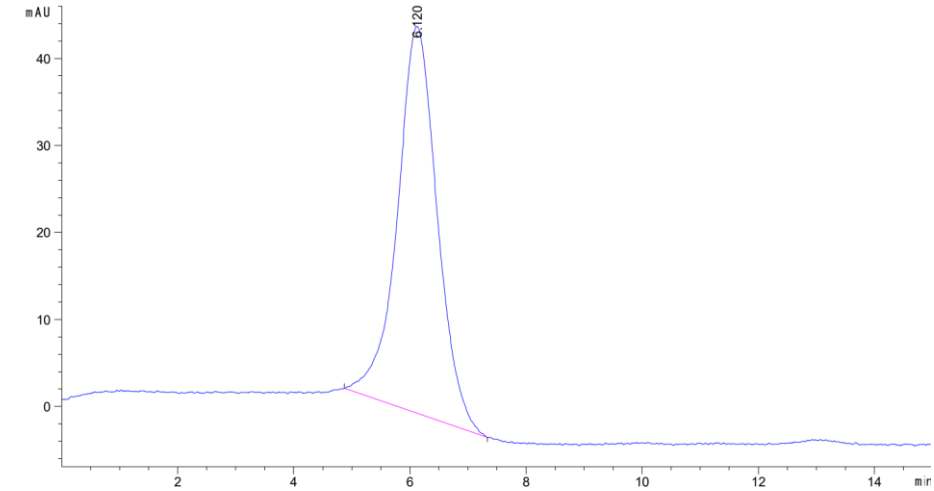

Signal 1: DAD1 B, Sig=254,4 Ref=off

Peak #	RetTime [min]	Type	Width [min]	Area [mAU*s]	Height [mAU]	Area %
1	6.120	BB	0.6205	2126.85034	44.42670	100.0000

Characterization ESI-MS and HPLC of HL2

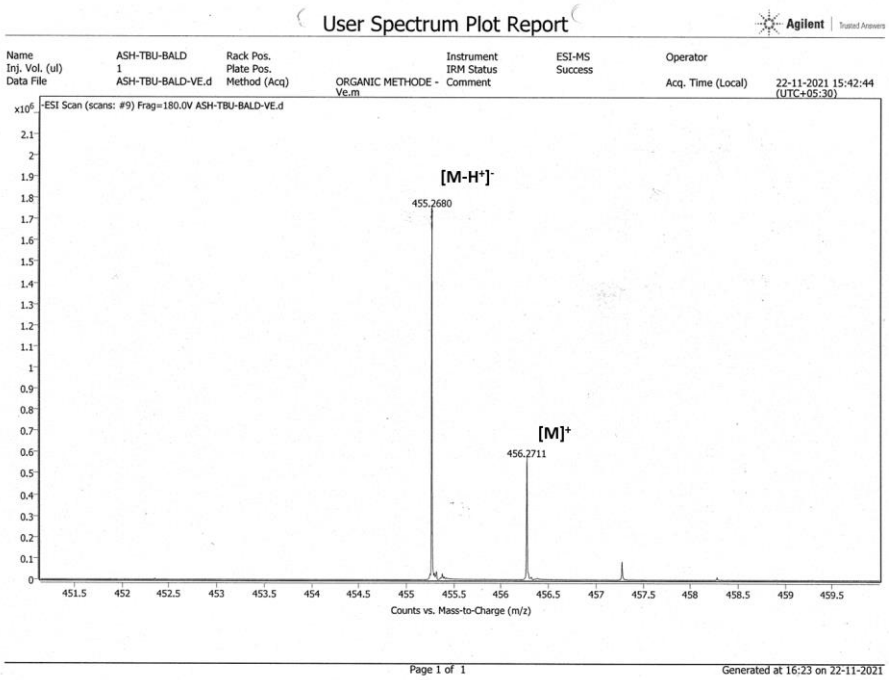

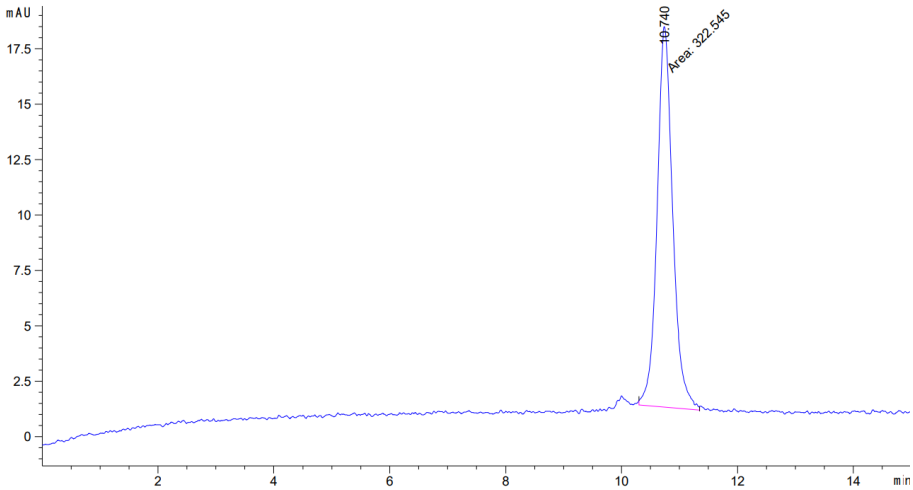

Signal 1: DAD1 B, Sig=254,4 Ref=off

Peak #	RetTime [min]	Type	Width [min]	Area [mAU*s]	Height [mAU]	Area %
1	10.740	MM	0.3131	322.54471	17.17070	100.0000

Figure S11: Characterization ESI-MS and HPLC of $Cu(L3)_2$

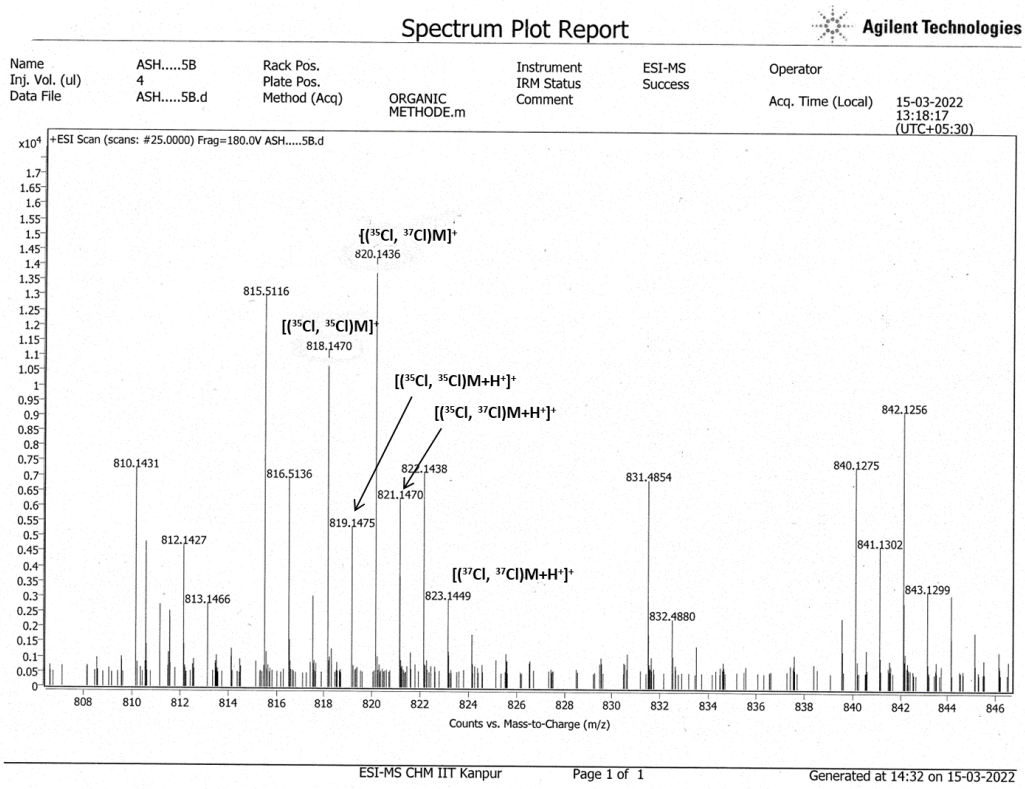

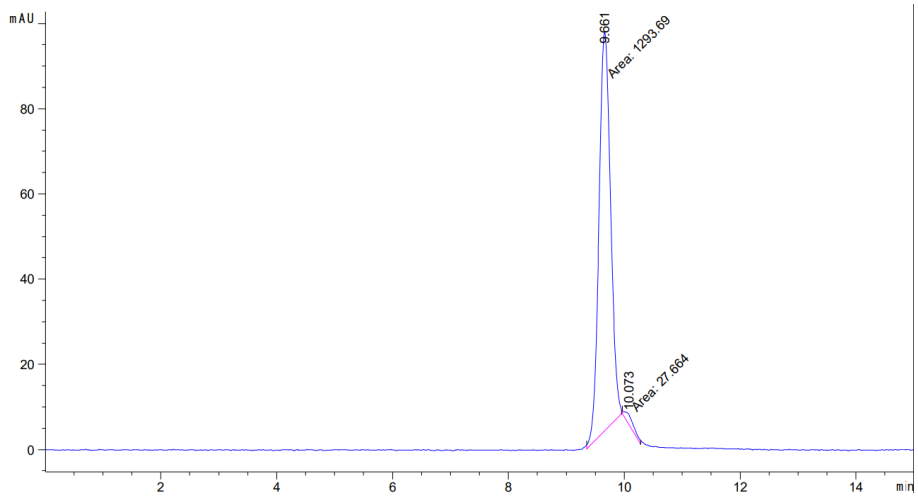

Signal 1: DAD1 B, Sig=254,4 Ref=off

Peak #	RetTime [min]	Type	Width [min]	Area [mAU*s]	Height [mAU]	Area %
1	9.661	MM	0.2305	1293.69250	93.55347	97.9064
2	10.073	MM	0.2019	27.66400	2.28311	2.0936

Characterization ESI-MS and HPLC of HL3

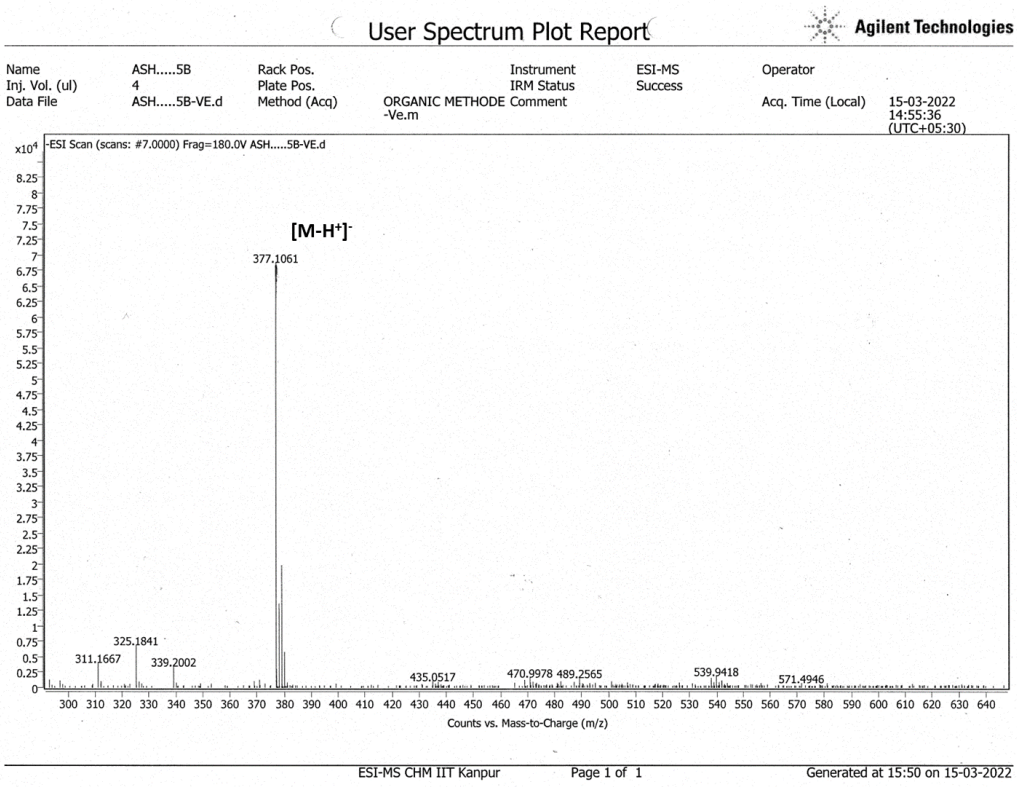

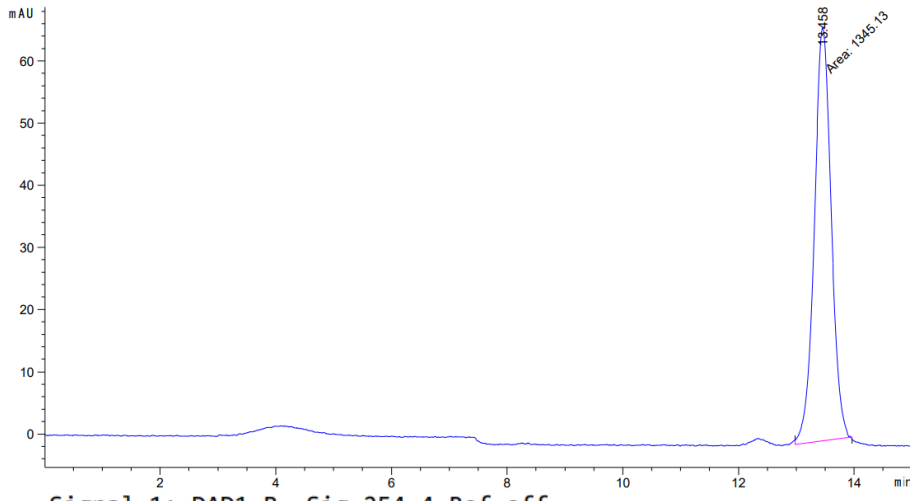

Signal 1: DAD1 B, Sig=254,4 Ref=off

Peak #	RetTime [min]	Type	Width [min]	Area [mAU*s]	Height [mAU]	Area %
1	13.458	MM	0.3373	1345.13049	66.45680	100.0000

Figure S12: Characterization ESI-MS and HPLC of $Cu(L4)_2$

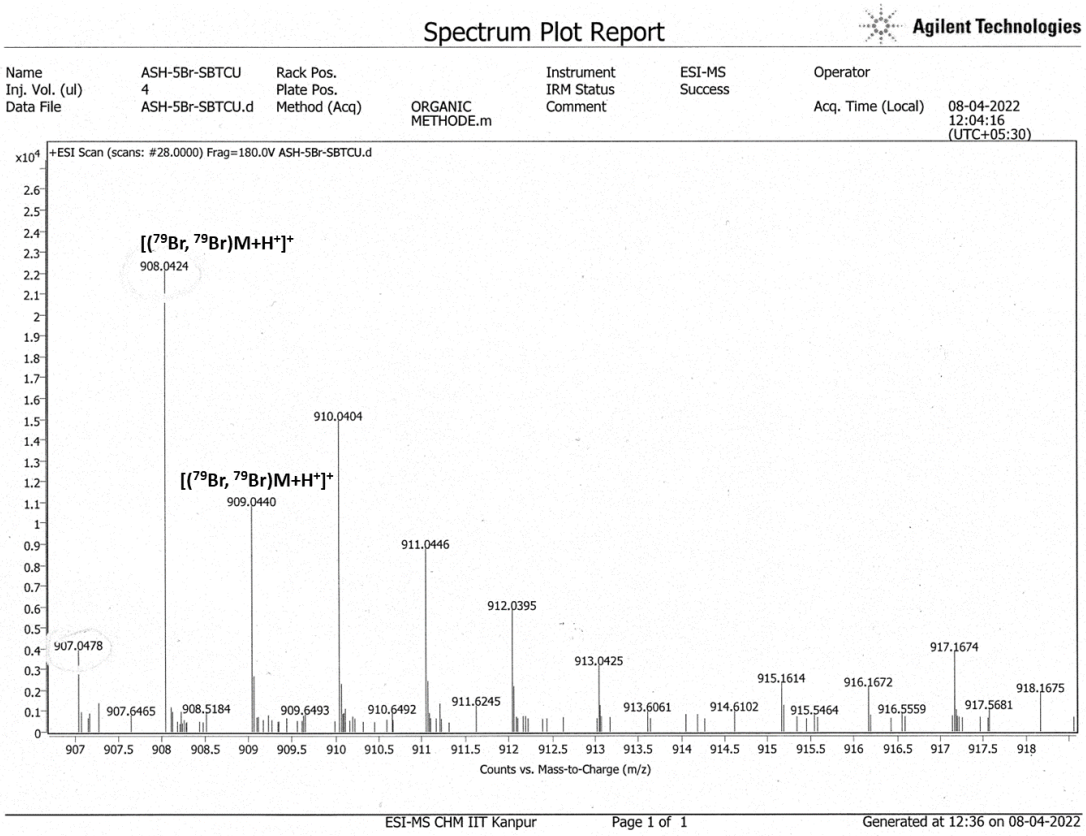

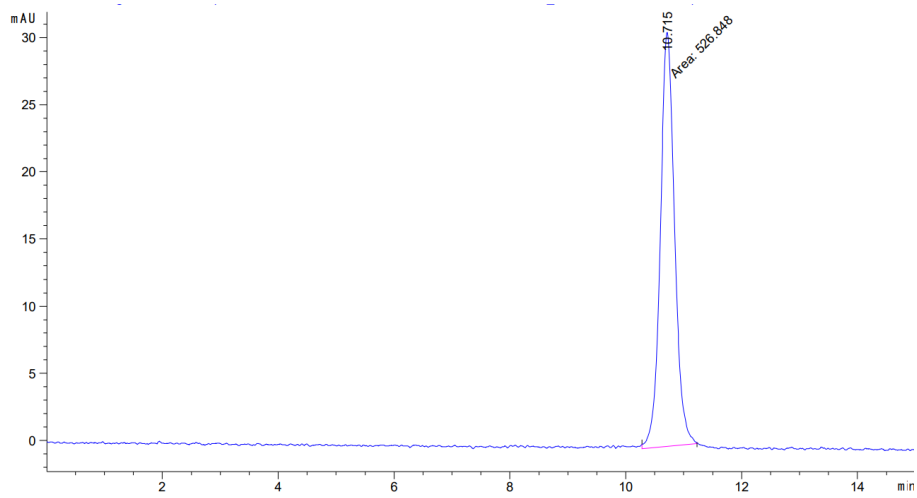

Signal 1: DAD1 B, Sig=254,4 Ref=off

Peak #	RetTime [min]	Type	Width [min]	Area [mAU*s]	Height [mAU]	Area %
1	10.715	MM	0.2845	526.84766	30.86158	100.0000

Characterization ESI-MS and HPLC of HL4

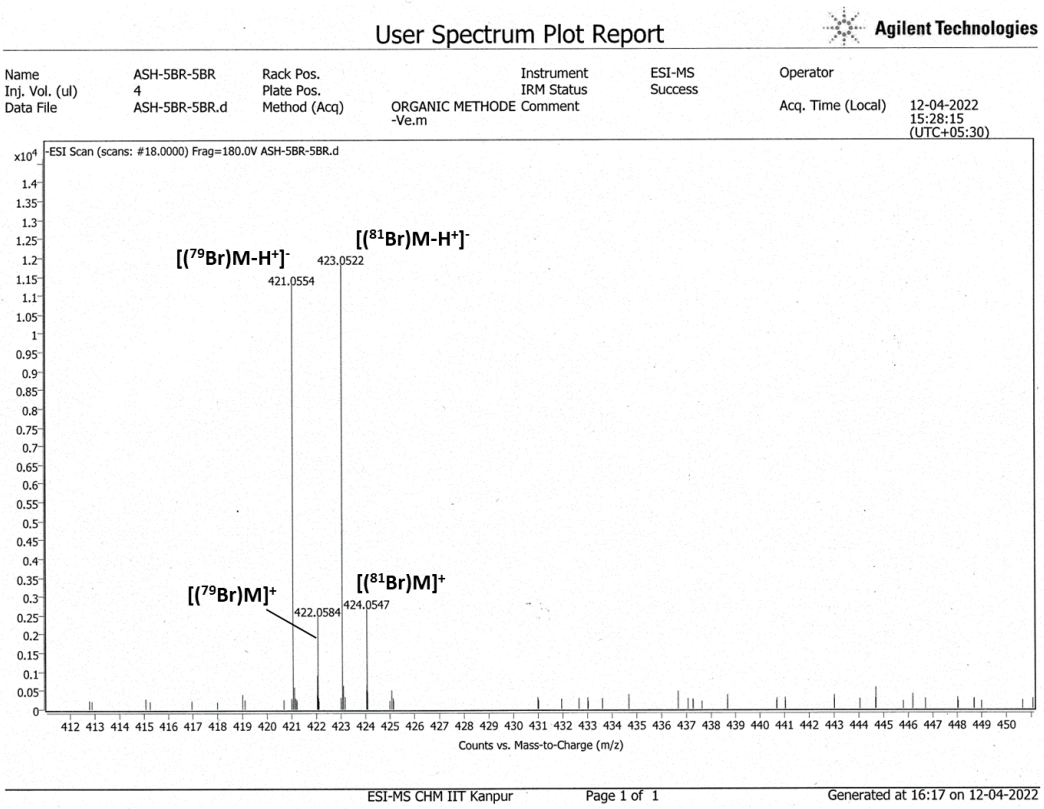

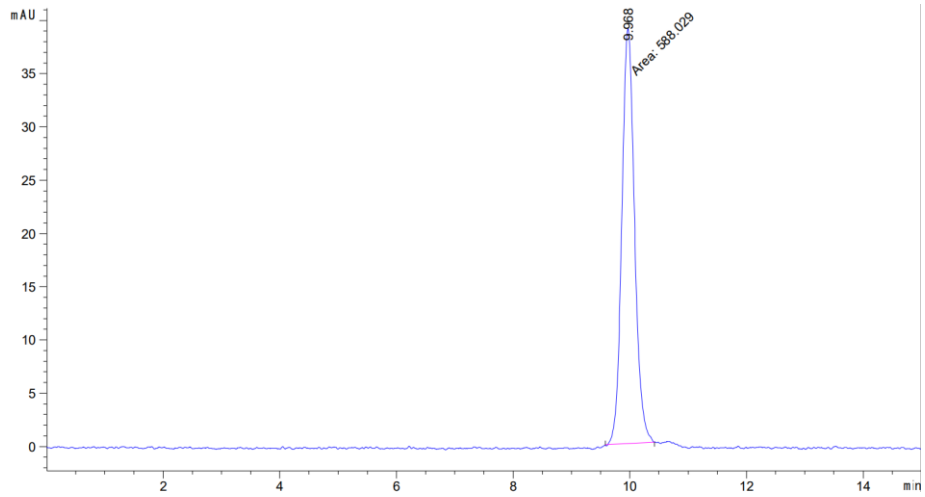

Signal 1: DAD1 B, Sig=254,4 Ref=off

Peak #	RetTime [min]	Type	Width [min]	Area [mAU*s]	Height [mAU]	Area %
1	9.968	MM	0.2517	588.02869	38.93793	100.0000

Figure S13: Characterization ESI-MS and HPLC of $Cu(L5)_2$

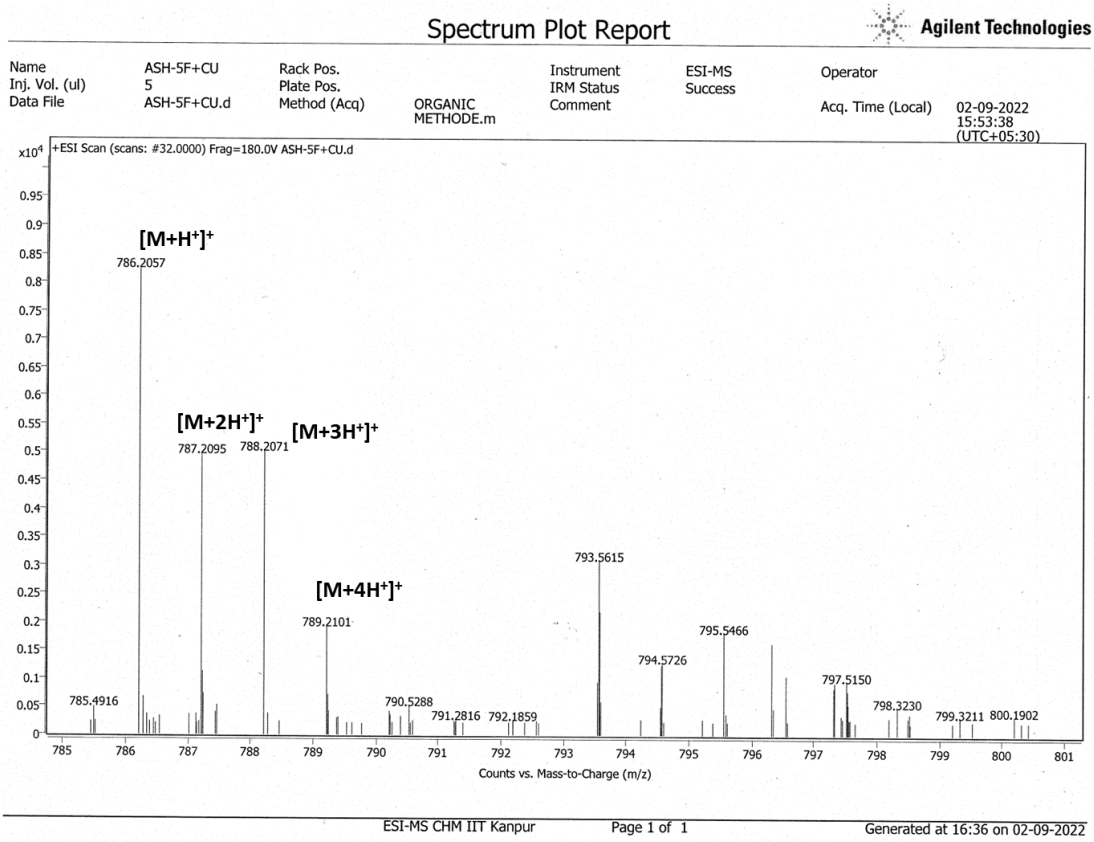

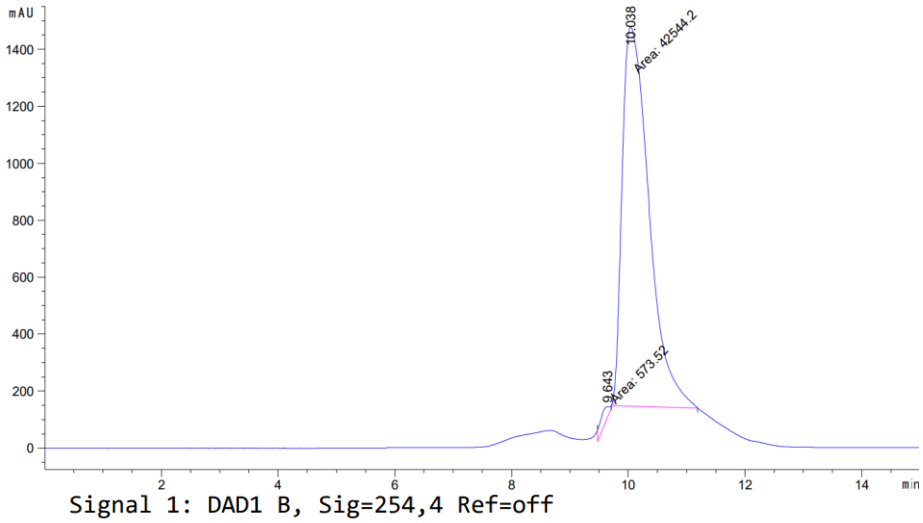

Signal 1: DAD1 B, Sig=254,4 Ref=off

Peak #	RetTime [min]	Type	Width [min]	Area [mAU*s]	Height [mAU]	Area %
1	9.643	MM	0.2449	573.51996	39.02641	1.3301
2	10.038	MM	0.5328	4.25442e4	1330.92615	98.6699

Characterization ESI-MS and HPLC of HL5

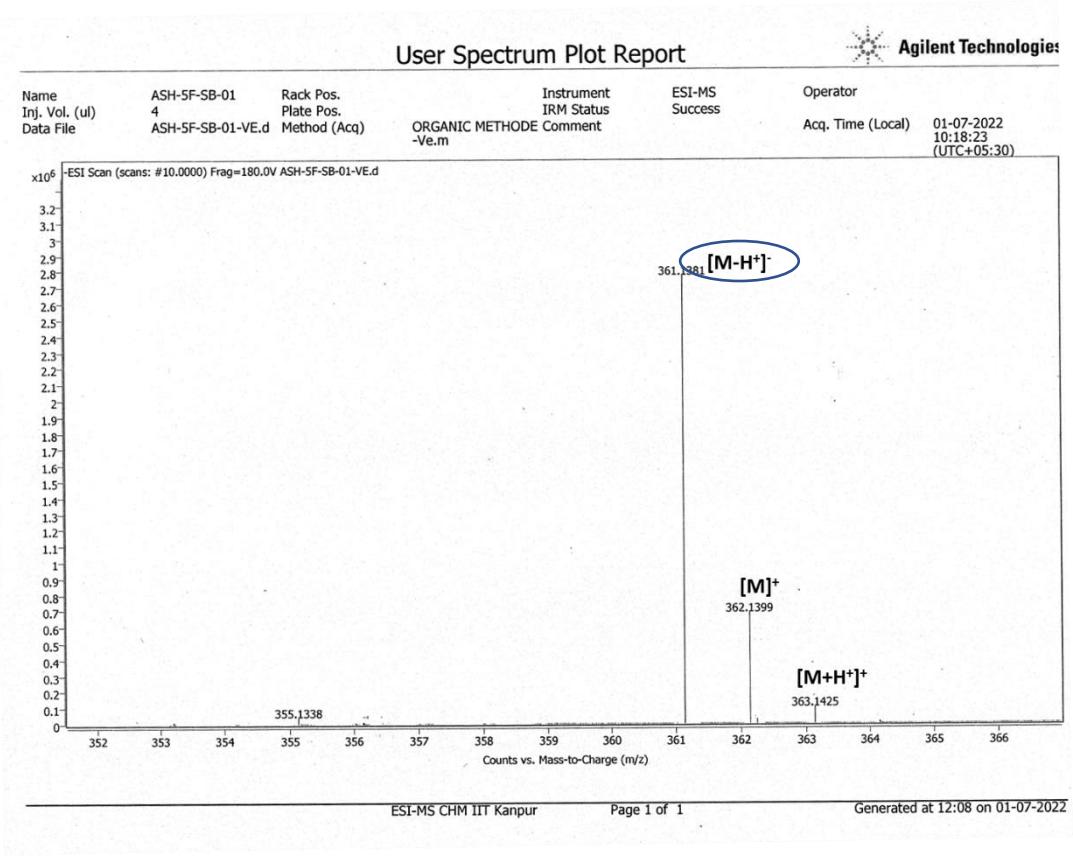

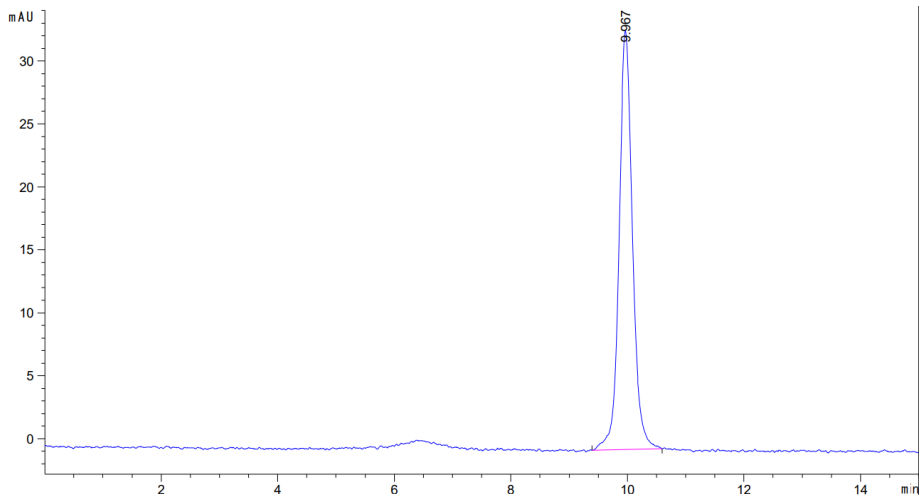

Signal 1: DAD1 B, Sig=254,4 Ref=off

Peak #	RetTime [min]	Type	Width [min]	Area [mAU*s]	Height [mAU]	Area %
1	9.967	BB	0.2461	530.71185	33.26481	100.0000

Figure S14: Characterization ESI-MS and HPLC of $Cu(L6)_2$

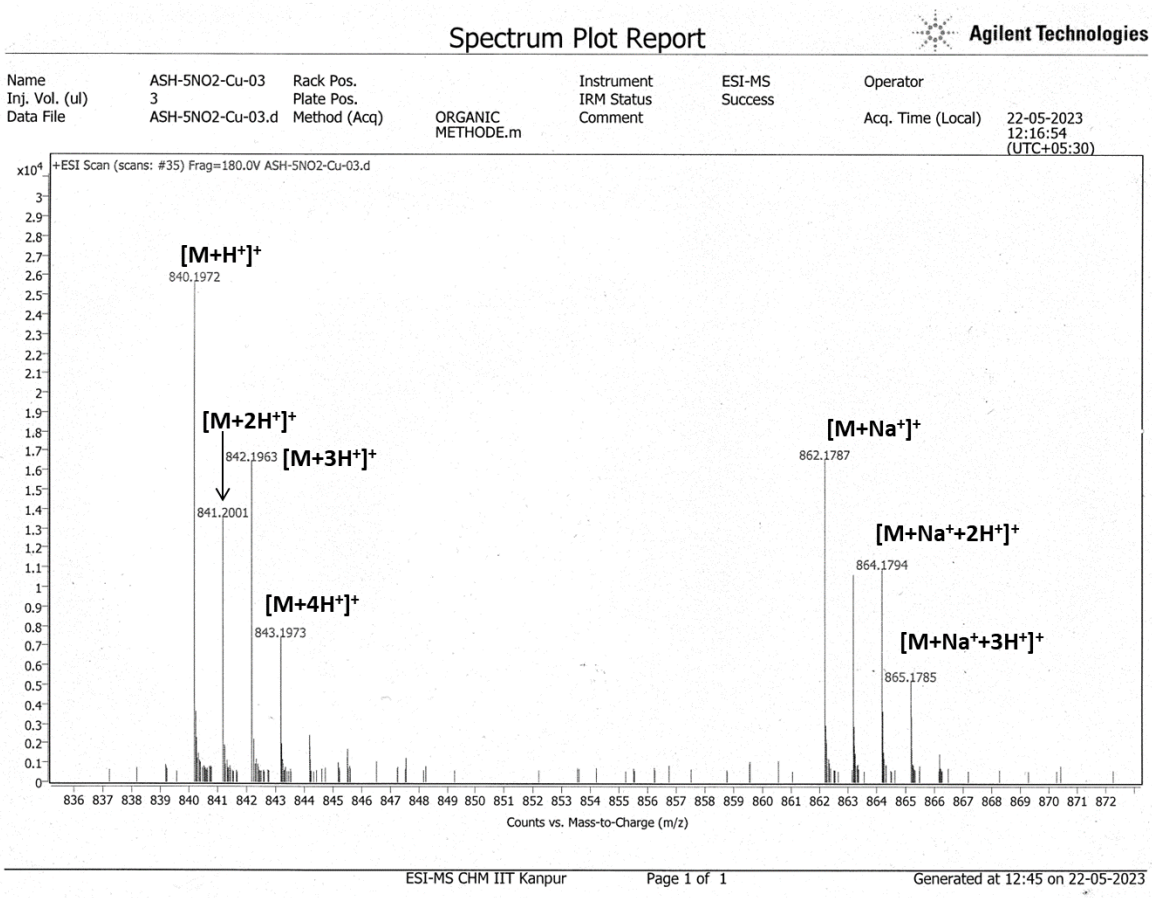

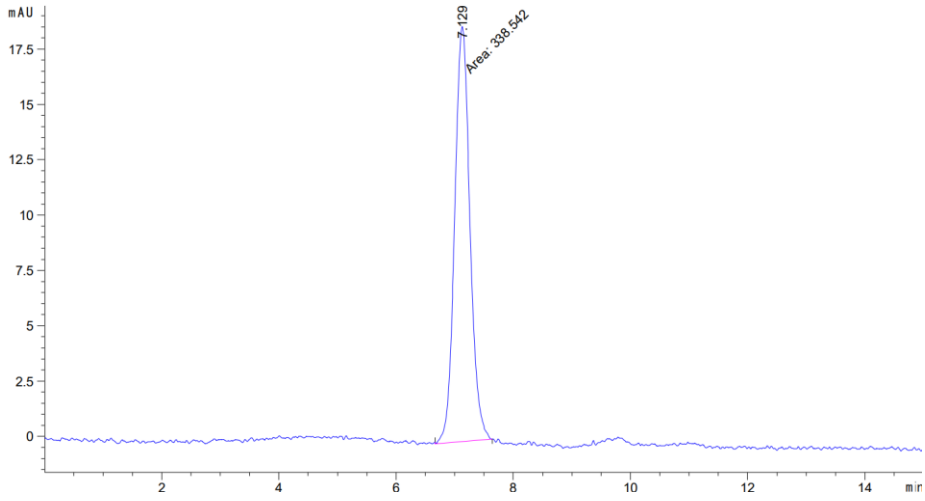

Signal 1: DAD1 B, Sig=254,4 Ref=off

Peak #	RetTime [min]	Type	Width [min]	Area [mAU*s]	Height [mAU]	Area %
1	7.129	MM	0.3010	338.54233	18.74357	100.0000

Characterization ESI-MS and HPLC of HL6

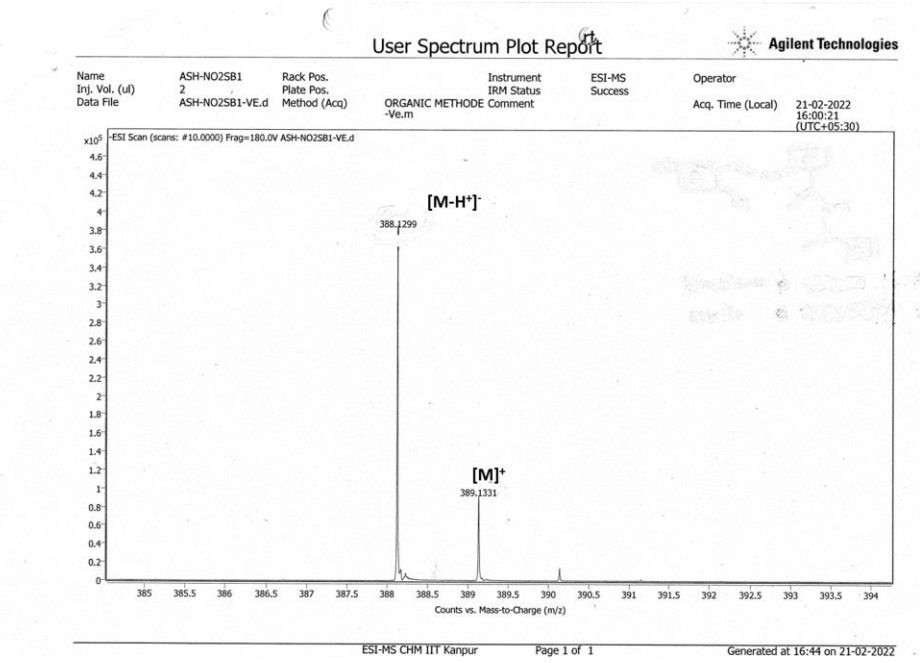

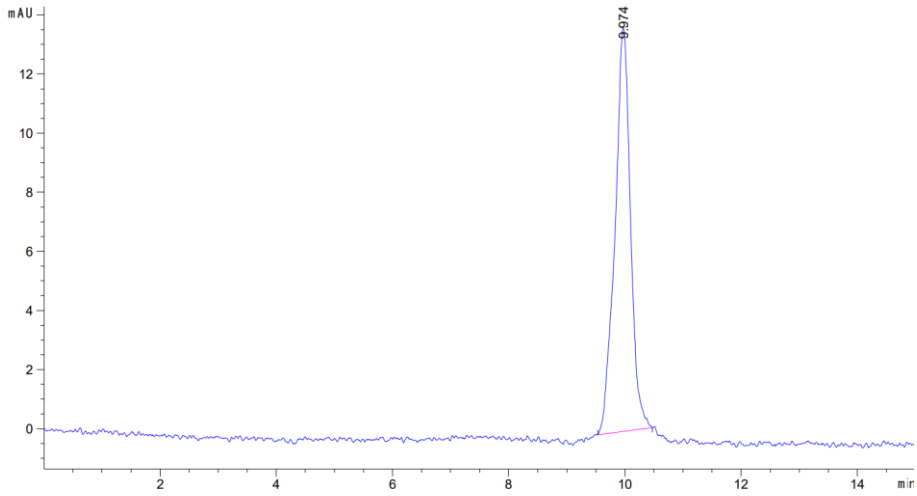

Signal 1: DAD1 B, Sig=254,4 Ref=off

Peak #	RetTime [min]	Type	Width [min]	Area [mAU*s]	Height [mAU]	Area %
1	9.974	BB	0.2682	253.33157	13.67233	100.0000

Figure S15: Characterization ESI-MS and HPLC of $Cu(L7)_2$

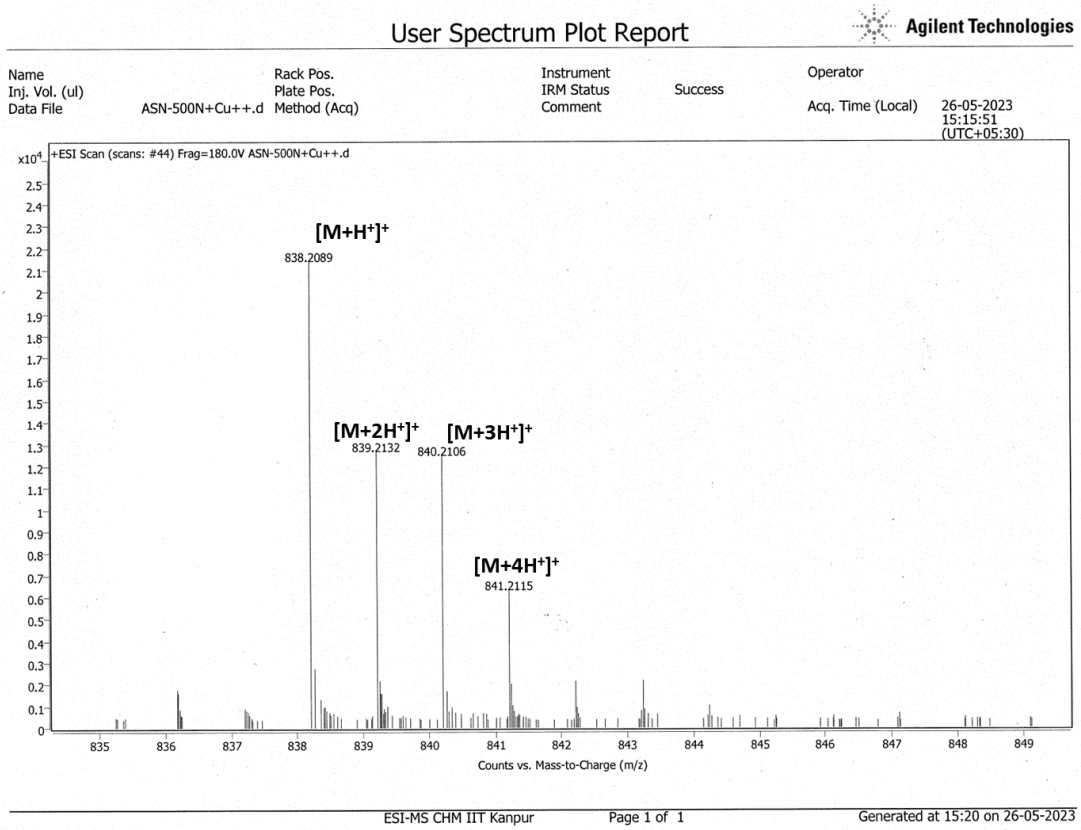

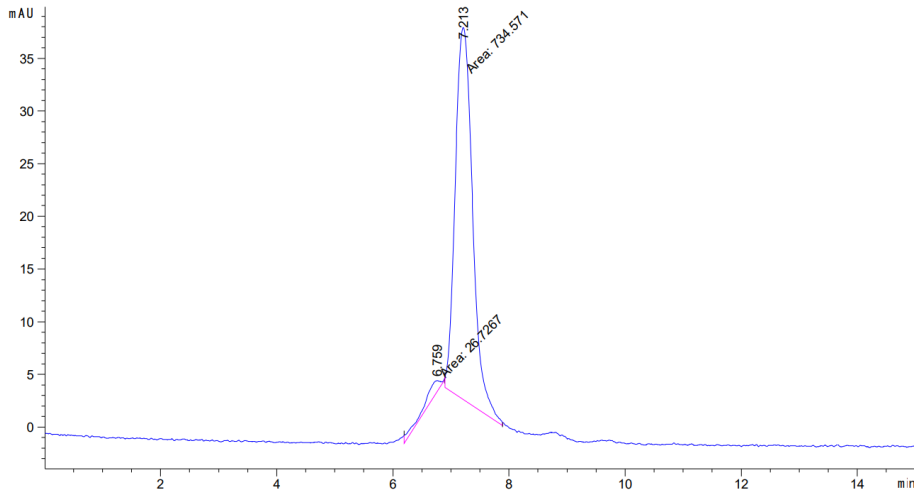

Signal 1: DAD1 B, Sig=254,4 Ref=off

Peak #	RetTime [min]	Type	Width [min]	Area [mAU*s]	Height [mAU]	Area %
1	6.759	MM	0.2908	26.72666	1.09632	3.5107
2	7.213	MM	0.3467	734.57123	35.31448	96.4893

Characterization ESI-MS and HPLC of HL7

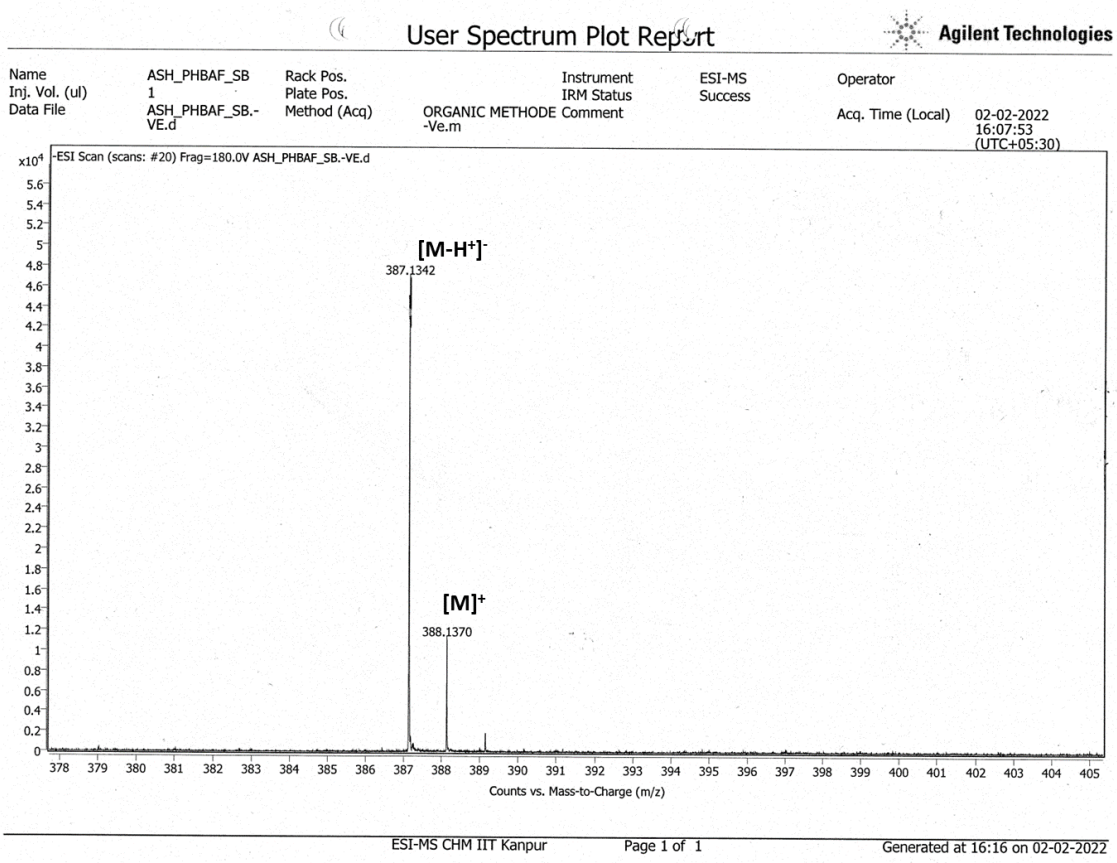

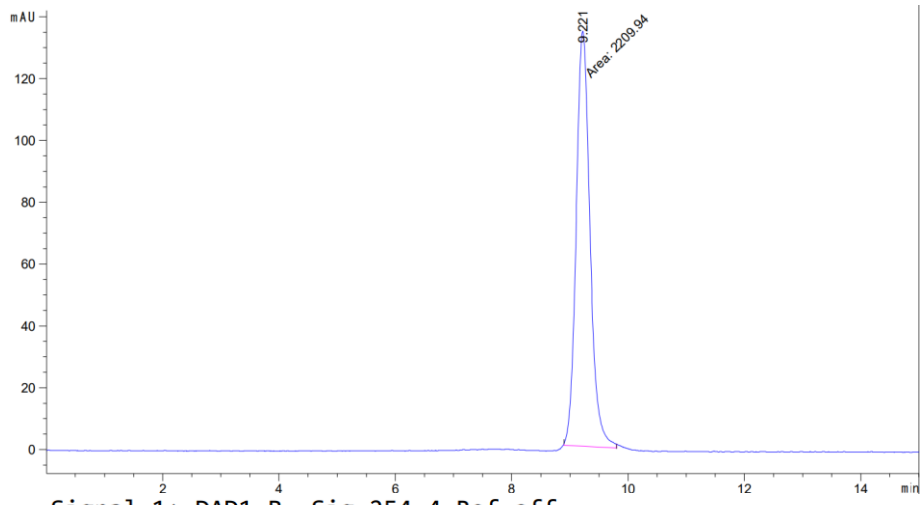

Signal 1: DAD1 B, Sig=254,4 Ref=off

Peak #	RetTime [min]	Type	Width [min]	Area [mAU*s]	Height [mAU]	Area %
1	9.221	MM	0.2744	2209.94409	134.24728	100.0000

Figure S16: Characterization ESI-MS and HPLC of $Cu(L8)_2$

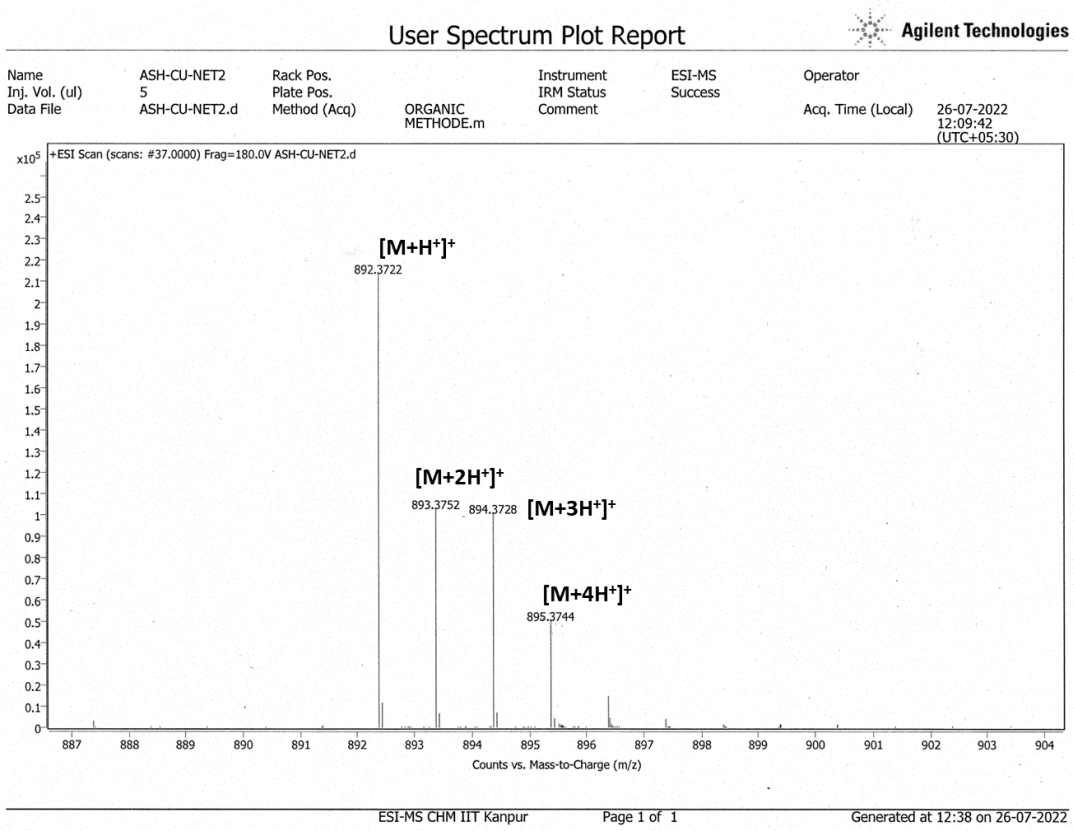

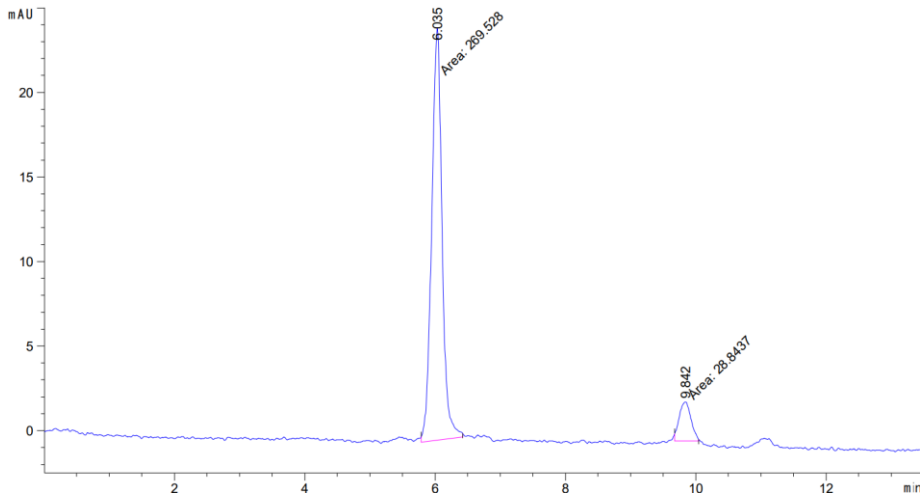

Signal 1: DAD1 B, Sig=254,4 Ref=off

Peak #	RetTime [min]	Type	Width [min]	Area [mAU*s]	Height [mAU]	Area %
1	6.035	MM	0.1843	269.52768	24.37045	90.3330
2	9.842	MM	0.2085	28.84371	2.30580	9.6670

Characterization ESI-MS and HPLC of HL8

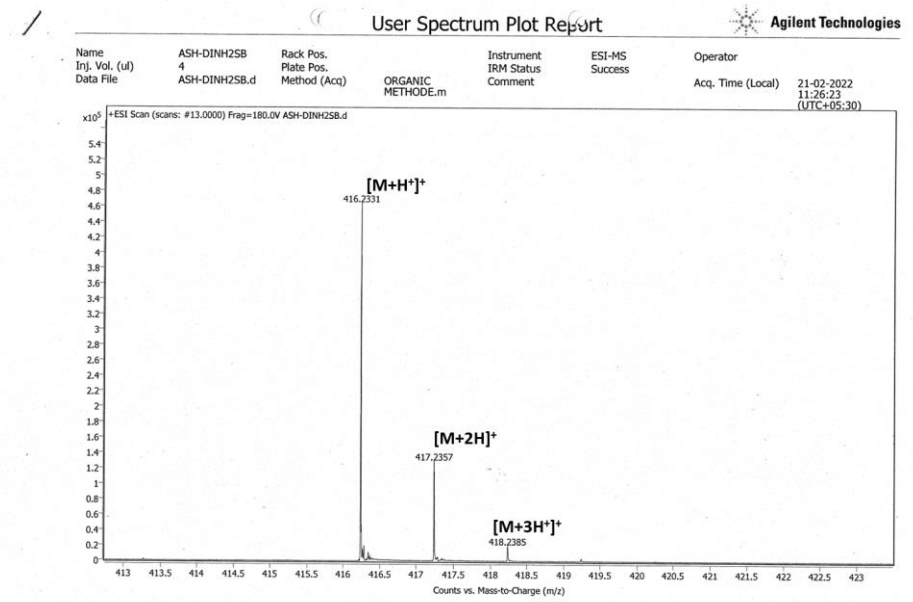

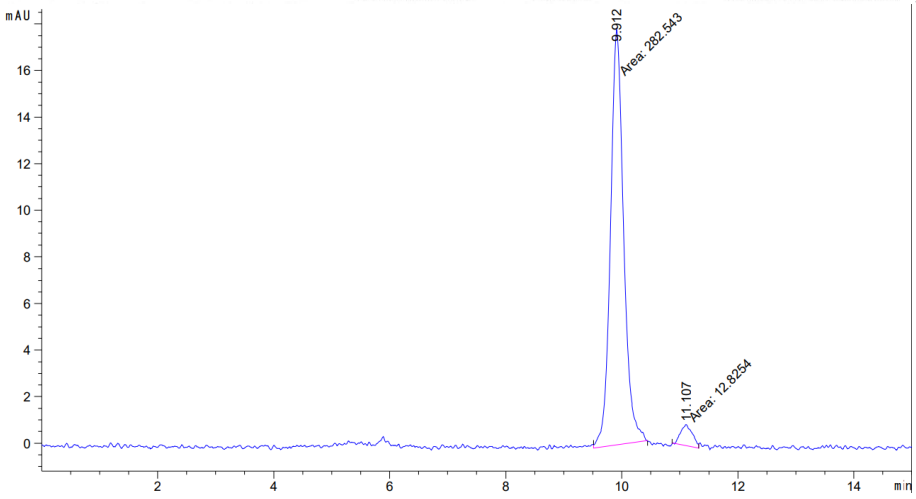

Signal 1: DAD1 B, Sig=254,4 Ref=off

Peak #	RetTime [min]	Type	Width [min]	Area [mAU*s]	Height [mAU]	Area %
1	9.912	MM	0.2642	282.54321	17.82419	95.6578
2	11.107	MM	0.2349	12.82540	9.09826e-1	4.3422

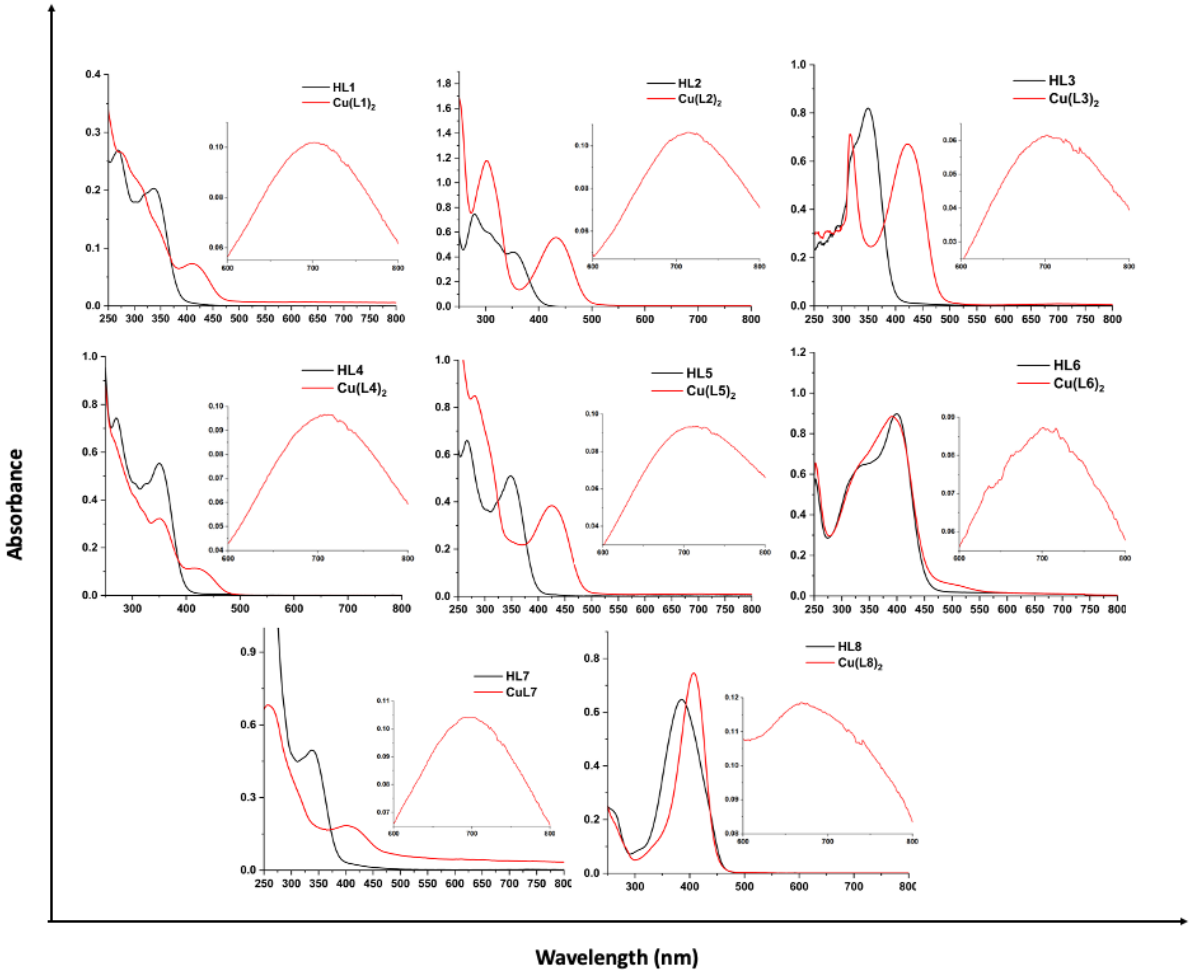

Figure S17: UV-visible absorption spectra of ligands **HL1-HL8**, complexes **$Cu(L1)_2$-$Cu(L8)_2$** recorded at room temperature in methanol.

UV-visible Spectroscopic Titration and Binding Isotherm

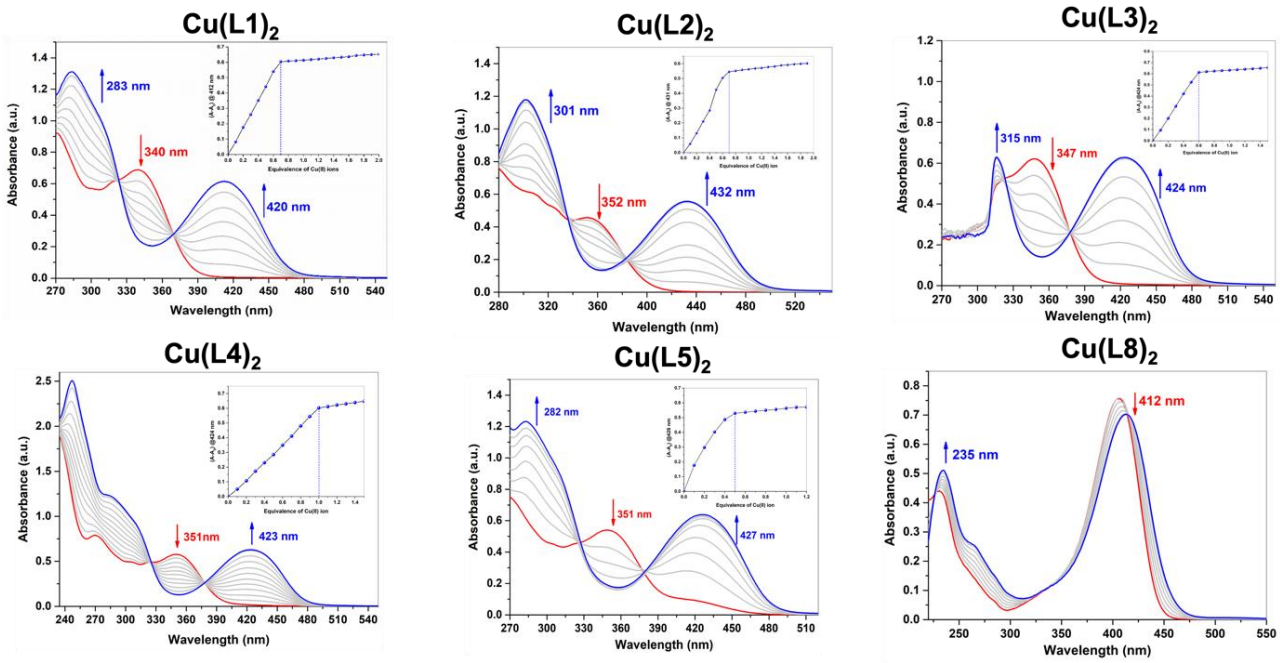

Figure S18: UV-visible absorption spectra were obtained on an JASCO V-770 UV-Visible-NIR spectrophotometer equipped at 25.0 °C. For Cu(II) titration experiments, a stock solution of $Cu(OAc)_2 \bullet H_2O$ (25.8 μM) was prepared in dry methanol. Additions (0−1.5 equiv. Cu(II)) to the ligands **HL1-HL8** solution in methanol were carried out with a glass syringe. After each addition, the solution was allowed to equilibrate.

Infrared Spectroscopic Characterization

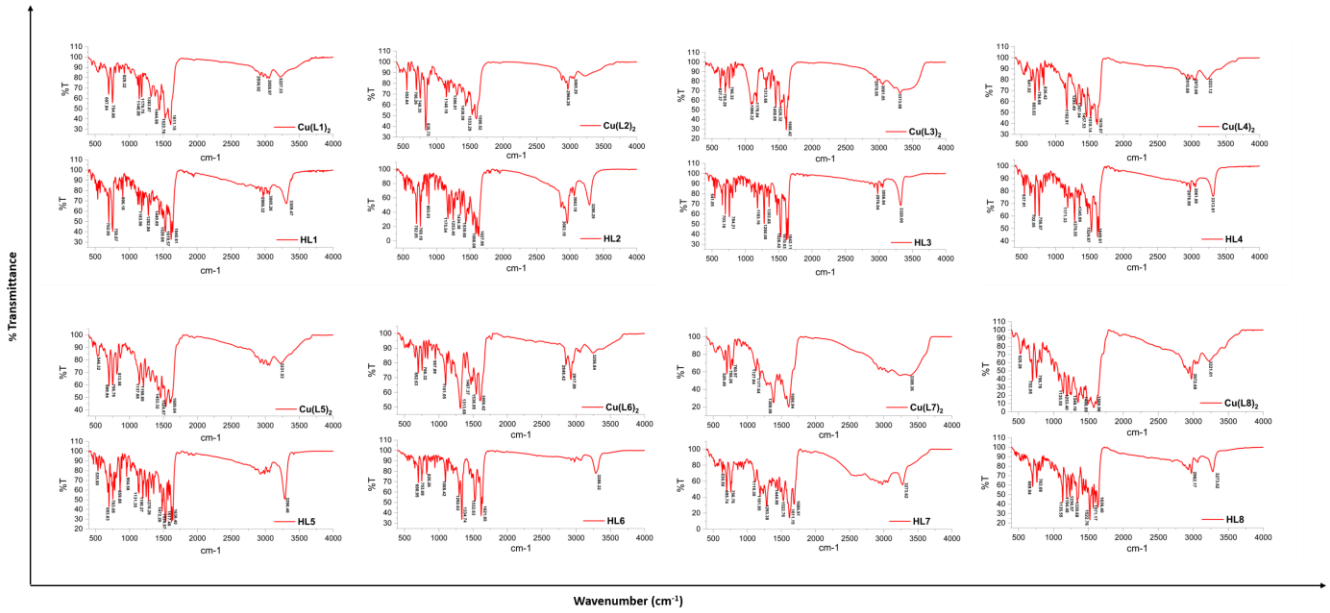

Figure S19: The FT-IR spectra of the ligands **HL1-HL8** and complexes **Cu(L1)$_2$-Cu(L8)$_2$** recorded at room temperature.

Electron Paramagnetic Resonance Data.

The X-band EPR spectrum of $Cu(L1)_2$ – $Cu(L8)_2$ was recorded at room temperature. The EPR spectrum of the complex provides a very constructive information about the extent of the delocalization of unpaired electron and gives valuable information concerning the environment present around the Cu(II) ion. The EPR spectrum of the powdered complex at 300 K, showed signal having $g_{\perp}$, g_{II} and g_{iso} in the range 2.123- 2.048, 2.433-2.210 and 2.12-2.05.

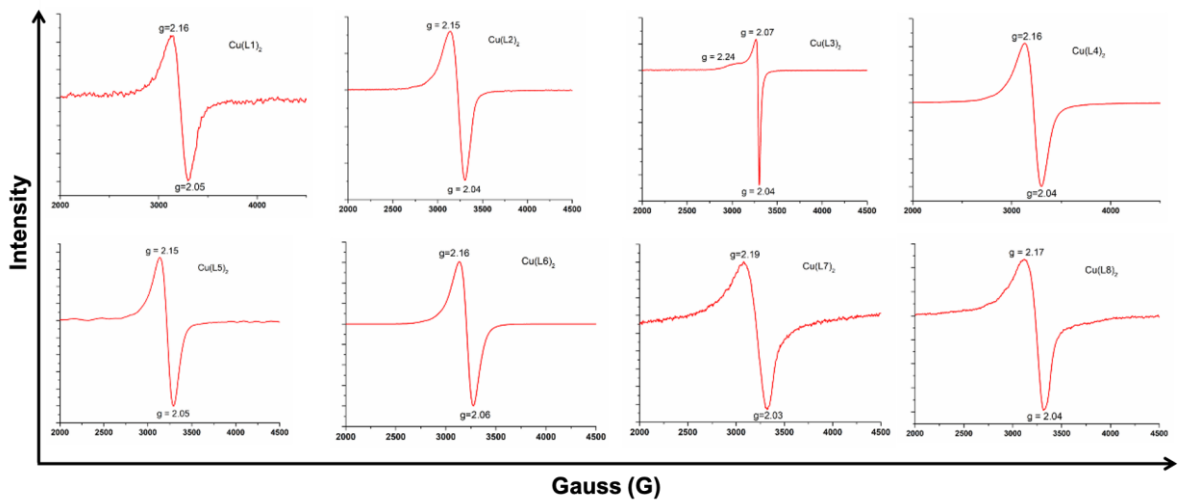

Figure S20: The X-band EPR spectra of the complexes **$Cu(L1)_2$-$Cu(L8)_2$** recorded at room temperature.

Single Crystal X-Ray Diffraction Characterization

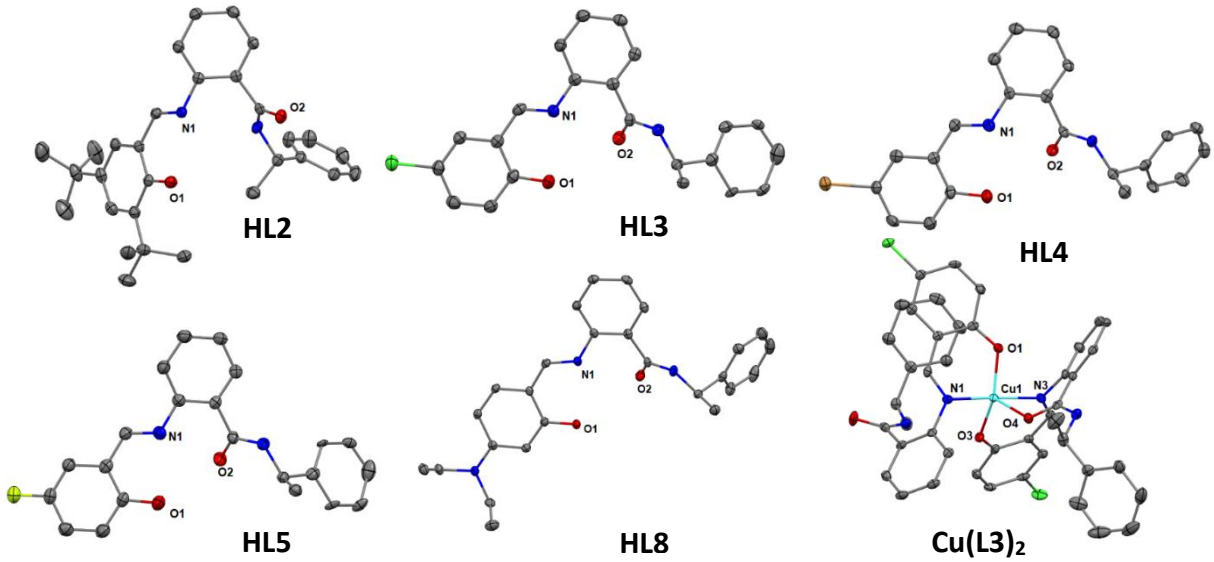

Figure S21: Thermal ellipsoid plot (50 % probability) of HL2, HL3-HL5, HL8 and $Cu(L3)_2$ Nonessential hydrogen atoms omitted for clarity (nitrate ion and water molecule are omitted for clarity from HL8).

Table S1 Crystal data and refinement parameters of ligands

CCDC Identification code	**2252221** **HL2**	**2251966** **HL3**	**2251968** **HL4**	**2251967** **HL5**	**2251965** **HL8**
Chemical formula	$C_{30}H_{36}N_2O_2$	$C_{22.10}H_{19.70}ClN_2O_2$	$C_{44}H_{36}Br_2N_4O_4$	$C_{44}H_{39.2}F_2N_4O_4$	$C_{26}H_{30}N_4O_6$
Formula weight	456.61	380.75	844.59	725.99	494.54
Temperature	100	100	100	100	100
Wavelength	0.71073	0.71073	0.71073	0.71073	0.71073
Crystal size	0.25 × 0.23 × 0.15	0.25 × 0.21 × 0.16	0.28 × 0.28 × 0.18	0.27 × 0.25 × 0.16	0.26 × 0.25 × 0.18
Crystal system	orthorhombic	monoclinic	monoclinic	monoclinic	triclinic
Space group	$P2_12_12_1$	$P2_1$	$P2_1$	$P2_1$	P1
Unit cell dimensions					
a (Å)	90	90	90	90	78.4470(10)
β (Å)	90	105.532(9)	90.216(7)	107.667(5)	76.3600(10)
γ (Å)	90	90	90	90	89.9920(10)
a	9.7339(16)	13.596(4)	5.1334(11)	13.566(3)	5.3560(2)
b	12.884(2)	5.0457(13)	17.550(4)	5.0135(9)	10.9666(4)
c	20.882(4)	13.851(4)	20.516(4)	13.582(2)	11.0710(4)
Volume	2618.7(7)	915.5(4)	1848.4(6)	880.2(3)	618.38(4)
Z	4	18	2	1	1
Density (calculated)	1.158	1.381	1.518	1.370	1.328
F(000)	984.0	399.0	860.0	381.0	262.0
Goodness-of-fit on F^2	1.066	1.045	1.031	1.033	1.042

Final R indices I>2σ(I)	R_1 = 0.0414, wR_2 = 0.0984	R_1 = 0.0482, wR_2 = 0.1124	R_1 = 0.0515, wR_2 = 0.0943	R_1 = 0.0642, wR_2 = 0.1423	R_1 = 0.0394, wR_2 = 0.0932
R indices (all data)	R_1 = 0.0503, wR_2 = 0.1051	R_1 = 0.0651, wR_2 = 0.1223	R_1 = 0.0766, wR_2 = 0.1030	R_1 = 0.1146, wR_2 = 0.1727	R_1 = 0.0442, wR_2 = 0.0962

Table S2 Crystal data and refinement parameters of complex **Cu(L3)$_2$**

CCDC	**2251969**
Identification code	**Cu(L3)$_2$**
Chemical formula	$C_{22}H_{18}ClCu_{0.5}N_2O_2$
Formula weight	409.60
Temperature	100
Wavelength	0.71073
Crystal size	0.13 × 0.12 × 0.1
Crystal system	monoclinic
Space group	$P2_12_12_1$
Unit cell dimensions	
a (Å)	90
β (Å)	100.864(3)
γ (Å)	90
a	13.9547(13)
b	16.5604(16)
c	16.4837(15)
Volume	3741.0(6)
Z	8
Density (calculated)	1.454
F(000)	1692.0
Goodness-of-fit on F^2	1.038
Final R indices I>2σ(I)	R_1 = 0.0391, wR_2 = 0.0813
R indices (all data)	R_1 = 0.0500, wR_2 = 0.0856

Table S3 Selected bond distances (Å) and bond angles (°) for HL2-HL5 and HL8

	HL2	**HL3**	**HL4**	**HL5**	**HL8**
Bond distance(Å)					
C1-O1	1.357(2)	1.338(4)	1.367(7)	1.352 (6)	1.342 (3)
C7-N1	1.285(3)	1.277(4)	1.273(8)	1.277 (6)	1.328 (3)
C14-O2	1.236(2)	1.232(4)	1.243(7)	1.240 (5)	1.238 (3)
C14-N2	1.332(3)	1.339(4)	1.334(7)	1.329 (6)	1.340 (3)
Bond angle **(°)**					
O1-C1-C2	120.25(18)	118.4(3)	117.9(6)	117.8(4)	122.2(2)
C7-N1-C8	116.92(17)	122.2(3)	123.1(6)	121.3(4)	125.1(2)
O2-C14-C13	119.31(18)	121.6(3)	121.1(5)	121.6(4)	120.8(2)
O2-C14-N2	123.97(19)	123.0(3)	123.4(6)	122.3(4)	123.3(2)

Table S4 Selected bond distances (Å) and bond angles (°) for $Cu(L3)_2$

	Cu(L3)$_2$
Bond distance(Å)	
Cu1-O1	1.925(3)
Cu1-N1	1.974(3)
Cu1-O3	1.933(3)
Cu1-N3	1.986(3)
Cu1-O4	2.354(3)
Bond angle **(°)**	
O1-Cu1-N1	92.31(13)
O1- Cu1-N3	89.61(13)

O1-Cu1-O3	151.85(12)
O1-Cu1-O4	98.81(12)
O1-Cu1-O3	88.28(13)
N1-Cu1-N3	176.75(14)
N1-Cu1-O4	99.41(11)
N3-Cu1-O3	91.27(13)
N3-Cu1-O4	77.69(11)
O3-Cu1-O4	108.86(12)

Stability profile of $Cu(L1)_2$ – $Cu(L8)_2$ by UV-visible spectroscopic characterization: The stability of $Cu(L1)_2$–$Cu(L8)_2$ (Fig. S22, ESI†) under simulated physiological conditions (phosphate buffer saline (PBS) solution at pH 7.4 containing 1% DMSO) showed no obvious bathochromic and hypsochromic shift at 0, 1, and 2 h.

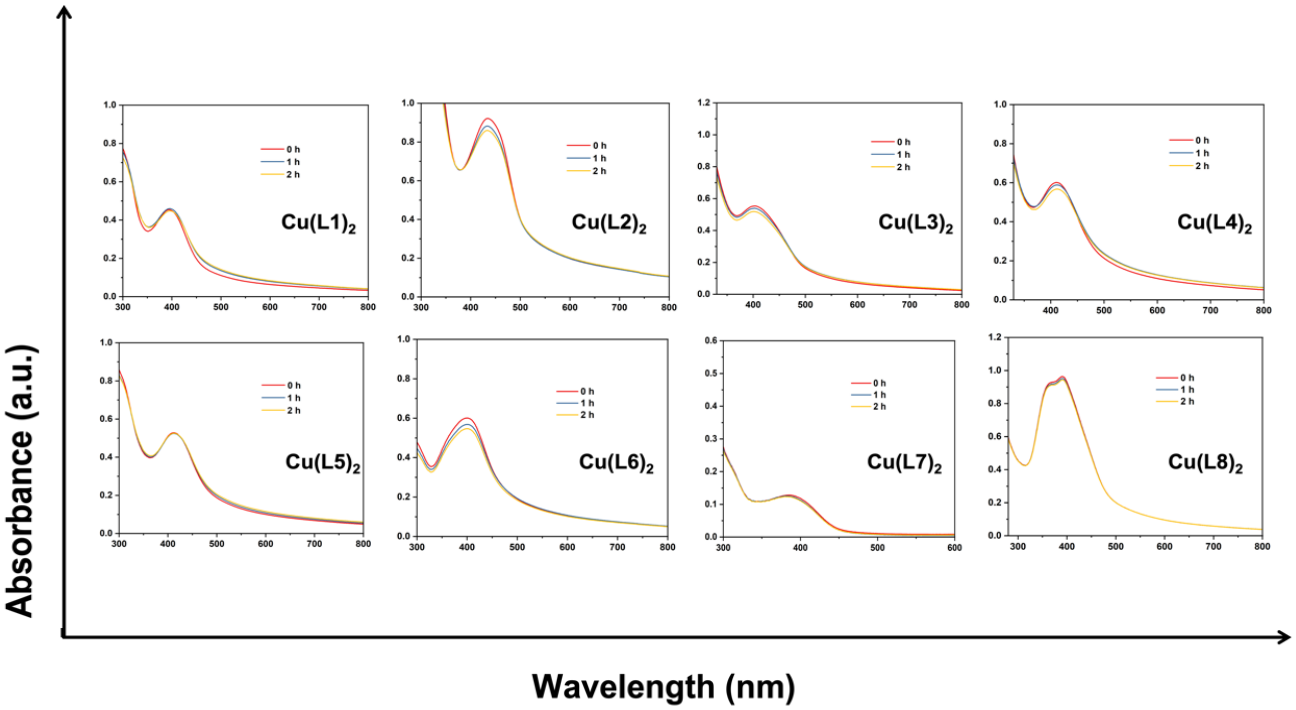

Figure S22: Stability profile: UV-Visible absorption spectra of complexes **$Cu(L1)_2$-$Cu(L8)_2$** in PBS buffer containing 1% DMSO solution at time = 0 h, 1 h and 2 h.

Electrochemical profile of Cu(L2)$_2$: Cyclic Voltammetry (CV) analysis was performed on a CHI610E electrochemical analyzer under oxygen-free conditions. The CV studies were performed on the copper complex (10^{-3} M) using 0.1 M [nBu$_4$N] [ClO$_4$] as a supporting electrolyte in DMF solvent at a scan rate of 50 mV/s The three-component electrode consisted of a glassy carbon working electrode, a Ag/AgCl reference electrode, and a platinum wire as the counter electrode. The CV plot of Cu(II) complex showed one quasi-reversible peak at $E_{1/2}$ = 0.53 V vs. Ag/AgCl ($E_{p/a}$ = 0.49 V, $E_{p/c}$ = 0.57 V vs. Ag/AgCl) corresponding to the Cu^{II}/Cu^{I} redox couple. [1] Scan rates effect on the electrochemical behaviour of the CuL^{11} was investigated in the potential range of 0.0 to 1.2 V in 0.1 M [nBu$_4$N] [ClO$_4$]. A linear correlation exists between the peak current and the square root of the scan rate. However, the voltammetric data shows that at higher scan rates, the reduction ($E_{p/c}$) and oxidation ($E_{p/a}$) peaks are shifted to more negative and positive values, respectively. Therefore, the process can be considered to be quasi-reversible.

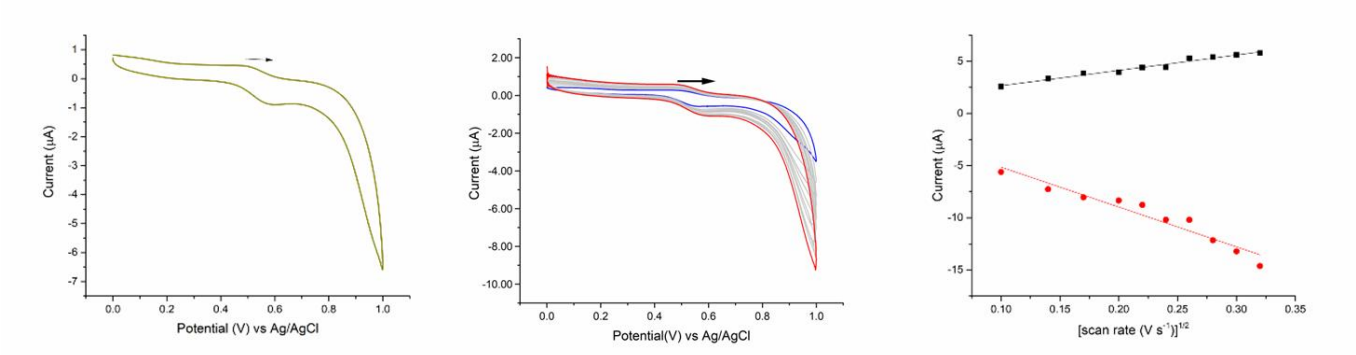

Figure S23 Electrochemical characterization of Cu(L2)$_2$ (Left): Cyclic voltammogram at a glassy carbon electrode in DMF with [nBu$_4$N] [ClO$_4$] as a supporting electrolyte. (Centre): Data collected at different scan rate 0.01-0.1 V/s using an Ag/AgCl reference electrode and a platinum wire electrode. (Right): Plot of measured anodic peak current vs square root of applied scan rate for both the reduction (circle) and oxidation (square) events on the cyclic voltammogram.

Biological Profile

Cell lines and culture conditions. Breast adenocarcinoma cell lines MDA-MB-231 and MCF-7, Human lung adenocarcinoma cell line A549, Human colon cancer cell line HCT-116, and Human embryonic kidney cell line HEK-293 was obtained from National Centre for Cell Science (NCCS Pune, India). The cell lines were maintained in RPMI 1640 (MDA-MB-231, MCF-7 and A549) or DMEM medium (HCT-116, HEK-293), supplemented with 10% fetal bovine serum, 10,000 Units/mL penicillin and 10,000 µg/mL streptomycin, at 37 °C humidified atmosphere with 5% CO_2. All stocks of the compound were prepared in DMSO.

Resazurin assay. The cytotoxicity of the compounds was determined by the resazurin assay. For each cell type 0.35×10^6 cells were plated in culture flasks, The cells were harvested from culture flasks by trypsinization and 2,500 cells per well were seeded into 96-well microculture plates for the viability assay. After the cells were allowed to resume exponential growth for 24 h, they were exposed to drugs at different concentrations in media for 72 h. Cisplatin (10 µM) and DMSO (0.5-0.2% of the media) were used as positive and negative control, respectively. After the exposure of 72 h, the cells were washed once with 1xPBS (100 µL/well) and then treated with resazurin solution (150 µL/well, 0.02 mg/mL) for 4 h in the dark and then fluorescence was taken at emission wavelength range 580-640 nm (λ_{ex} = 520 nm) by SpectraMax M5^e microplate reader. All procedures were carried out in triplicate of three independent experiments. IC_{50} values were calculated using GraphPad Prism 8.0 software and the results were presented as a mean ± SD.

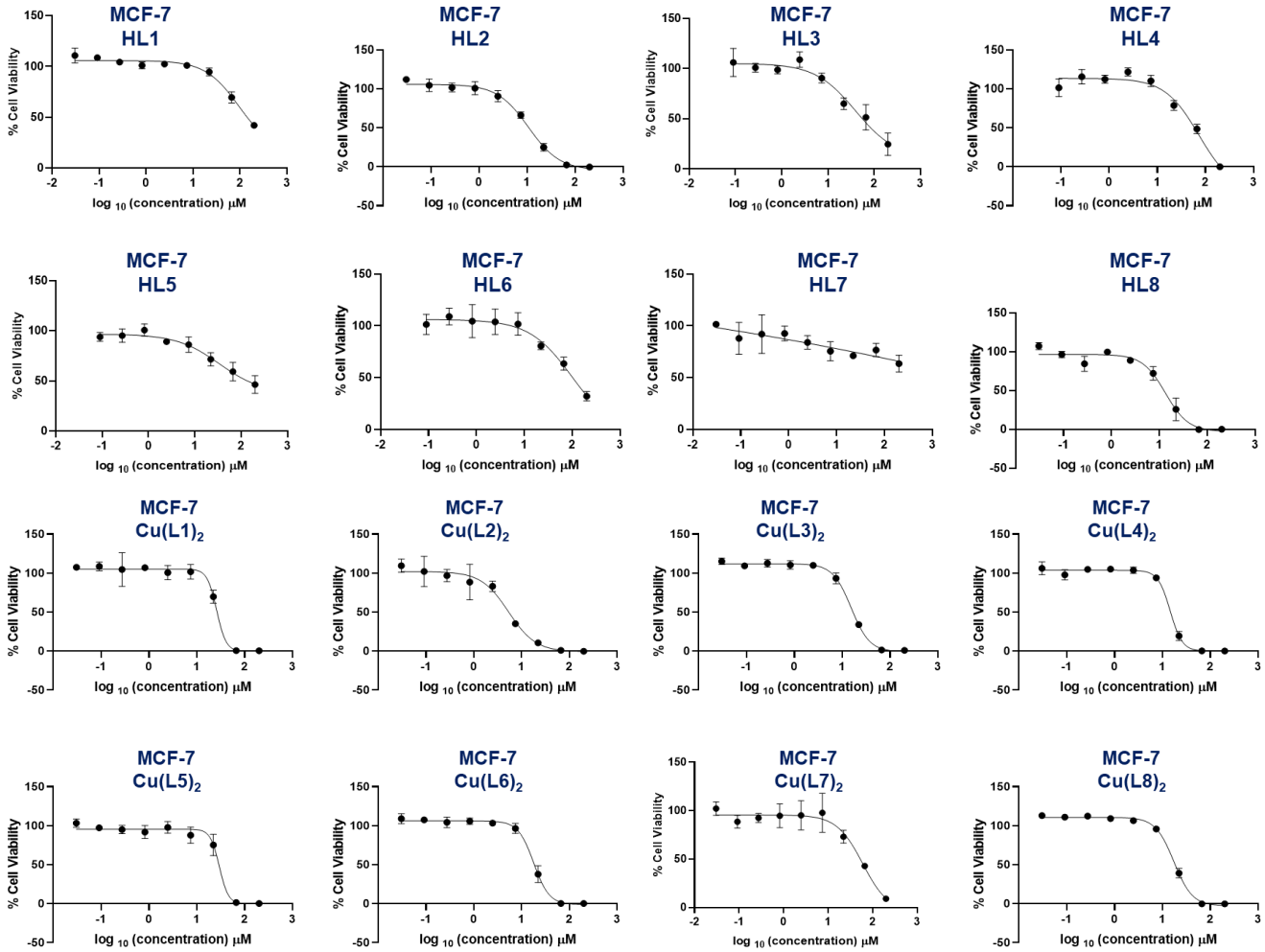

Figure. S24: Cytotoxicity profile of HL1 – HL8 and $Cu(L1)_2$ – $Cu(L8)_2$ in MCF-7 cell lines by Resazurin Assay

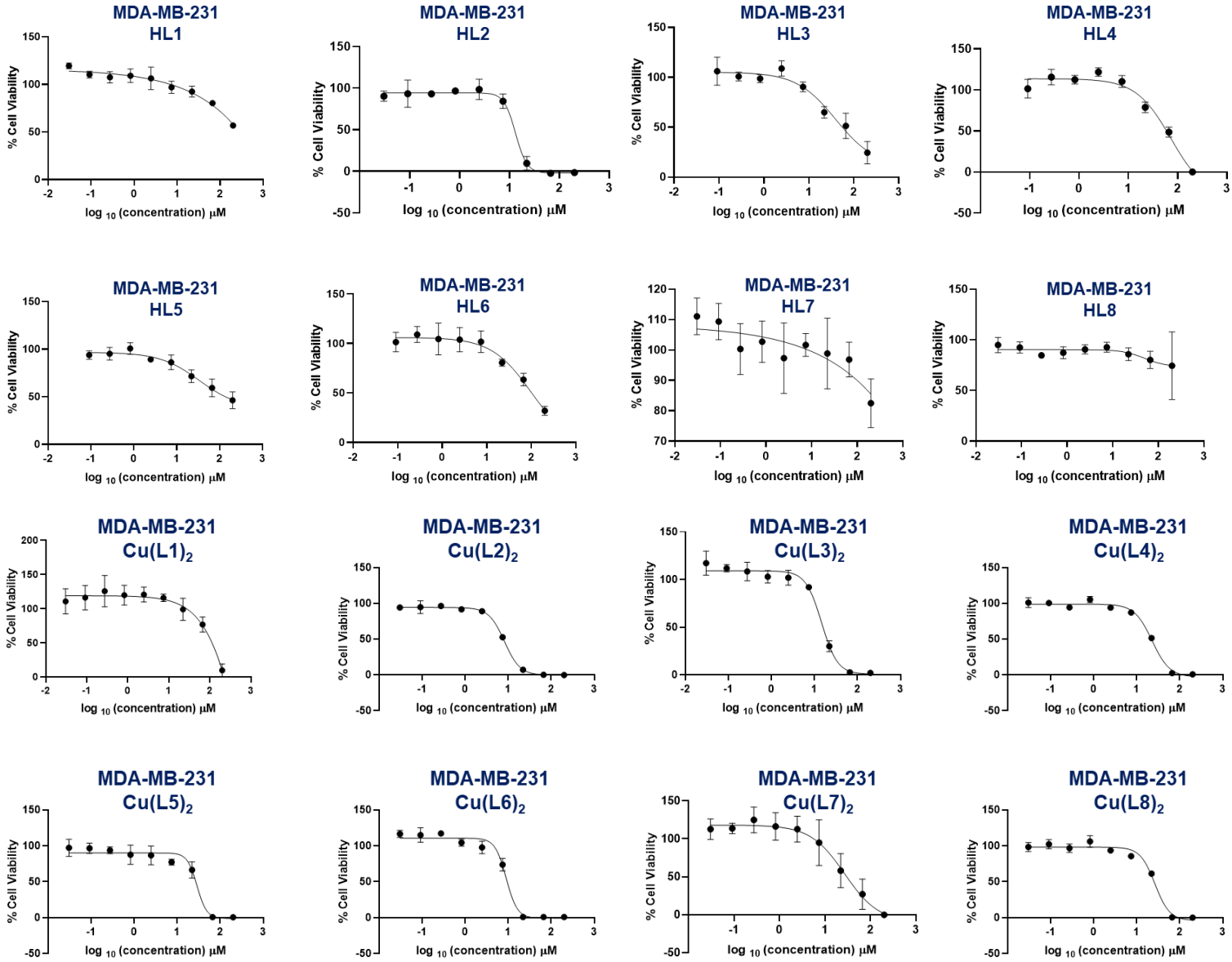

Figure. S25: Cytotoxicity profile of HL1 – HL8 and $Cu(L1)_2$ – $Cu(L8)_2$ in MDA-MB-231 cell lines by Resazurin Assay

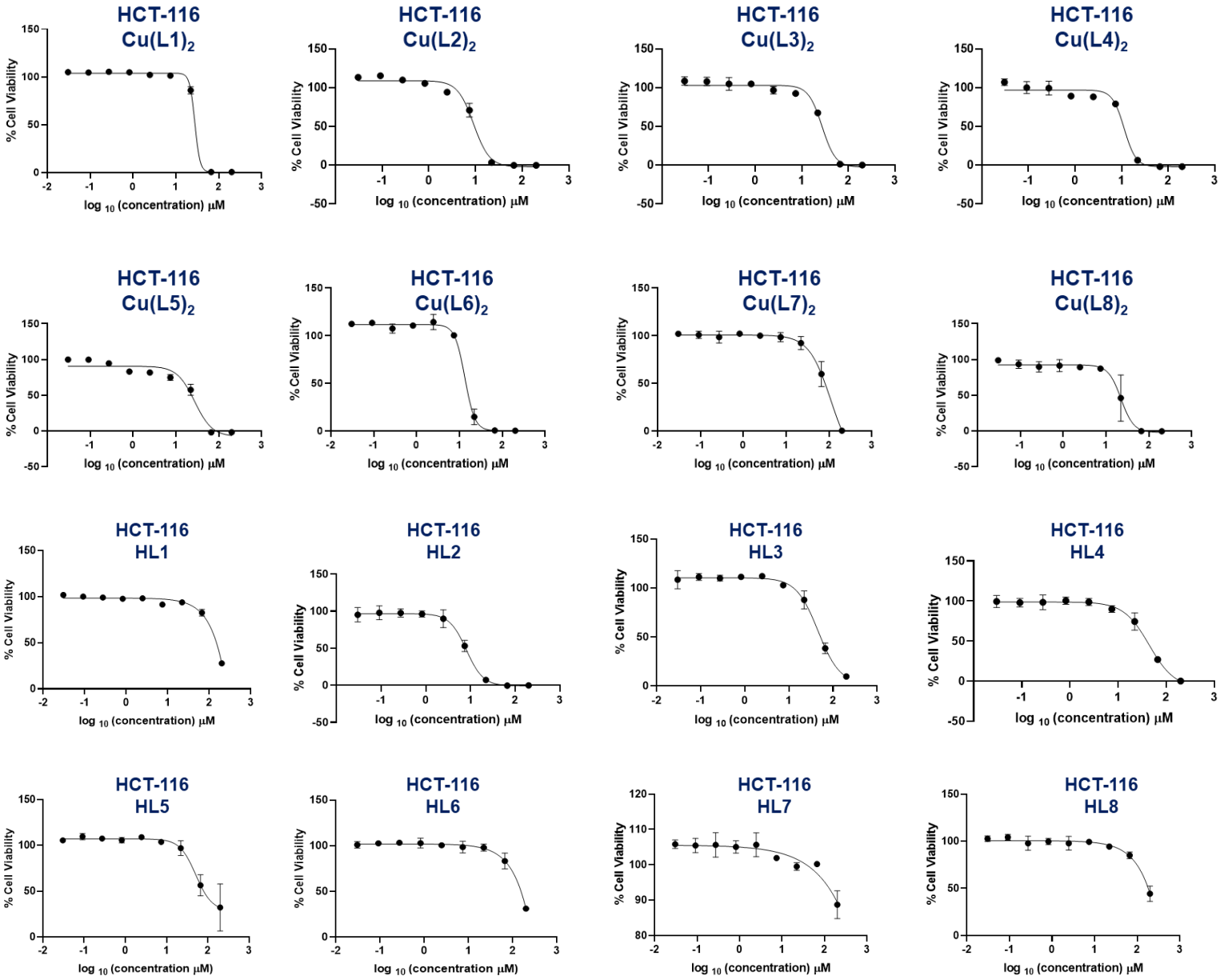

Figure. S26: Cytotoxicity profile of HL1- HL8 and $Cu(L1)_2$ – $Cu(L8)_2$ in HCT-116 cell lines by Resazurin

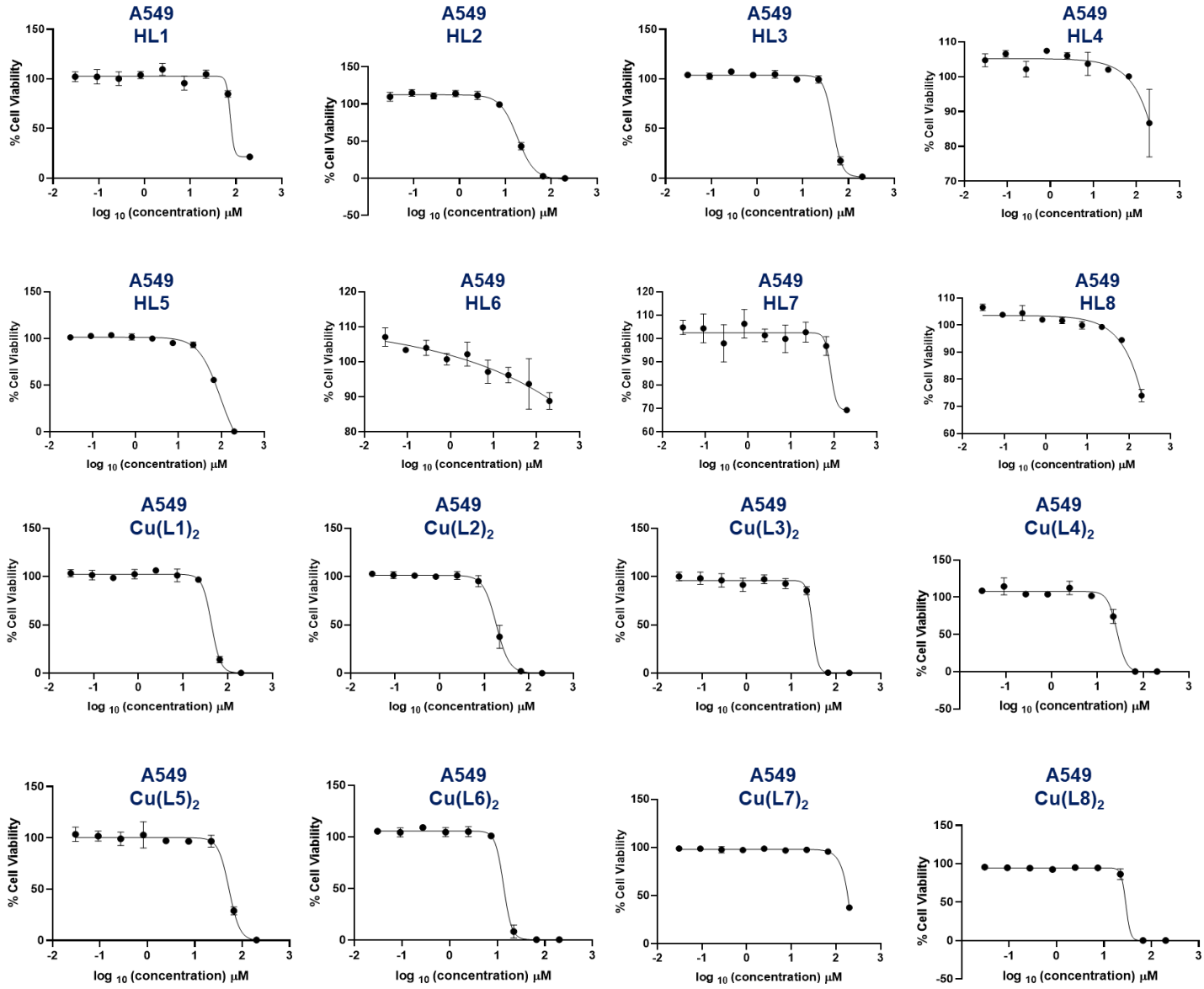

Figure. S27: Cytotoxicity profile of HL1 – HL8 and $Cu(L1)_2$ – $Cu(L8)_2$ in A549 cell lines by Resazurin

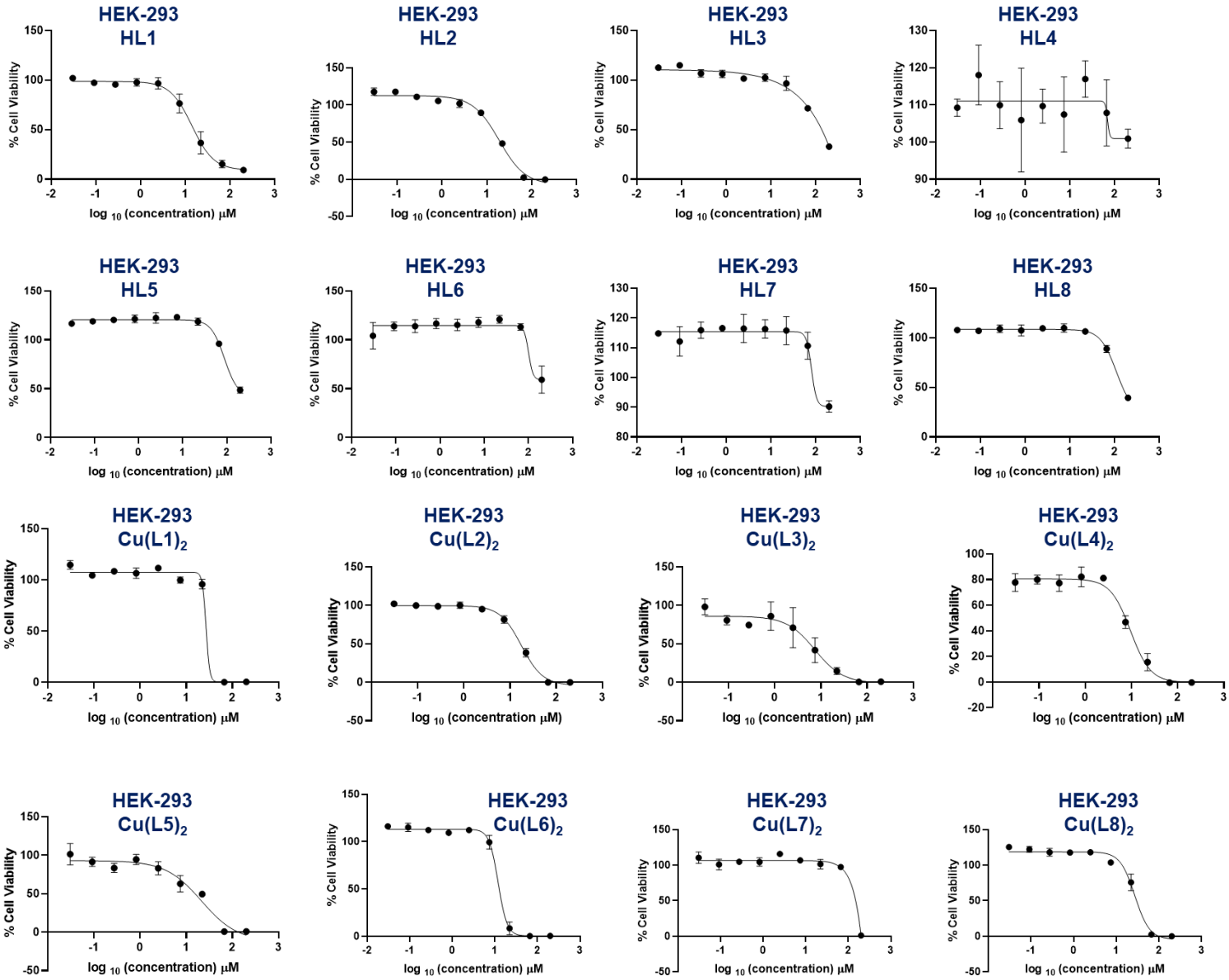

Figure. S28: Cytotoxicity profile of HL1 – HL8 and $Cu(L1)_2$ – $Cu(L8)_2$ in HEK-293 cell lines by Resazurin Assay

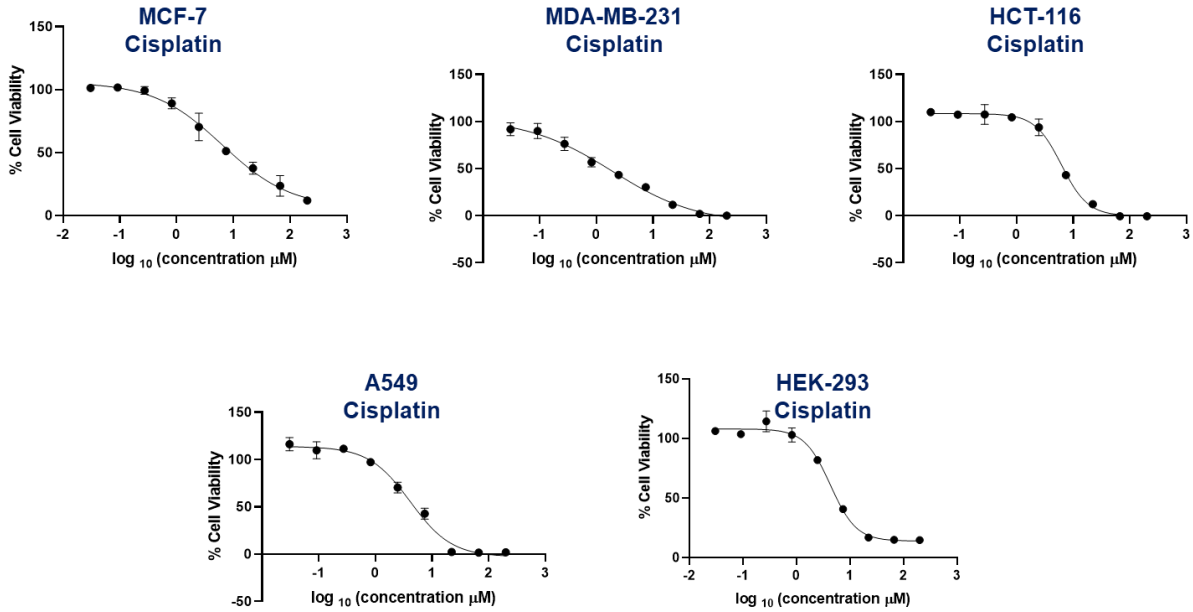

Figure. S29: Cytotoxicity profile of FDA approved cisplatin in 5 cell lines (A549. HCT-116. HEK-293, MCF-7, MDA-MB-231) by Resazurin Assay

Live/Dead assay. To investigate cytotoxicity of **Cu(L2)$_2$** Live/Dead assay was performed. Cytotoxicity was detected by calcein-AM and propidium iodide (PI) dual-color fluorescence staining. In brief, 1 x 10^6 cells/well of MCF-7 were seeded in a 6 well plate and cultured overnight. The cells were treated with **Cu(L2)$_2$** at different concentrations for 48 h. Untreated cells and cisplatin (20 μM) were used as negative and positive control, respectively. Then the medium was aspirated and washed three times with PBS. The cells were incubated with Calcein-AM/PI in working buffer for 30 min. The staining medium was aspirated, washed with PBS and the cells were observed by fluorescent cell imager.

Benzoate Hydroxylation Assay. Stock solutions of ligands were prepared in methanol and EDTA in ultrapure water. Ligand stock solutions were added to the test solutions prepared in 10 mM phosphate buffer (pH 7.40) and it also contains benzoate. The amount of methanol (0.46% v/v) was maintained the same in all test solutions. Following addition of $FeSO_4$, the hydroxylation reaction was initiated by addition of 30% H_2O_2. The final volume of each test solution was 3000 μL, containing 1.0 mM benzoate, 30 μM Fe(II), 1 mM H_2O_2, and varying concentrations of ligands. Test solutions were incubated for 3.5 h at room temperature, and then fluorescence emission was collected at 410 nm (ex. 290 nm). Measurements were conducted in triplicate and reported as average ± standard deviation.

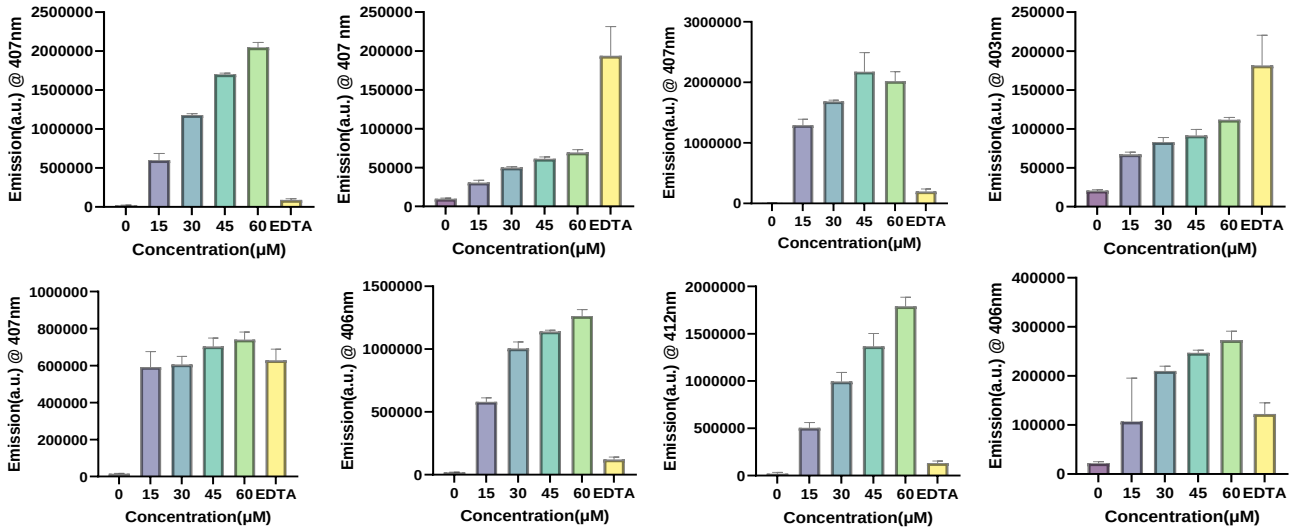

Figure. S30: Effect of synthesised ligands (HL1-HL8) on the rate of benzoate hydroxylation that results the formation of fluorescent salicylate(s) (ex. 290 nm, em. 400-410 nm) in the presence of Fe(II) ions (30 μM) and H_2O_2 (1.0 mM). All the solutions had been prepared in phosphate buffer (10 mM, pH 7.40), and after adding H_2O_2, they were all incubated for 3 hours. As a positive control, 30 μM of EDTA was used.

Methylene Blue degradation assay. A fixed concentration of Methylene Blue (MB) solution was prepared in 1x PBS buffer solution (pH 7.4) with 8 mM H_2O_2, 100 mM GSH, and 128 μM **Cu(L2)$_2$** complex. After the mixing system had been incubated for 30 min at room temperature, the absorbance of MB was determined using UV-vis spectroscopy.

Detection of ·OH by EPR. Equal molar Cu(L2)$_2$ complex (50 μM) and GSH (50 μM) were dissolved in DMF and distilled water, respectively. Subsequently, they were mixed and reacted. After 5 min, H_2O_2 (8 mM) and DMPO (100 mM) were added. The spectra of ·OH signals were recorded on a Bruker EMX (X-band) Spectrometer.

Measurement of intracellular reactive oxygen species (ROS). MCF-7 cells (2.5 x 10^4 cells/well) were plated in 96 well plate and allowed to adhere overnight. Afterwards, the cells were treated with Cu-complex **Cu(L2)$_2$** as well as metal free ligand **HL2**. Hydrogen peroxide (H_2O_2) was used as positive control whereas DMSO treated cells were used as a negative control in this experiment. After 3 h of incubation, the media containing compounds was removed and the cells were washed with PBS. Then, a solution of 2′,7′-dichlorodihydrofluorescein diacetate (H_2DCF-DA; 10 μM, 100 μL) in PBS was added to the cells and incubated in the dark at 37 °C for 15 min. The cells were then washed thrice with PBS to remove excess H_2DCF-DA and fluorescence microscopy images were captured immediately using BIO-RAD ZOE™ fluorescent cell imager.

Copper complex interaction with GSH by NMR. GSH and the Cu(II) complex **Cu(L2)$_2$** were both dissolved in D_2O and 60:1(v/v) DMSO-d_6, respectively. The complex's disassociated ligand was observed by ^{1}H NMR spectra after a 2-hour mixing period. Additionally, 1:5 (v/v) DMSO-d_6 and D_2O were used to dissolve the copper (II) complex and GSH, in order to identify the GSSG (oxidation product of GSH) using 1H NMR spectra.

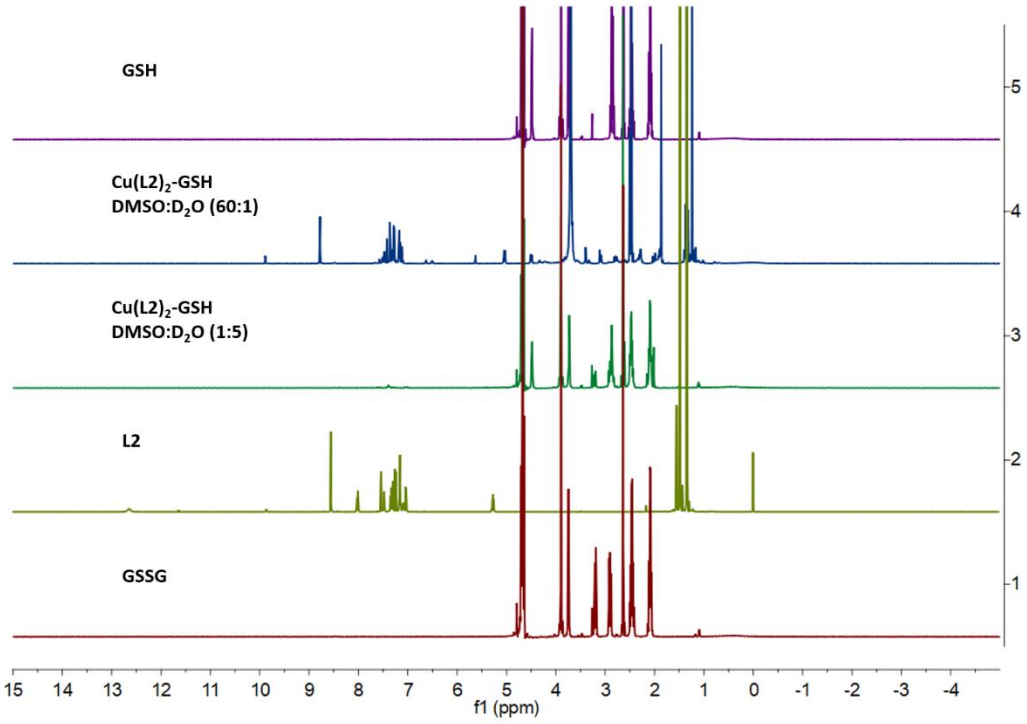

Figure S31: ^{1}H NMR spectra of (a) reduced glutathione (GSH); (b) GSH with $Cu(L2)_2$ in DMSO:D_2O (60:1); (c) GSH with $Cu(L2)_2$ in DMSO:D_2O (1:5); (d) HL2; and (e) oxidized glutathione (GSSG).

Glutathione depletion by Ellman's reagent. Glutathione (GSH) depletion was investigated using Ellman's reagent in cell-free as well as in-cell environment. At first, solutions with 20 mM GSH and 40 μM of **Cu(L2)$_2$** complex were incubated at 37 °C for 0–6 h. Then the samples were centrifuged at 12000 rpm for 10 min, and the supernatants were collected. A DTNB solution was added to the supernatant and co-incubated for 5 min at 25 °C, and then the absorbance at 412 nm was measured with a microplate reader. The same procedure was followed with a higher concentration of **Cu(L2)$_2$** (400 μM).
Afterwards, the depletion in GSH level was estimated in MCF-7. In brief, 1 x 10^6 cells were plated in 6-well plate and incubated for 24 h. After that, cells were treated with different concentrations of **Cu(L2)$_2$** and kept for incubation. After 24 h, cells were collected by centrifugation, and the cellular protein was precipitated by incubating 250 μL of the sonicated cell suspension with 250 μL TCA (10%) and was placed on ice for 1 h and then by centrifugation for 10 min at 3000 rpm. The supernatant was added to 500 μL of 0.4 M Tris buffer (pH 8.9) containing 0.02 M EDTA, followed by the addition of 0.01 M 5,5′-dithionitrobenzoic acid (DTNB) to a final volume of 1.5 ml. At 37 °C, for 10 min of incubation in a shaking water bath, the tubes were kept. The absorbance was recorded at 412 nm.

GSH-Glo™ Glutathione Assay for. The GSH-Glo™ Glutathione Assay is a luminescence-based assay for detecting and quantifying glutathione (GSH). The experiment was performed according to the assay protocol. In the 96-well plate, 2500 cells of MCF-7 were seeded and allowed to adhere overnight. The cells were treated with five different concentrations of **Cu(L2)$_2$** and incubated for 24 h. Afterwards, media was removed and cells of each well were treated with 100μl of prepared 1X GSH-Glo™ Reagent and incubated for 30 minutes at room temperature. Furthermore, 100μl of reconstituted Luciferin Detection Reagent was added to each well and incubated for 15 minutes again and then recorded the luminescence using plate reader.

ICP-MS. MCF-7 cells were plated in 6-well plate (1×10^6 cells/well). After incubation for 24 h, the medium was replaced by medium containing copper complex **Cu(L2)$_2$** and $Cu(OAc)_2.H_2O$. After 8 h, the medium was aspirated. Cells were trypsinized, counted and washed three times with PBS. Then, cells were centrifuged at 3000 rpm at 4 ^{o}C for 10 min digested in HNO_3 overnight. Each sample was diluted to 10 mL before test. The amount of Cu was determined by ICP-MS. Each result was repeated three times.

Lipophilicity by ICP-MS. The flask-shaking method and ICP-MS analysis were utilised to determine the lipophilicity ($logP_{o/w}$) of $Cu(L2)_2$. An equivalent amount of 0.9% (w/v) NaCl solution, saturated with octanol, was introduced into a 1 mL stock solution of the $Cu(L2)_2$ in n-octanol. The resulting mixture was agitated for 24 hours in an incubator set at 37 °C. Following this, the mixtures underwent centrifugation at 10000×rpm for 10 minutes. Subsequently, the distinct oil and water phases were carefully isolated. A total of 100 μL from each of the oil and water phases were subjected to dissolution using 65% HNO_3 (300 μL) and subsequently diluted to a final volume of 10 mL using distilled water. The concentration of copper(II) (C_o or C_w) was determined via the ICP-MS technique utilising an internal reference. The $P_o/_w$ value is directly proportional to the ratio of the concentration of the organic phase (C_o) to the concentration of the aqueous phase (C_w).

Table S5: Lipophilicity for Cu(L1)2 - Cu(L8)2

Compound	Lipophilicity ($P_{o/w}$)	$\log P_{o/w}$
$Cu(L1)_2$	0.65	-0.18
$Cu(L2)_2$	0.89	-0.050
$Cu(L3)_2$	1.63	0.21
$Cu(L4)_2$	1.71	0.23
$Cu(L5)_2$	0.86	-0.065
$Cu(L6)_2$	0.38	-0.42
$Cu(L7)_2$	0.074	-1.13
$Cu(L8)_2$	1.36	0.13

DNA Binding: In analyzing the UV-vis titration spectra with DNA, it was observed that increasing the concentration of DNA resulted in hypochromism, indicating an intercalation binding mode between $Cu(L2)_2$ and DNA base pairs. Additionally, an isosbestic point was observed at 380 nm (can be seen when 0.1 eq.- 1 eq. of DNA was added, as shown in fig.) suggests that equilibrium was established between DNA and $Cu(L2)_2$. The intrinsic binding constant (K_b) of $Cu(L2)_2$ with CT-DNA was determined by using the equation: $[DNA]/(\varepsilon_a-\varepsilon_f) = [DNA]/(\varepsilon_b-\varepsilon_f) + 1/ Kb (\varepsilon_b-\varepsilon_f)$, where ε_a is the extinction coefficient of the complex at a given DNA concentration, ε_b is the extinction coefficient of complex when fully bound to DNA, ε_f is the extinction coefficient of the complex in free solution. The plot $[DNA]/(\varepsilon_a-\varepsilon_f)$ vs. [DNA] gave the slope $1/(\varepsilon_b-\varepsilon_f)$ and intercept $1/ K_b (\varepsilon_b-\varepsilon_f)$, K_b was calculated as ratio of slope to intercept. The value of intrinsic binding constant was found to be $K_b=1.28 \times 10^5\ M^{-1}$, which is consistent to the previous reported studies. [7,8]

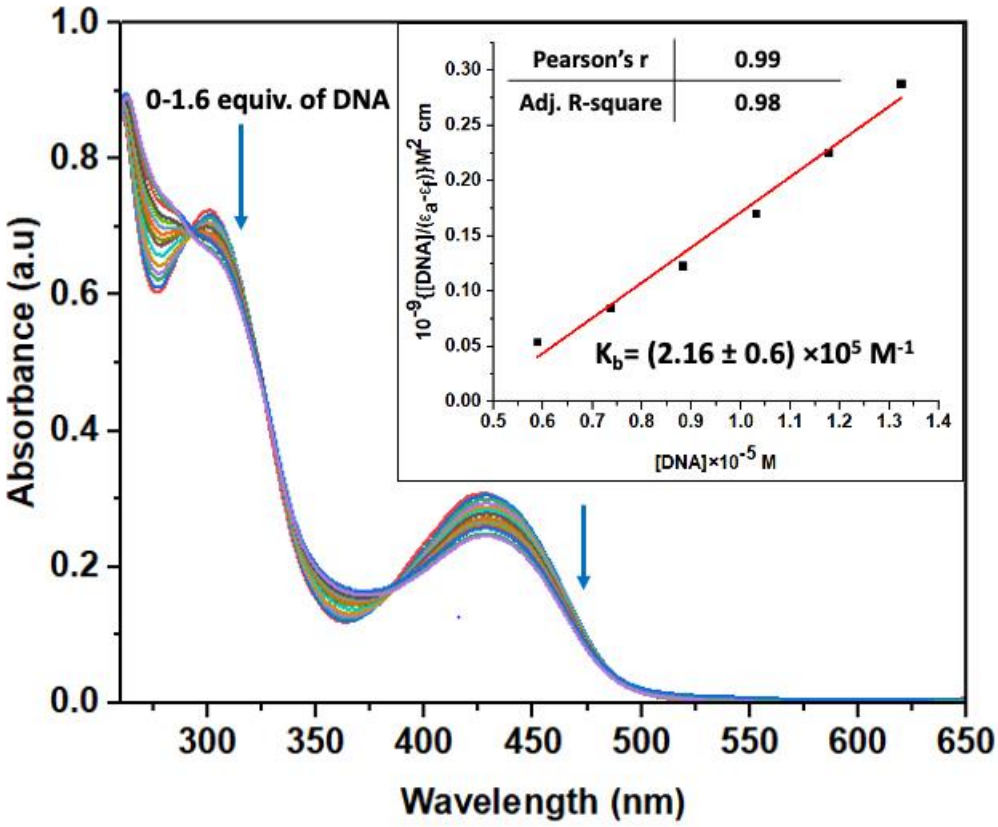

Figure S32: Absorption spectra of $Cu(L2)_2$ (50 μM) at pH 7 (50 mM Tris-buffer) with increasing CT-DNA concentration (0.1 – 1.6 equivalent). (Inset) Linear Point for binding constant of $Cu(L2)_2$ (50 μM) with increasing CT-DNA (0.1 – 1.6 equivalent).

TMRM assay. MCF-7 cells (2.5 x 10^4 cells/well) were plated in 96 well plate and allowed to adhere overnight. Afterwards, the cells were treated with Cu-complex **Cu(L2)$_2$** as well as metal free ligand **HL2**. Hydrogen peroxide (H_2O_2) was used as positive control whereas DMSO treated cells were used as a negative control in this experiment. After 3 h of incubation, the media containing compounds was removed and the cells were washed with PBS. Then, a solution of Tetramethyl rhodamine methyl ester perchlorate (TMRM; 10 nM, 100 μL) in RPMI-1640 media was added to the cells and incubated in the dark at 37 °C for 15 min. The cells were then washed thrice with PBS to remove excess TMRM and fluorescence microscopy images were captured immediately using BIO-RAD ZOE™ fluorescent cell imager.

ATP assay. ATP production was measured using the Cell Titer-Glo luminescence cell viability assay kit (Promega) according to the manufacturer's instructions. MCF-7 cells were cultured in an opaque-walled 96-well plate and treated with **Cu(L2)$_2$** at the indicated concentrations for 12 h. 100 μL Cell Titer-Glo reagent was added to each well. The plate was incubated at room temperature for 30 min. Luminescence intensity was measured in a microplate reader.

Lipid peroxidation assay. MCF-7 cells (1.5 x 10^4 cells/well) were plated in 96 well plate and allowed to adhere overnight. Afterwards, the cells were treated with Cu-complex **Cu(L2)$_2$** with its 20-fold and 10-fold IC_{50} values, respectively. DMSO treated cells were used as a negative control in this experiment. After 3 h of incubation, the media containing compounds was removed and the cells were washed with PBS. Then, a solution of C11-BODIPY in media was added to the cells and incubated in the dark at 37 °C for 15 min. The cells were then washed thrice with PBS to remove excess C11-BODIPY and fluorescence microscopy images were captured immediately using BIO-RAD ZOE™ fluorescent cell imager. Oxidation of BODIPY-C11 581/591 was calculated as the ratio of the green (fluorescence emission of the oxidized probe)/red fluorescence mean intensity (fluorescence emission of reduced probe) within the cell outlines.

Hemolytic assay. To check the induction of hemolysis, fresh human blood has been used in this experiment.[4] Briefly, The blood was collected and centrifuged at 1500 rpm for 10 min to remove blood plasma. The pellet of red blood cells (RBCs) were then washed thrice in PBS. Afterwards, RBCs were resuspended in 4% v/v in the PBS buffer. Compound **Cu(L2)$_2$** and the corresponding ligand **HL2** were dissolved in DMSO and serially diluted. In the 96 well plate, 20 μL of each concentration were added to the 100 μL of RBC suspension in each well and volume of 200 μL was achieved by adding PBS. The plate was immediately kept for the incubation of 1 h. After incubation, the plates were centrifuged again at 1500 rpm for 10 min. the supernatant (20 μL) was added to 80 μL of PBS in a fresh 96-well plate and hemoglobin release was measured. The optical density (OD) at 414 nm was measured for the hemoglobin release by using SpectraMax M5^e microplate reader. For positive control, 0.1% Triton X-100 was used whereas untreated cells were used as negative control. Percentage hemolysis was calculated using formula –

% hemolysis = [(OD of Sample – OD of PBS)/ (OD of Triton X – OD of PBS)] × 100

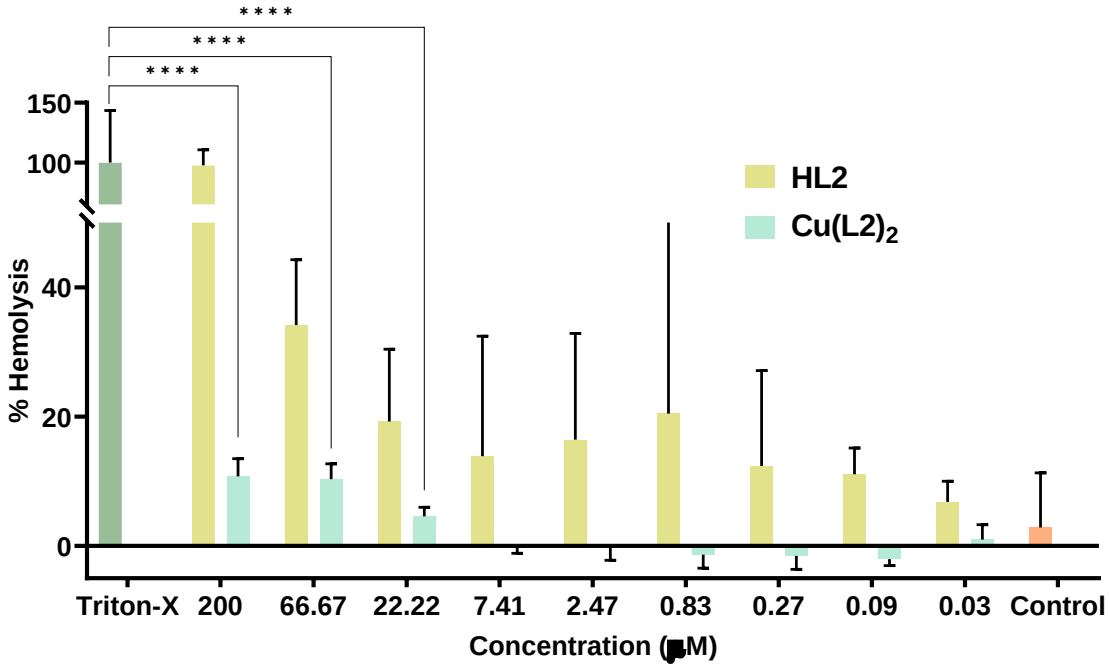

Figure S33: The experiment was performed in accordance with the guidelines of Institutional Animal Ethics Committee. Significance is denoted by asterisks from one-way ANOVA, ****P < 0.0001 versus control, nonsignificant analysis is not indicated.

Combination Analysis:

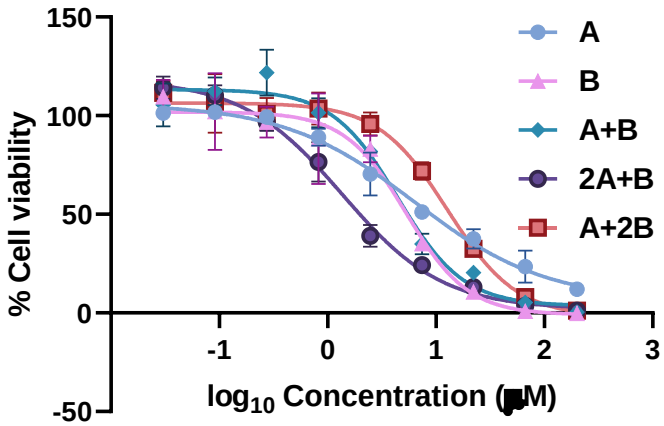

Figure S34: The combination analysis of the antiproliferative activity of the 1:1, 2:1 and 1:2 cisplatin/$Cu(L_2)_2$ combinations against MCF-7 cells for 72 h and the cytotoxicity curve of corresponding combinations.

When the combination was Cisplatin : $Cu(L2)_2$ :: 1:1, the combination IC_{50} value will be divided by 2. The Combination Index (CI) would be -

$$CI = \frac{D_{IC50}1}{D1} + \frac{D_{IC50}2}{D2}$$

$$CI = \frac{2.21}{6.39} + \frac{2.21}{5.32}$$

$$CI = 0.34 + 0.41$$

$$CI = 0.75$$

When the combination was Cisplatin : $Cu(L2)_2$ :: 2:1, the combination IC_{50} value will be divided by 3. The Combination Index (CI) would be -

$$CI = \frac{2(D_{IC50}1)}{D1} + \frac{D_{IC50}2}{D2}$$

$$CI = \frac{2(0.45)}{6.39} + \frac{0.45}{5.32}$$

$$CI = 0.141 + 0.085$$

$$CI = 0.226$$

When the combination was Cisplatin : $Cu(L2)_2$ :: 1:2, the combination IC_{50} value will be divided by 3. The Combination Index (CI) would be -

$$CI = \frac{D_{IC50}1}{D1} + \frac{2(D_{IC50}2)}{D2}$$

$$CI = \frac{4.24}{6.39} + \frac{2(0.42)}{5.32}$$

$$CI = 2.253$$

Western Blot. Cell and tissue protein extracts were prepared for western blotting. The protein mixtures were separated on SDS-PAGE gel (10%) and then transferred to a PVDF membrane (G-Biosciences, USA). Afterward, the membrane was blocked in 5% BSA for 1 h and incubated with primary antibodies [CST: PERK (D11A8) rabbit mAb #5683] overnight at 4 °C. The samples were subsequently incubated with β-actin antibody [CST: β-Actin (D6A8) rabbit mAb #8457] as a loading control. The membranes were washed three times (5 min each) with TBST and incubated for 2 h with a secondary antibody. After incubation, the membranes were washed again with TBST three times (5 min each) and visualized Supersignal™ West Pico Plus Chemiluminescent Substrate (Thermo scientific) and a chemiluminescence imaging machine (ChemiDoc Touch Imaging System, BioRad). The level of expression for each protein was analyzed using Bio-Rad Image Lab Software.

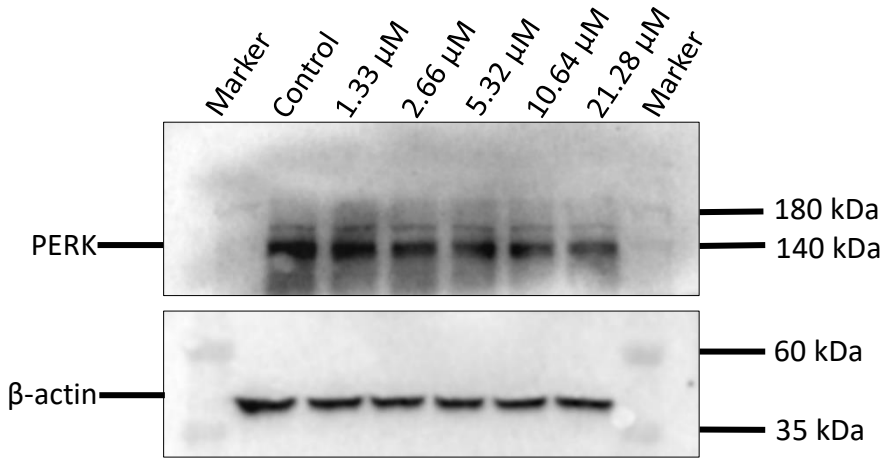

Cell Cycle Arrest:

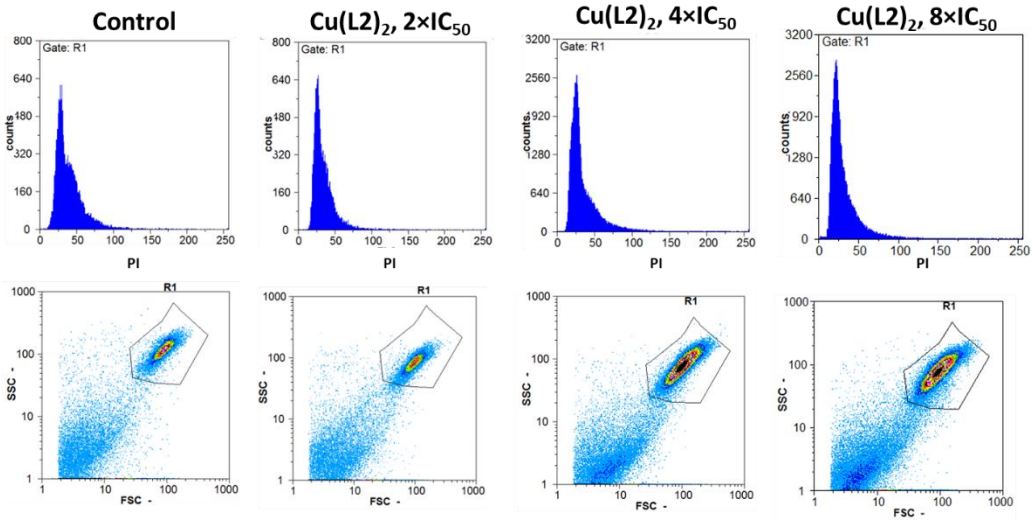

Figure S35: Cell cycle arrest: The MCF-7 cells were initially seeded and cultured overnight. Subsequently, they were treated with Cu(L2)2 at varying concentrations of 10 µM, 20 µM, and 40 µM for 24 hours. Following overnight incubation with ice ethanol, the cells were collected, subjected to centrifugation, washed, and subsequently incubated with a staining buffer solution containing PI/RNAse for 30 min. Later, the flow cytometry technique was employed to calculate the change in MCF-7 cells arrested at distinct stages.

Antimicrobial Activity: The antibacterial activities of (HL1−HL8) and their corresponding $Cu(L1)_2$ −$Cu(L8)_2$ complexes were ascertained by the broth microdilution method according to CLSI guidelines. Staphylococcus aureus ATCC 29213 was inoculated to LB agar plate and cultured overnight at 37 °C. Single colonies from the agar plate were added to Muller Hinton Broth (MHB) medium and grown overnight at 37 °C with agitation (170 rpm). The overnight cell cultures were diluted and grown to the mid-log phase (OD 600: 0.4–0.6). This culture was then diluted to ~10^5 CFU/mL in MHB medium. The prepared compounds were dissolved in DMSO to prepare the stock solutions, which were serially diluted two fold in 96- well plates in Mueller−Hinton broth. After that, 100 µL of diluted

bacterial suspension was added to the 96-well plate containing 100 µL of compound solution. The plates were then kept in incubator for 24 h at 37 °C. The MIC of the compounds that inhibited microbial growth was determined by recording the optical density at 600 nm using a microplate reader.

Table S6: Antimicrobial Profile of HL1-HL8 and $Cu(L1)_2$ - $Cu(L8)_2$

MIC (µM)			
Compounds	*S. aureus* ATCC 29213	Compounds	*S. aureus* ATCC 29213
HL1	164.89	$Cu(L1)_2$	85.42
HL2	154.13	$Cu(L2)_2$	65.74
HL3	170.16	$Cu(L3)_2$	78.32
HL4	152.36	$Cu(L4)_2$	70.85
HL5	177.71	$Cu(L5)_2$	81.50
HL6	23.38	$Cu(L6)_2$	76.17
HL7	140.88	$Cu(L7)_2$	76.35
HL8	154.88	$Cu(L8)_2$	71.79
Levofloxacin	0.69	Levofloxacin	0.69

Morphological Changes in S. aureus ATCC 29213 Observed by Atomic Force Microscope: Bacterial samples for AFM measurements were prepared as described earlier.[5-6] The incubated culture of *S. aureus* ATCC 29213 was inoculated in Mueller–Hinton Broth to make OD600 (0.4-0.6). The cells were treated with 25 and 50 µM HL6 for 1 and 4 h at 37 °C with shaking. Ampicillin (50 µg/mL)-treated cells and untreated bacterial cells were used as the control. After incubation, the 1 mL of culture was centrifuged at 15000 rpm for 1 min, the cell pellet was washed twice with Milli-Q water. Then drop of dispersed pellet in Milli-Q water was taken on a glass slide. The glass slide was then air dried and stored under vacuum in a desiccator. After drying, these cells were characterized by Atomic Force Microscopy (AFM) in order to assess the integrity of cells.

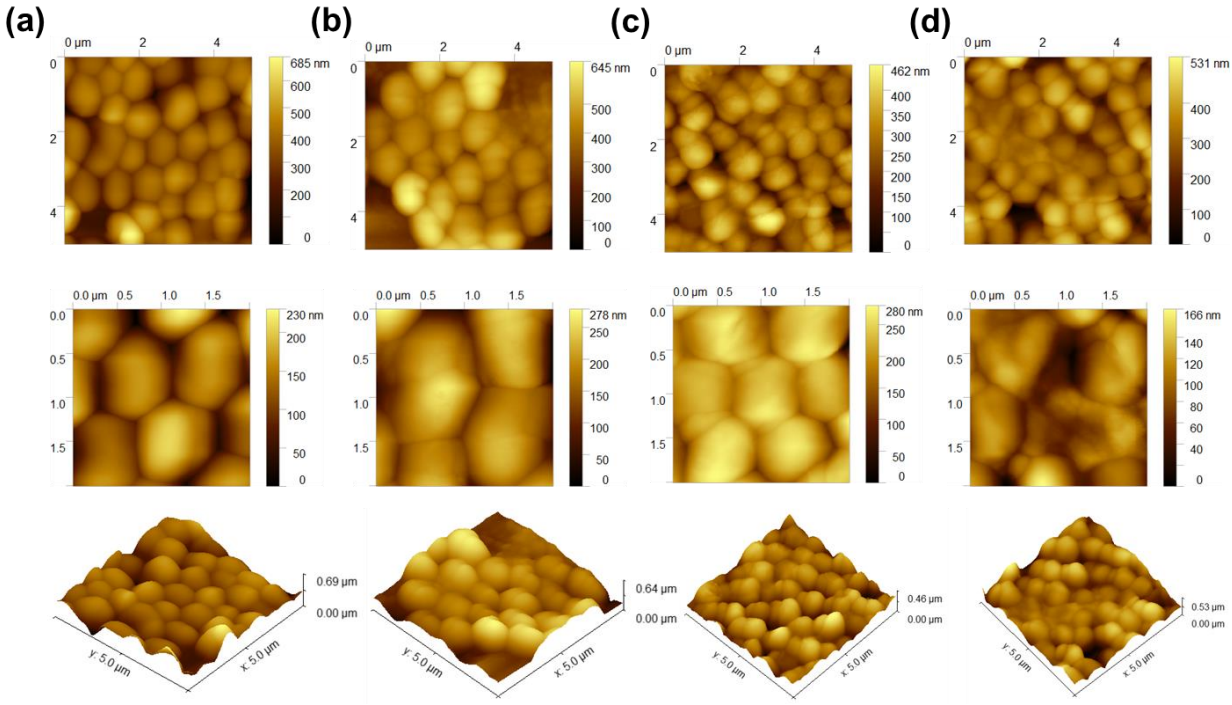

Figure S36: Atomic force microscopic images 2D topography (top two panel) and the corresponding 3D reconstructions (bottom panel) of *S. aureus* cells; (a) in the absence of drug treatment, showing typical round *S. aureus* cells with a smooth surface; (b) in the presence of treatment with 143.1 µM ampicillin (positive control); (c-d) in the presence of treatment with 25 and 50 µM HL6 respectively after 1 h; the treatment resulted in bacterial cell membrane damage with engraving and flat surface of *S. aureus* cells. The image was acquired in tapping mode using a scan size of 5 and 2 µm.

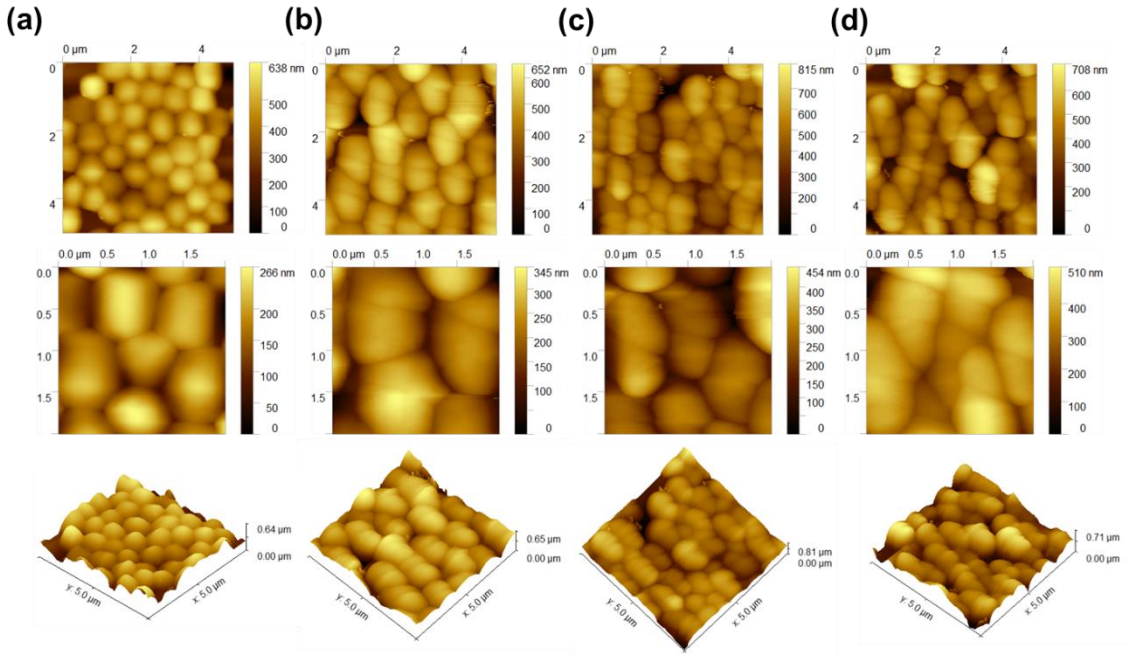

Figure S37: Atomic force microscopic images 2D topography (top two panel) and the corresponding 3D reconstructions (bottom panel) of *S. aureus* cells; (a) in the absence of drug treatment, showing typical round *S. aureus* cells with a smooth surface; (b) in the presence of treatment with 143.1 µM ampicillin (positive control); (c-d) in the presence of treatment with 25 and 50 µM HL6 respectively after 4 h; the treatment resulted in bacterial cell membrane damage with engraving and flat surface of *S. aureus* cells. The image was acquired in tapping mode using a scan size of 5 and 2 µm.

Morphological Changes for *S. aureus* ATCC 29213 observed by SEM

Bacterial samples for SEM measurements were prepared as described earlier. [4]Briefly, mid-logarithmic phase cells of *S. aureus* ATCC 29213 (OD_{600} 0.4-0.6) were treated with 25, 50 and 100 µM HL6 for 1 h and 4 h at 37 °C with shaking. Untreated bacterial cells and ampicillin (143.1 µM)-treated cells were used as the control. After incubation, the 1 mL of culture was centrifuged at 15000 rpm for 1 min, the cell pellet was washed twice with 1x PBS buffer. Then drop of dispersed pellet in 1x PBS was taken on a pre-cleaned coverslip. The sample was air dried and then fixed with 2.5% glutaraldehyde for 60 min. Then the cells were again washed thrice with the same buffer and dehydrated sequentially with 30–100% ethanol for 10 min each. The coverslips were then dried under vacuum in a desiccator. Finally, the cells were coated with gold and viewed via a scanning electron microscope available at IITK.

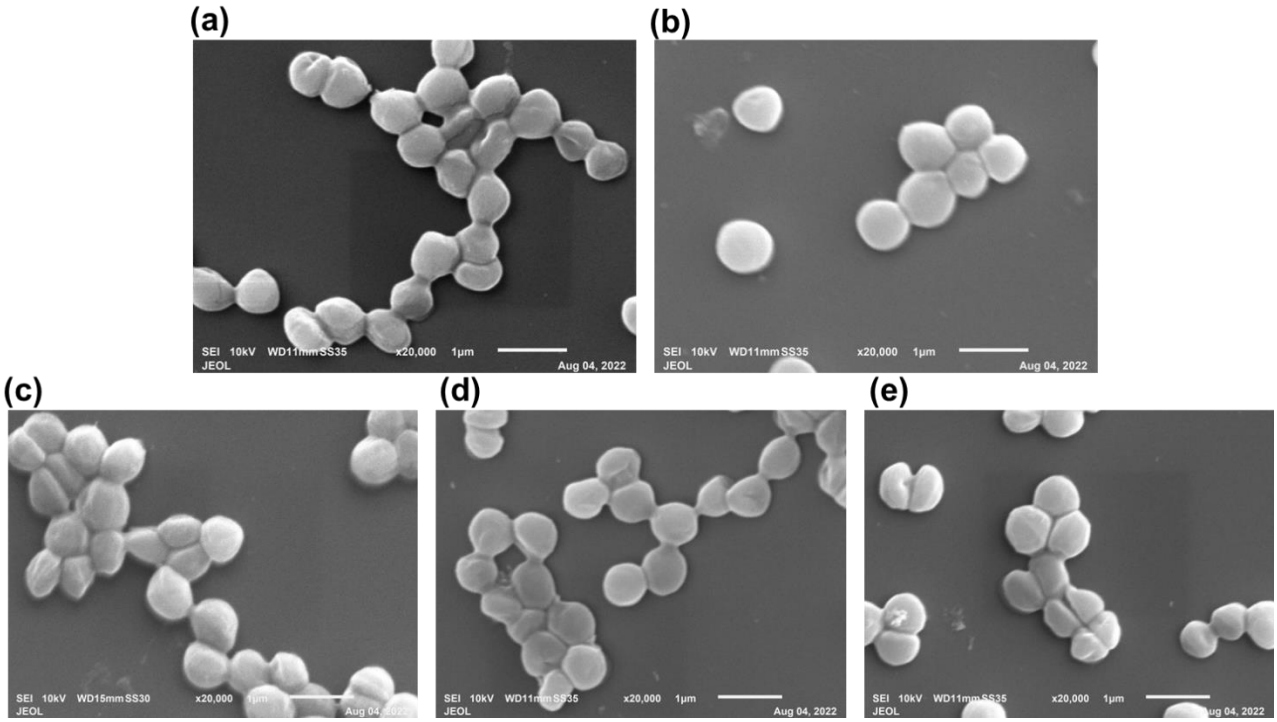

Figure S38: Scanning electron microscope images of *S. aureus* ATCC 29213 cells; (a) untreated cells showing smooth well-defined morphology; (b) treated cells with ampicillin (positive control) 143.1 µM respectively; (c-e) treated cells with HL6 25, 50 and 100 µM respectively after 1h; the treated *S. aureus* cells shows irregular shape fractured cells with cellular debris. Scale bar = 1 µm, magnification = 20 K.

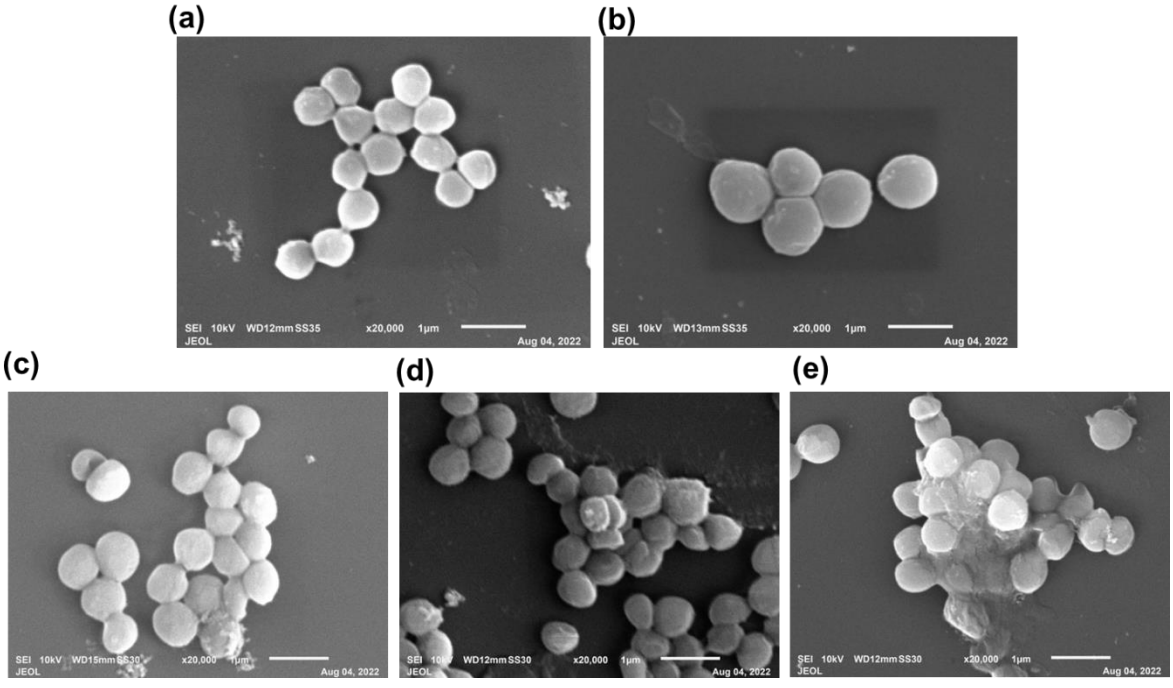

Figure S39: Scanning electron microscope images of *S. aureus* ATCC 29213 cells; (a) untreated cells showing smooth well-defined morphology; (b) treated cells with ampicillin (positive control) 143.1 µM respectively; (c-e) treated cells with HL6 25, 50 and 100 µM respectively after 4h; the treated *S. aureus* cells show irregular shape fractured cells with cellular debris. Scale bar = 1 µm, magnification = 20 K.

Table S7: The SMILES strings for the ligands (HL1 – HL8) and complexes $Cu(L1)_2$ – $Cu(L8)_2$

Compound	SMILES	MDA-MB-231	MCF-7	HCT-116	A549	HEK-293
HL1	O=C(N([H])[C@@H](C1=CC=CC=C1)C(C=CC=C2)=C2/N=C/C3=CC=CC=C3O	> 100	95.4 ± 20.0	> 100	> 100	14.9 ± 7.9
HL2	O=C(N([H])[C@@H](C1=CC=CC=C1)C(C=CC=C2)=C2/N=C/C3=CC(C(C)(C)C)=CC(C(C)(C)C)=C3O	13.2 ± 3.9	10.7 ± 2.7	8.1 ± 1.4	18.2 ± 0.7	18.6 ± 1.6
HL3	O=C(N([H])[C@@H](C1=CC=CC=C1)C(C=CC=C2)=C2/N=C/C3=CC(Cl)=CC=C3O	39.5 ± 43.0	39.8 ± 43.0	45.8 ± 7.0	45.5 ± 1.1	> 100
HL4	O=C(N([H])[C@@H](C1=CC=CC=C1)C(C=CC=C2)=C2/N=C/C3=CC(Br)=CC=C3O	73.4 ± 7.0	73.1 ± 7.0	44.3 ± 2.5	> 100	> 100
HL5	O=C(N([H])[C@@H](C1=CC=CC=C1)C(C=CC=C2)=C2/N=C/C3=CC(F)=CC=C3O	33.8 ± 36.4	34.2 ± 36.0	51.3 ± 27.9	95.9 ± 3.7	88.1 ± 9.5
HL6	O=C(N([H])[C@@H](C1=CC=CC=C1)C(C=CC=C2)=C2/N=C/C3=CC([N+]([O-])=O)=CC=C3O	> 100	> 100	> 100	> 100	> 100
HL7	O=C(N([H])[C@@H](C1=CC=CC=C1)C(C=CC=C2)=C2/N=C/C3=CC(C(O)=O)=CC=C3O	> 100	> 100	> 100	> 100	> 100
HL8	O=C(N([H])[C@@H](C1=CC=CC=C1)C(C=CC=C2)=C2/N=C/C3=CC=C(N(CC)CC)C=C3O	50.1 ± 0.0	13.4 ± 6.0	> 100	> 100	> 100
$Cu(L1)_2$	[H]N([C@@H](C1=CC=CC=C1)C2=O[Cu]34([N](C5=C(C(N([H])[C@@H](C6=CC=CC=C6)C)=O)C=CC=C5)=CC7=CC=CC=C7O4)OC8=CC=CC=C8C=[N]3C9=C2C=CC=C9	> 100	25.9 ± 0.6	27.6 ± 0.8	43.4 ± 1.3	> 100
$Cu(L2)_2$	[H]N([C@@H](C1=CC=CC=C1)C2=O[Cu]34([N](C5=C(C(N([H])[C@@H](C6=CC=CC=C6)C)=O)C=CC=C5)=CC7=CC(C(C)(C)C)=CC(C(C)(C)C)=C7O4)OC8=C(C(C)(C)C)C=C(C(C)(C)C)C=C8C=[N]3C9=C2C=CC=C9	8.1 ± 0.4	5.3 ± 0.7	9.1 ± 1.4	9.4 ± 4.2	17.6 ± 1.7
$Cu(L3)_2$	[H]N([C@@H](C1=CC=CC=C1)C2=O[Cu]34([N](C5=C(C(N([H])[C@@H](C6=CC=CC=C6)C)=O)C=CC=C5)=CC7=CC(Cl)=CC=C7O4)OC8=CC=C(Cl)C=C8C=[N]3C9=C2C=CC=C9	14.6 ± 1.3	15.4 ± 0.9	27.3 ± 0.6	30.0 ± 1.4	7.4 ± 0.1
$Cu(L4)_2$	[H]N([C@@H](C1=CC=CC=C1)C2=O[Cu]34([N](C5=C(C(N([H])[C@@H](C6=CC=CC=C6)C)=O)C=CC=C5)=CC7=CC(Br)=CC=C7O4	22.7 ± 1.1	14.5 ± 0.4	11.4 ± 1.2	26.8 ± 2.3	9.5 ± 1.3

	)OC8=CC=C(Br)C=C8C=[N]3C9=C2C=CC=C9					
$Cu(L5)_2$	[H]N([C@@H](C1=CC=CC=C1)C)C2=O[Cu]34([N](C5=C(C(N([H])[C@@H](C6=CC=CC=C6)C)=O)C=CC=C5)=CC7=CC(F)=CC=C7O4)OC8=CC=C(F)C=C8C=[N]3C9=C2C=CC=C9	28.0 ± 1.5	29.5 ± 4.6	27.3 ± 2.5	52.7 ± 1.4	21.4 ± 5.3
$Cu(L6)_2$	[H]N([C@@H](C1=CC=CC=C1)C)C2=O[Cu]34([N](C5=C(C(N([H])[C@@H](C6=CC=CC=C6)C)=O)C=CC=C5)=CC7=CC([N+]([O-])=O)=CC=C7O4)OC8=CC=C([N+]([O-])=O)C=C8C=[N]3C9=C2C=CC=C9	9.0 ± 2.0	17.9 ± 2.9	13.3 ± 1.2	13.5 ± 1.4	12.0 ± 0.4
$Cu(L7)_2$	[H]N([C@@H](C1=CC=CC=C1)C)C2=O[Cu]34([N](C5=C(C(N([H])[C@@H](C6=CC=CC=C6)C)=O)C=CC=C5)=CC7=CC(C(O)=O)=CC=C7O4)OC8=CC=C(C(O)=O)C=C8C=[N]3C9=C2C=CC=C9	26.9 ± 21.9	59.9 ± 4.9	> 100	> 100	> 100
$Cu(L8)_2$	[H]N([C@@H](C1=CC=CC=C1)C)C2=O[Cu]34([N](C5=C(C(N([H])[C@@H](C6=CC=CC=C6)C)=O)C=CC=C5)=CC7=CC=C(N(CC)CC)C=C7O4)OC8=CC(N(CC)CC)=CC=C8C=[N]3C9=C2C=CC=C9	17.9 ± 0.7	17.3 ± 1.2	22.4 ± 6.6	28.9 ± 1.4	27.2 ± 2.6

Table S8: Table S8: 50% Inhibitory concentrations (IC_{50}, μM) of HL1–HL8 and $(Cu(L1)_2–Cu(L8)_2$ in comparison with the FDA approved cisplatin determined by the resazurin assay after incubation for 72 h.

Compounds	MDA-MB-231	MCF-7	HCT-116	A549	HEK-293
HL1	>100	95.4 ± 20.0	>100	>100	14.9 ± 7.9
HL2	13.2 ± 3.9	10.7 ± 2.7	8.1 ± 1.4	18.2 ± 0.7	18.6 ± 1.6
HL3	39.5 ± 43.0	39.8 ± 43.0	45.8 ± 7.0	45.5 ± 1.1	>100
HL4	73.4 ± 7.0	73.1 ± 7.0	44.3 ± 2.5	>100	>100
HL5	33.8 ± 36.4	34.2 ± 36.0	51.3 ± 27.9	95.9 ± 3.7	88.1 ± 9.5
HL6	>100	>100	>100	>100	>100
HL7	>100	>100	>100	>100	>100
HL8	50.1 ± 0.0	13.4 ± 6.0	>100	>100	>100
$Cu(L1)_2$	>100	25.9 ± 0.6	27.6 ± 0.8	43.4 ± 1.3	>100
$Cu(L2)_2$	8.1 ± 0.4	5.3 ± 0.7	9.1 ± 1.4	9.4 ± 4.2	17.6 ± 1.7
$Cu(L3)_2$	14.6 ± 1.3	15.4 ± 0.9	27.3 ± 0.6	30.0 ± 1.4	7.4 ± 0.1
$Cu(L4)_2$	22.7 ± 1.1	14.5 ± 0.4	11.4 ± 1.2	26.8 ± 2.3	9.5 ± 1.3
$Cu(L5)_2$	28.0 ± 1.5	29.5 ± 4.6	27.3 ± 2.5	52.7 ± 1.4	21.4 ± 5.3
$Cu(L6)_2$	9.0 ± 2.0	17.9 ± 2.9	13.3 ± 1.2	13.5 ± 1.4	12.0 ± 0.4
$Cu(L7)_2$	26.9 ± 21.9	59.9 ± 4.9	>100	>100	>100
$Cu(L8)_2$	17.9 ± 0.7	17.3 ± 1.2	22.4 ± 6.6	28.9 ± 1.4	27.2 ± 2.6
Cisplatin	1.9 ± 0.1	6.4 ± 1.6	6.2 ± 0.1	4.1 ± 0.1	4.3 ± 0.1

References

1. X. R. Zhou, Y. Liu, Z. T. Huang, Q. X. Yao, F. F. He and Y. Gao, *Bioconjug. Chem.*, 2021, **32**, 106-110
2. A. L. Shi, D. F. Wang, H. Wang, Y. Wu, H. Q. Tian, Q. Guan, K. Bao and W. G. Zhang, *RSC Adv.*, 2016, **6**, 114879-114888.
3. J. N. Liu, W. Q. Tang, L. Sheng, Z. Du, T. Zhang, X. Su and S. X. A. Zhang, *Chem. Asian J.*, 2019, **14**, 438-445.
4. T. Saha, P. Kumar, N. Sepay, D. Ganguly, K. Tiwari, K. Mukhopadhyay and S. Das, *Acs Omega*, 2020, **5**, 16342-16357.
5. S. Ali, S. Perveen, M. Ali, M.R. Shah, E. Khan, A.S. Sharma, H. Li, Q. Chen. *J. Clust. Sci*. 2019, **31**, 811–821.
6. R. Niranjan, S. Zafar, B. Lochab and R. Priyadarshini, *Nanomater.*, 2022, **12**, 191-209.
7. K. Sakthikumar, R. V. Solomon and J. D. Raja, *RSC Adv.*, 2019, **9**, 14220-14241.
8. I. Warad, H. Suboh, N. Al-Zaqri, A. Alsalme, F. A. Alharthi, M. M. Aljohani and A. Zarrouk, *RSC Adv.*, 2020, **10**, 21806-21821.